THERMODYNAMIC MODELING OF SUPERCOOLED WATER

By
Jana Kalová

UNIVERSITY OF WEST BOHEMIA
FACULTY OF MECHANICAL ENGINEERING

The undersigned hereby certify that they have read and recommend to the Faculty of Mechanical Engineering for acceptance a thesis entitled "**Thermodynamic modeling of supercooled water**" by **Jana Kalová** in partial fulfillment of the requirements for the degree of **Doctor of Philosophy**.

Dated: 2012

Supervisor: Prof. Radim Mareš
University of West Bohemia, Czech Republic

Supervisor Specialist: Prof. Mikhail A. Anisimov
The University of Maryland, U.S.A.

UNIVERSITY OF WEST BOHEMIA

Date: **2012**

Author: **Jana Kalová**

Title: **Thermodynamic modeling of supercooled water**

Faculty: **Mechanical Engineering**

Department: **Power System Engineering**

Degree: **Ph.D.**

Permission is herewith granted to the University of West Bohemia to circulate and to have copied for non-commercial purposes, at its discretion, the above title upon the request of individuals or institutions.

Signature of Author

To Marie, Stanislav, Jaroslav, Michael, Vladimír.

With love.

Table of Contents

List of Tables

List of Figures

Abstract

Thermodynamic properties of supercooled water are often used in many atmospheric applications. Clouds are often composed from deeply supercooled water. Supercooled water can also occur on some of our neighboring planets. Properties of supercooled water play an important role in aqueous solutions. Knowledge of behavior of aqueous solutions below 0 °C is important for deep ocean science, underwater communication and navigation. Supercooled water is of great importance for biological systems. Four scenarios can be described to explain behavior of supercooled water: retracing spinodal, singularity free, critical point and critical point free scenarios. Mainly the second critical point scenario is discussed in the thesis, because a lot of work was made recently in this particular area. It is shown that the complete scaling method can describe existing experimental data both in the linear scaling equation and in the mean-field approximation. One of the models was tested by the author in the mean-field approximation. A modification of the IAPWS vapor pressure equation was developed to describe vapor pressure data from 123 K to 647 K. A possible existence of the second inflection point in the temperature dependence of the surface tension is discussed and a new term to IAPWS equation for surface tension is added to describe behavior of surface tension from 228 K to 647 K. The influence of the new calculated and measured values of critical exponents on the linearity of a parametric equation was tested and the necessity of linearity tests when new values of exponents are used is identified.

Acknowledgements

I would like to thank Professor Radim Mareš, my supervisor, for his constant support and help during my Ph.D. study. He provided encouragement, advice, good guidance and company. One simply could not wish for a better and friendlier supervisor. I am grateful to Professor Mikhail A. Anisimov, my supervisor specialist, for his many valuable suggestions and advice during this research. He provided many useful references and friendly encouragement. It is an honor for me to thank Professor Jan V. Sengers for his inspiration, advice and kindness. Their support was crucial to the successful completion of this project.

D. A. Fuentevilla, C. E. Bertrand and V. Holten from the Institute of Physical Science and Technology, The University of Maryland, shared with me their knowledge and gave me a better perspective on my own results.

I would like to thank those many people who have taught me, especially Professor Pavel Drábek and Professor Stanislav Míka from The Faculty of Applied Science, The University of West Bohemia and Dr. Josef Blažek from The Pedagogical Faculty, The University of South Bohemia.

I am indebted to my many friends for providing a stimulating, kind and pleasant background. I am especially grateful to Lenka Kudrličková, Věra Kurcová, Deepa Subramanian, Dagmar Šimková, Jan Eisner, Vlastimil Křivan, Radek Trča.

I also wish to acknowledge The Czech National Committee for the Properties of Water and Steam for their support, namely to Dr. Jan Hrubý. I also would like to mention that my research at The University of Maryland, U.S.A in 2010 was supported by a grant from The International Association for the Properties of Water and Steam and by the Ministry of Education, Youth, and Sports of the Czech Republic.

The Department of Mathematics and Biomathematics, The University of South Bohemia has provided the support and equipment I have needed to produce and complete my thesis.

Finally, and most importantly, I am grateful to my family for an unending love and support, to my marvellous mum Marie Novotná, my amazing sons Jaroslav Kala and Michael Kala, and my beloved partner Vladimír Blažek. They always support me and they love me. They all have been my primary motivation for everything. It would have been impossible for me to finish this work without them. I remember my dad Stanislav Novotný. I owe my loving thanks to them and I dedicate this thesis to them.

Nomenclature

S	Entropy
U	Internal energy
V	Volume
S	Numbers of moles
T	Temperature
P	Pressure
C_V	Isochoric heat capacity
C_P	Isobaric heat capacity
κ_T	Isothermal compressibility
α_V	Coefficient of thermal expansion
σ_{ik}	Element of stress tensor
ϵ_{ik}	Element of strain tensor
T_S	Thermodynamic limit for liquid water
T_H	Kinetic limit for liquid water
T_B	Boiling point temperature
T_M	Melting point temperature
T_G	Glass transition temperature
T_X	Spontaneous crystallization temperature

HDA	High density amorphous ice
LDA	Low density amorphous ice
HDL	High density liquid
LDL	Low density liquid
T_S	Spinodal (singular) temperature
X_{b}	Regular background
X_{cr}	Critical part of properties
LLCP	Liquid-liquid critical point
ρ	Density
A	Helmholtz energy per mol
φ	Order parameter
h_1	"Ordering" field
h_2	"Thermal" field
h_3	Critical part of scaling field
χ	Susceptibility
$\alpha, \beta, \gamma, \delta, \nu, \eta$	Universal critical exponents
$A_0^{\pm}, B_0, \Gamma_0^{\pm}$	Ising critical amplitudes
$\hat{X}$	Circumflex accent indicates dimensionless property
μ	Chemical potential (Gibbs energy per mol)
$L_{liq}(T)$	Enthalpy of vaporization
R	Molar gas constant
σ	Surface tension
EOS	Equation of state
LLT	Liquid-liquid transition
IAPWS	International Association for the Properties of Water and Steam

Introduction

The thermodynamic properties of ordinary water exhibit anomalous behavior upon supercooling. A variety of explanations for the anomalous thermodynamic behavior of supercooled water has been suggested. In this thesis we considered the existence of a liquid-liquid critical point and its possible effects on the temperature dependence of the thermodynamic properties of water - the heat capacity, the isothermal compressibility, and the thermal expansivity of supercooled water.

The following goals of this thesis were established:

- to test possibilities of describing supercooled water experimental data using the complete scaling method and the mean-field approximation
- to analyze experimental data for the surface tension of supercooled water and to test the possibility of the existence of the second inflection point in the temperature surface tension dependence.

This thesis is divided into nine chapters. Chapter 1 explains conditions of the thermodynamics stability, a concept of metastable liquids, describes thermodynamic and kinetic limits for liquid water, existing experimental data, and leading theories for anomalous behavior of supercooled water. Chapter 2 introduces a critical point theory. Chapter 3 describes the parametric scaled equation of state for supercooled liquid water and the influence of critical exponents values on the linearity of the model.

Chapter 4 covers a simple, revised and complete scaling method and summarizes the scaled equation of state developed by Fuentevilla and Anisimov. Chapter 5 describes the vapor pressure of supercooled water in the temperature interval from 123 K to 647 K. A deriving this equation for vapor pressure is based on the crossover equation. These results we published in the International Journal of Thermophysics in 2010. Experimental data of the surface tension of supercooled water are analyzed in Chapter 6. The paper with these results has been submitted in the International Journal of Thermophysics and is under review. Chapter 7 contains a recent development of the scaled equation of supercooled water based on the linear model. The mean-field approximation of the scaled equation is described in the Chapter 8. The paper with this research conclusions has been submitted to the International Journal of Thermophysics, with Jana Kalová as a co-author. The Summary in Chapter 9 contains a more detailed overview of results and conclusions, and suggestes possibilities of future research.

The list of publications is in the appendix.

Chapter 1

Metastable liquids and supercooled water

Water at atmospheric pressure and temperature below 0 °C can exist as liquid . Such water is called supercooled. Liquid water at above 100 °C is called superheated. All liquids and their mixtures have the same properties. The states of liquids below the normal freezing point and above the normal boiling point are called metastable. At atmospheric pressure, water can exist in the liquid state (stable and metastable) in the temperature range from -41 °C to 280 °C [28, 29]. It is possible to get a metastable state of water also for stretched water (or other liquids). Water has been stretched to a remarkably large negative pressure -140 MPa ([30]).

1.1 Metastable liquids

To get a metastable state of liquid, it is essential to remove suspended and dissolved impurities carefully and to minimize contact with rough bounding surfaces. Minor perturbations in metastable states can trigger a sudden appearance of a nucleus of stable phases - ice in supercooled water and vapor in superheated water. The process

of nucleation is called "heterogeneous" when it is influenced by the presence of defects, impurities, walls or radiation. The process is common in nature - for example, water droplets in clouds freeze roughly at -20 °C due to the presence of dust particles and various chemicals. The process of nucleation in the absence of defects, walls etc. is an intrinsic property of the system and is called "homogeneous". Metastability is possible because there is an energy barrier against nucleation of the stable phase. In homogeneous nucleation, a new phase is formed when some fluctuation overcomes the free energy barrier and forms a nucleus of a critical size ([31]).

To be able to study thermodynamic properties of metastable liquids, the lifetime of the system must be longer than the relaxation time (the time when the system returns to the equilibrium) plus the observation time (the necessary time for the measurement of properties). That is why it is not possible to obtain any experimental data near the limit of thermodynamic stability -the lifetime of the system becomes too low in this case. The limit of superheating or supercooling restricts the region where one can measure thermodynamic properties of liquids. These limits are called homogeneous nucleation limits. Calculation of the metastable system lifetime is a matter of kinetics. A concept of a kinetic spinodal is introduced as a locus where the lifetime of the metastable state becomes shorter than the relaxation time to the local equilibrium [32, 33, 34].

We can also use a phenomenological approach to derive criteria for the thermodynamic stability of a macroscopic system. When the system is isolated and located in equilibrium, some microscopic fluctuation always decreases the system entropy. For an isolated system, one can write the following condition:

$$[\Delta S]_{U,V,N} \leq 0,$$

where S, U, V and N stand for the system's entropy, internal energy, volume, and the number of moles [35]. The stability criterium is equivalent to the condition

$$[\Delta U]_{S,V,N} \geq 0.$$

Using this, one can derive six criteria of a system stability [31]:

$$\left(\frac{\partial T}{\partial S}\right)_{P,N} > 0, \qquad \left(\frac{\partial T}{\partial S}\right)_{\mu,V} > 0,$$
$$\left(\frac{\partial P}{\partial V}\right)_{\mu,S} < 0, \qquad \left(\frac{\partial P}{\partial V}\right)_{T,N} < 0,$$
$$\left(\frac{\partial \mu}{\partial N}\right)_{P,S} > 0, \qquad \left(\frac{\partial \mu}{\partial N}\right)_{T,V} > 0.$$

The criteria can be expressed in measurable quantities - positive values of the isochoric heat capacity C_V or the isothermal compressibility κ_T are necessary for the stability:

$$\left(\frac{\partial T}{\partial S}\right)_{V,N} = \frac{T}{C_V} > 0, \qquad \left(-\frac{\partial P}{\partial V}\right)_{T,N} = \frac{1}{V \cdot \kappa_T} > 0.$$

The criteria mean, that either temperature must increase due to added heat, or the pressure must increase when the body is compressed. It is not possible to reach the limit of thermodynamic stability experimentally because the homogeneous nucleation limit is reached first.

The criteria of stability of a fluid phase with a respect to a solid phase are more complex. It is required to add the terms $\sigma_{ik}\epsilon_{ik}$, where σ_{ik} is an element of stress tensor and ϵ_{ik} is the element of strain tensor, $(i, k = 1, 2, ..., 6)$ [36]. The terms denote works of deformation of the solid phase. The complexity of the description of the stability limits between fluid and solid phases causes that criteria of stability have not yet been developed [30].

1.2 Thermodynamic and kinetic limits for liquid water

Thermodynamic (T_S) and kinetic (T_H) limits for liquid water are schematically shown in Figure 1.1 [1].

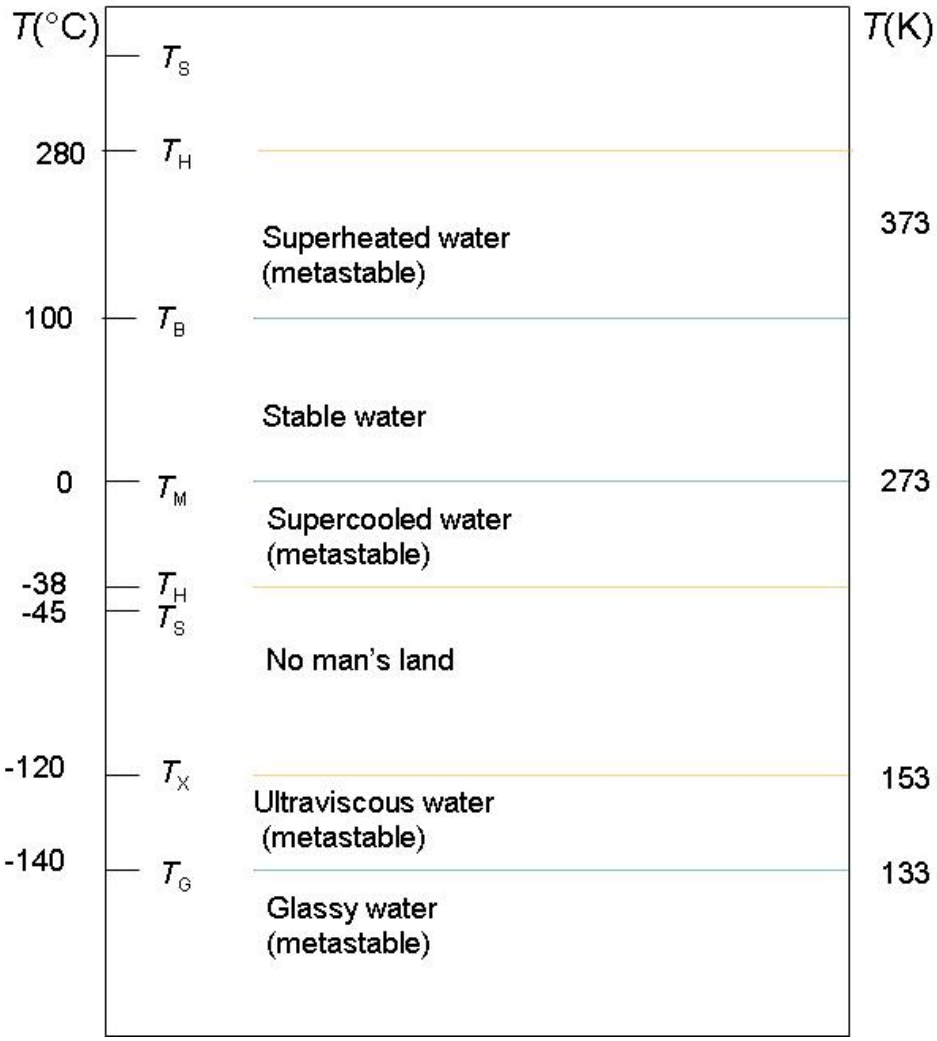

Figure 1.1: Thermodynamic and kinetic limits for ordinary liquid water at ambient pressure [1].

The liquid status of water starts at the hypothetic thermodynamic limit of stability T_S. This limit is called "spinodal" [37, 38]. Only one criterium of stability is often used for a spinodal definition:

$$\left(\frac{\partial P}{\partial V}\right)_{T,N} = 0.$$

It becomes impossible to avoid boiling above the kinetic spinodal temperature T_H. The temperatures T_B (the boiling point) and T_M (the melting point) are the higher and lower limits of the stable region of liquid water. If water is cooled below the melting temperature, then ice is formed. If extremely clean, water can be cooled to T_H=-38 °C, to the kinetic spinodal between liquid and ice. Below this temperature it is impracticable to avoid crystallization. The region below T_H is called "No man's land", because no data for bulk water exist from this region. Only huge quenching rates ($> 10^5$ degrees per second) can prevent crystallization.

When the temperature drops below T_G = -140 °C (the glass transition temperature), amorphous ice is created. Amorphous ice is also called glassy water. Although amorphous ice is solid, its structure shows features similar to liquid. When amorphous ice is heated above the glass transition temperature, it transforms into a highly viscous (ultraviscous) liquid. Ultraviscous liquid is metastable, but as the viscosity of liquid is very high, the lifetime of the state is longer and it is possible to measure its thermodynamic properties. Above the spontaneous crystallization temperature T_X, the "No man's land" region is reached again and one cannot avoid crystallization [1, 39].

A new form of amorphous ice was discovered in 1984 [40, 41]. This phenomenon is called polyamorphism [39]. The new kind of amorphous ice has higher density and this form of amorphous ice is called High Density Amorphous ice (HDA ice), while the

original form is called Low Density Amorphous ice (LDA). LDA ice can be formed directly from HDA ice, when thermodynamic parameters (temperature, pressure) are changed. The volume changes significantly when thermodynamic parameters are changed infinitesimally. It is expected that the first order transition exists between HDA and LDA ice.

When amorphous ice is heated, it changes into an ultraviscous liquid. It is expected (similarly to amorphous states of ice), that two different liquid phases are created - Low Density Liquid (LDL) and High Density Liquid (HDL).

1.3 Supercooled liquid water

Water has many of unusual properties. One of the best-known is the fact that the maximum density of water is at 4 °C. In 1971, Voronel [42] predicted a "scaling" relation for several substances:

$$\frac{C_V}{T} = A \cdot \tau^{-\alpha} + B, \tag{1.3.1}$$

where C_V is specific isochoric heat capacity, T is the temperature in K and where $\tau = (T - T_0)/T_c$, T_0 is temperature below the melting point and cannot be determined directly from any experiment. T_c is the critical temperature. The value 0.13 was used for index α. Anisimov *et al.* [9] measured the isobaric heat capacity C_P to -7.5 °C in the adiabatic calorimeter. He and his co-workers found T_0=255 K.

Subsequent experiments found that isothermal compressibility and thermal expansivity also change rapidly with respect to temperature below 0 °C. The overview of experimental data for supercooled water supported the statement is in Table 1.3.

Table 1.1: Overview of the experimental data

Properties	Range	Reference
isothermal compressibility	0.1 MPa, -26/45 °C	Speedy and Angell 1976 [12]
	0.1/190 MPa, -30/25 °C	Kanno and Angell 1979 [13]
density, thermal expansion	0.1 MPa, -23/4 °C	Schufle 1965 [43]
	0.1 MPa, -40/24 °C	Schufle and Venugopalan 1967 [44]
	0.1 MPa, -34/24 °C	Zheleznyi 1967 [45]
	0.1 MPa, -35/5 °C	Rasmussen and MacKenzie 1973 [46]
	0.1 MPa, -34/0 °C	Sorensen 1983 [47]
	0.1 MPa, -34/40 °C	Hare and Sorensen 1986 [14]
	0.1 MPa, -34/0 °C	Hare and Sorensen 1987 [15]
	0.1 MPa, -243/100 °C	Mallamace et al. [48]
	40/400 MPa, -73/2 °C	O. Mishima [17]
isobaric heat capacity	0.1 MPa, -7.5/30 °C	Anisimov et al. 1972 [9]
	0.1 MPa, -35/5 °C	Rasmussen and MacKenzie 1973 [46]
	0.1 MPa, -35/5 °C	Rasmussen at al 1973 [49]
	0.1 MPa, -38/4 °C	Angell at al 1973 [50]
	0.1 MPa, -37/17 °C	Angell at al 1982 [7]
	0.1 MPa, -28.5/10 °C	Tombari at al 1982 [8]
	0.1 MPa, -37/12 °C	Archer and Carter 2000 [10]

Three different scenarios have been proposed to explain metastable behavior of water, observed anomalies, and two types of amorphous ice. Experimental verification of the scenarios is difficult because nucleation of ice prevents detailed supportive measurements.

Retracing spinodal scenario

The stability limit conjecture scenario was suggested by Speedy [51, 52]. This spinodal is (according to the hypothesis) a retracing liquid-gas spinodal, that is continuous from the liquid-gas critical point to the very low temperatures. According to this scenario, water has a continuous spinodal curve bounding the superheated, supercooled and stretched states of water. The observed anomalies in the supercooled region are caused by the spinodal, where isobaric heat capacity, isothermal compressibility and the thermal expansion coefficient diverge. The scenario predicts power-law behavior of the properties,

$$X = A \cdot \left(\frac{T}{T_{\mathrm{S}}} - 1 \right)^{-c} + X_{\mathrm{b}},$$

where X is a property that diverges at the spinodal, T_{S} is spinodal temperature, c is an experimental exponent, and X_{b} is a background (analytical) function of the temperature. It is assumed that cooled or streched liquid water cannot exist beyond the line $T_{\mathrm{S}}(P)$ in the pressure - temperature $(P - T)$ phase diagram.

Debenedetti has argued that retracing spinodal scenario is implausible for supercooled water [53, 54, 55].

Singularity free scenario

The theory shows that the increase in compressibility at constant pressure, when the temperature decreases, are not primarily an indication of any singular behavior [56].

This scenario is the simplest one that is consistent with experimental data. The singularity free scenario is supported by several models showing anomalous increases of properties without corresponding singularity [57].

Critical-point scenario

The third recent attempt to explain anomalous behavior of water is called the liquid-liquid critical point (LLCP) hypothesis [58]. This scenario is based on the molecular dynamics studies and ascribes the anomalous properties of water to the presence of a liquid-liquid critical point. The critical point is associated with a phase transition between a low-density and a high-density liquid phase. The scenario is supported by experimentally observed first order transition between low density and high density amorphous ice [59, 40, 41] and by extensive Monte Carlo and molecular dynamics simulations of various water and water-like models [60, 61].

Chapter 2

Critical point theory

A phase transition is a change of a substance from one phase to another. During a phase transition, a thermodynamic system changes its properties when some external conditions, such as the temperature and the pressure, are slightly changed. For example, liquid becomes gas when the temperature is increased above the boiling point, resulting in an abrupt change in volume. The classical Paul Ehrenfest classification of phase transitions is based on behavior of thermodynamic free energy. The first-order phase transitions mean that the first derivative of free energy shows discontinuity, e.g. molar entropy, molar volume, molar enthalpy or concentration. The second-order phase transitions are continuous in the first derivative, but the second derivative of free energy exhibits discontinuity, e.g. molar heat capacity, isothermal compressibility, thermal expansivity [62].

Typically, a phase transition is brought about by a change in the temperature of the system. An example of the first-order phase transition is melting, where liquid is disordered and thus has higher entropy than solid. The solid-liquid transition occurs at the melting point. This is characterized by the amount of latent heat that must

be added to the solid (ice) for it to be disordered into the liquid phase. Other examples of phase transitions are the gas-liquid transition (condensation), the normal-to-superconducting transition in electrical conductors, the paramagnet-to-ferromagnet transition in magnetic materials, and the superfluid transition in liquid helium, transitions involving amorphous or glassy structures, spin glasses, charge-density waves, and spin-density waves [63, 34].

In first-order phase transitions the metastable states can exist. The two distinct phases may coexist. The boundary of the two phases is called binodal or coexistence curve. The binodal can be defined by the condition at which the chemical potentials of both components are equal. The metastable states of the first order transitions are limited by spinodal, also called the limit of stability. The extremum of a binodal curve in temperature coincides with the extremum of a spinodal curve and the extremum is called a critical point. The critical point is a common point of a binodal and a spinodal, that is why the parameters of the critical point can be determined from the following equations

$$\left(\frac{\partial P}{\partial \rho}\right)_T = 0, \qquad \left(\frac{\partial^2 P}{\partial \rho^2}\right)_T = 0.$$

Since the isothermal compressibility is defined as $\rho^{-1}(\partial\rho/\partial P)_T$, the compressibility diverges as the critical point is approached.

For fluids, the critical point terminates the coexistence curve between two fluid phases, usually vapor and liquid. For supercooled water - the liquid-liquid critical point scenario expects the coexistence curve between a low-density and a high-density liquid phase terminated by the critical point. Beyond the critical point, the difference between the two phases disappears and fluid becomes homogeneous. It means that it is possible to convert one phase into another one continuously without crossing the

phase equilibrium line.

The coexistence curve terminates in the critical point, it means the first derivatives of the free energy, i.e. molar volume and molar entropy, are also continuous, but the second derivatives (molar heat capacity, isothermal compressibility and thermal expansivity) are discontinuous. The phase transition at the critical point is classified as a second-order phase transition.

2.1 Classical (mean field) behavior

The general feature of the second-order phase transitions was discovered by Landau [63, 34]: a new element of symmetry appears at the transition point. To describe the second-order phase transition, Landau introduced a new parameter, which describes the higher symmetry of the system - order parameter φ. The parameter is equal to zero in the non-ordered phase and has a finite value in the ordered phase. The parameter is zero in the critical point. For example, in a ferromagnet, the order parameter is the magnetic moment per unit volume. It is zero in the paramagnetic state since the individual magnetic moments in the solid may point in any random direction, and as the temperature is lowered below the temperature of the phase transition, the magnetization (or the macroscopic magnetic moment per unit volume) grows. As the order parameter for the liquid-vapor phase transition, one can consider the difference in the densities of the liquid and gas phases.

The definition of the order parameter depends on the physical nature of the phase transition. But the concept of an order parameter is possible to be used to get some qualitative and quantitative features of a system behavior in the vicinity of the critical

point. Since the order parameter grows continuously from zero at the transition temperature, Landau suggested that an expansion of free energy $A(T, V, ...)$ in the Taylor expansion in the order parameter φ would tell us about the behavior near the transition. One can write:

$$A(\varphi) = A_0 + V(a\varphi^2/2 + b\varphi^4/4 + ...), \tag{2.1.1}$$

where V is volume of the system [34]. It is supposed the equation is independent of the transformation $\varphi \to -\varphi$. The equilibrium value of φ_0 can be obtained from the condition

$$\frac{\partial A(\varphi)}{\partial \varphi} = 0. \tag{2.1.2}$$

The coefficients a, b in Eq. (2.1.1) are functions of temperature and pressure. From Eq. (2.1.2) follows $a\varphi_0 + b\varphi_0^3 = 0$ and there are three possible roots of this equation:

$$\varphi_0 = \pm(-a/b)^{1/2}, \qquad \varphi_0 = 0. \tag{2.1.3}$$

If we define

$$a = \alpha\tau, \qquad \tau = \frac{T - T_c}{T_c}, \qquad \alpha > 0, \tag{2.1.4}$$

then the condition, that the order parameter at the critical point equals zero, is met. Below the critical point, there are three solutions of Eq. $a\varphi_0 + b\varphi_0^3 = 0$. Only one solution is above the critical point. We can see an analogy with the solutions of the Van der Waals equation, where also three solutions exist below the critical point of fluids (the middle one is unstable), and only one solution exists above the critical point.

Now it is reasonable to introduce a generalized external field h and to add the term $\Delta A = -Vh\varphi$ to free energy A [34]. From Eq. (2.1.2) we get

$$a\varphi_0 + b\varphi_0^3 = h. \tag{2.1.5}$$

If h is not equal to zero, $\varphi_0 = 0$ cannot be the root of Eq. (2.1.5), it means, if $h \neq 0$ then the order parameter is different from zero for arbitrary V and T. The second-order phase transition does not exist in this case.

One can define generalized susceptibility as

$$\chi = \frac{\partial \varphi_0}{\partial h}. \tag{2.1.6}$$

Eq. (2.1.6) yields $a\chi + 3b\varphi_0^2\chi = 0$, and finally χ could be stated as

$$\chi = \frac{1}{a + 3b\varphi_0^2}. \tag{2.1.7}$$

2.2 Ising model

The Ising model is originally the simplest model of ferromagnetism in statistical mechanics. The model consists of a set of magnetic spins arranged on a regular square lattice. Each spin can be in one of two states, called e.g. 'up' and 'down'. Energy of the system is determined by the sum of elementary interactions between a spin and its neighbors on the lattice. The general number of possible configurations of the system of spins $[\sigma]$ is equal to 2^N, where N is the number of nodes. It is reasonable to assign a variable $\sigma_{\mathbf{x}}$ with two possible values ± 1 to the lattice node $\mathbf{x}$, where $+1$ represents the spin "up", -1 the spin "down". Energy

$$H[\sigma] = \sum_{\mathbf{x}\mathbf{x}'} I(\mathbf{x}\text{-}\mathbf{x}')\sigma_{\mathbf{x}}\sigma_{\mathbf{x}'} - h\sum_{\mathbf{x}} \sigma_{\mathbf{x}}$$

is assigned for each configuration $[\sigma]$. Only the case of the nearest neighbor interactions is usually studied. In this case $I(\mathbf{x}) = 0$ for $\mathbf{x} \neq a$, where a is a base vector of the lattice.

The one-dimensional Ising model does not yield any phase transition. It was solved by Ising (1925) himself. The two-dimensional square lattice Ising model is much more difficult. An analytic description was given by Lars Onsager [64]. The three-dimensional Ising model can be solved only approximately.

The Ising model is a model of ferromagnets. The Ising model can be reinterpreted as a statistical model for the motion of atoms. Each node of the lattice either contains an atom or it doesn't. The model is called the lattice gas model. Each node of the lattice has an occupation number $n(\mathbf{x})$ equal to 0 or 1. The transformation $\sigma(\mathbf{x}) = 2n(\mathbf{x}) - 1$ leads to the Ising model of ferromagnetism. It means both models describe the same system, but using different variables. One of the most important results of the study of the phase transitions is the discovery that the thermodynamic system behavior in the vicinity of a critical point is universal [65].

There is a hypothesis that all fluids exhibit Ising-like asymptotic critical behavior. It is possible to characterize the thermodynamic behavior of fluids near the critical point by scaling laws with universal critical exponents and universal scaling functions of 3D Ising system. One of the problems of lattice gas is that the model is symmetric (in terms of order parameter), while phase transition of real fluids is not symmetric. Critical behavior of fluids is universal in terms of so-called scaling fields. Scaling fields are analytic functions of the physical fields.

It is commonly accepted, that the critical behavior of an Ising-like system can be described by two independent scaling fields: h_1 (so-called "strong" scaling field or "ordering" field) and h_2 (so-called "weak" scaling field or "thermal" field). Asymptotically near the critical point, a dependent scaling field h_3 has the form [66]:

$$h_3(h_1, h_2) \approx |h_2|^{2-\alpha} f^{\pm}\left(\frac{h_1}{|h_2|^{2-\alpha-\beta}}\right), \tag{2.2.1}$$

Table 2.1: Universal critical power laws

Critical power law	Thermodynamic path
$\phi_1 \approx \pm B_0 \lvert h_2 \rvert^{\beta}$	$h_2 < 0, \phi_1 = \pm\phi_{cxc}$
$\phi_2 \approx \frac{A_0^{\pm}}{1-\alpha} h_2 \lvert h_2 \rvert^{-\alpha}$	$\phi_1 = 0$
$\chi_1 \approx \Gamma_0^{+} \lvert h_2 \rvert^{-\gamma}$	$h_2 > 0, \phi_1 = 0$
$\chi_1 \approx \Gamma_0^{-} \lvert h_2 \rvert^{-\gamma}$	$h_2 < 0, \phi_1 = \pm\phi_{cxc}$
$\chi_2 \approx A_0^{+} \lvert h_2 \rvert^{-\alpha}$	$h_2 > 0, \phi_1 = 0$
$\chi_2 \approx A_0^{-} \lvert h_2 \rvert^{-\alpha}$	$h_2 < 0, \phi_1 = \pm\phi_{cxc}$
$\chi_{12} \approx \beta B_0 \frac{\lvert h_2 \rvert^{\beta}}{h_2}$	$h_2 < 0, \phi_1 = \pm\phi_{cxc}$

where $f^{\pm}$ is a universal scaling function except for two system-dependent amplitudes. The subscripts $\pm$ refer to $h_2 > 0$ and $h_2 < 0$, respectively. The exponents α and β are the universal critical exponents [67]. At the critical point $h_1 = h_2 = h_3$.

Now one can define two scaling densities, ϕ_1 is the "order parameter" and ϕ_2 is the "thermal" density [61]:

$$\phi_1 = \left(\frac{\partial h_3}{\partial h_1}\right)_{h_2}, \qquad \phi_2 = \left(\frac{\partial h_3}{\partial h_2}\right)_{h_1}. \tag{2.2.2}$$

The second derivatives of h_3 define three susceptibilities:

$$\chi_1 = \left(\frac{\partial \phi_1}{\partial h_1}\right)_{h_2}, \qquad \chi_2 = \left(\frac{\partial \phi_2}{\partial h_2}\right)_{h_1}, \qquad \chi_{12} = \left(\frac{\partial \phi_1}{\partial h_2}\right)_{h_1} = \left(\frac{\partial \phi_2}{\partial h_1}\right)_{h_2}. \tag{2.2.3}$$

The susceptibility χ_1 is called "strong", χ_2 is "weak" and χ_{12} is "cross" susceptibility.

The scaling laws result in asymptotic power laws along the path $\phi_1 = 0$ for $h_2 > 0$ and $h_2 < 0$ and along the two sides of the phase boundary $\phi_1 = \pm\phi_{cxc}$ for $h_2 < 0$ (Table 2.1). The universal critical exponents are related by

$$\gamma = 2 - \alpha - 2\beta \qquad 3\nu = 2 - \alpha \qquad \gamma = (2 - \eta)\nu. \tag{2.2.4}$$

Table 2.2: Comparison of critical exponents

Critical exponent	Source [71]	Calculated value [69]	Experimental value [67]	Classical value
α	0.110	0.110 ± 0.003	0.113 ± 0.009	0
β	0.325	0.326 ± 0.002	$0.3245 \pm 0.0.0105$	1/2
γ	1.24	1.239 ± 0.002	1.238 ± 0.012	1
δ	4.815	4.801 ± 0.017	4.815 ± 0.089	3
ν	0.63	0.630 ± 0.002	0.629 ± 0.003	1/2
η	0.0318	0.033 ± 0.004	0.032 ± 0.013	0

The Ising critical amplitude $\Gamma_0^{\pm}$ is related to B_0 and $A_0^{\pm}$ through universal ratios [68]

$$\frac{\alpha\Gamma_0^+ A_0^+}{B_0^2} = 0.0581, \qquad \frac{\Gamma_0^+}{\Gamma_0^-} = 4.8, \qquad \frac{A_0^+}{A_0^-} = 0.523.$$

The definition of the critical exponents is in Table 2.1. Characteristic of exponents δ and η is given e.g. in [67]. The critical exponents for the 3D Ising model are calculated from high-temperature expansions, the Monte Carlo simulation and perturbative field-theoretical methods [69]. The critical exponents are also measured in various experiments, e.g. from light-scattering data in an aqueous electrolyte solution [67, 70]. The comparison of calculated and measured critical exponents is in Table 2.2. Data from [71] are used in this paper.

One can define

$$z = \frac{h_1}{|h_2|^{2-\alpha-\beta}} = \frac{h_1}{|h_2|^{\beta+\gamma}}. \tag{2.2.5}$$

We have used the relation (2.2.4) between the universal critical exponents in the definition (2.2.5). Eq. (2.2.1) now can be written in the form [71]

$$h_3(h_1, h_2) \approx h_2^2 |h_2|^{-\alpha} f(z). \tag{2.2.6}$$

The scaling "densities" ϕ_1 and ϕ_2 are then

$$\phi_1 = -|h_2|^{\beta} f'(z), \tag{2.2.7}$$

$$\phi_2 = -h_2|h_2|^{-\alpha}\psi(z), \tag{2.2.8}$$

where $f'(z) = df/dz$ and $\psi(z) = (2-\alpha)f(z) - (\beta+\gamma)zf'(z)$.
Susceptibilities defined in Eq. (2.2.3) are now

$$\chi_1 = -|h_2|^{-\gamma}f''(z), \tag{2.2.9}$$

$$\chi_2 = -|h_2|^{-\alpha}\psi(z), \tag{2.2.10}$$

$$\chi_{12} = \chi_{21} = -|h_2|^{-\beta-1}[\beta f'(z) - (\beta+\gamma)f''(z)], \tag{2.2.11}$$

with $\Psi(z) = (1-\alpha)\psi(z) - (\beta+\gamma)z\psi'(z)$ and where $f''(z) = d^2f/dz^2$ and
$\psi'(z) = d\psi/dz$.

Near the critical point the scaling fields h_1 and h_2 are linear functions of the physical fields. The physical fields for one component fluid are pressure P, temperature T and chemical potential μ. For one-component fluids, the critical point can be specified by the critical temperature T_c, critical density ϱ_c and critical pressure P_c. One can define dimensionless thermodynamic properties as follows:

$$\begin{gathered}
\hat{T} = \frac{T}{T_\mathrm{c}}, \qquad \hat{\rho} = \frac{\rho}{\rho_\mathrm{c}}, \qquad \hat{P} = \frac{P}{\rho_\mathrm{c}RT_\mathrm{c}}, \\
\hat{\mu} = \frac{\mu}{RT_\mathrm{c}}, \qquad \hat{A} = \frac{A}{RT_\mathrm{c}}, \qquad \hat{S} = \frac{S}{R}, \qquad \hat{C_P} = \frac{C_P}{R}, \\
\hat{C_V} = \frac{C_V}{R}, \qquad \hat{\kappa}_T = \rho_\mathrm{c}RT_\mathrm{c}\kappa_T, \qquad \hat{\alpha}_P = T_\mathrm{c}\alpha_P, \\
\hat{\chi} = \left(\frac{\partial^2\hat{P}}{\partial\hat{\mu}^2}\right)_{\hat{T}} = \left(\frac{\partial\hat{\rho}}{\partial\hat{\mu}}\right)_{\hat{T}} = \hat{\rho}^2\hat{\kappa}_{\hat{T}},
\end{gathered} \tag{2.2.12}$$

where S is the molar entropy, C_V is the isochoric molar heat capacity, ρ is the molar density, C_P is the isobaric molar heat capacity, A is the molar Helmholtz energy, $\hat{\chi}$ is the isothermal susceptibility, $\hat{\alpha}_P$ is the thermal expansivity, R is the molar gas constant. It is common to define the physical fields to be zero at the critical point:

$$\Delta\hat{T} = \frac{T - T_c}{T_c}, \qquad \Delta\hat{\rho} = \frac{\rho - \rho_c}{\rho_c}, \qquad \Delta\hat{P} = \frac{P - P_c}{\rho_c R T_c}, \tag{2.2.13}$$
$$\Delta\hat{\mu} = \frac{\mu - \mu_c}{\mu_c}, \qquad \Delta\hat{S} = \frac{S - S_c}{S_c}, \qquad \Delta\hat{V} = \frac{V - V_c}{V_c},$$

where V is molar volume.

Chapter 3

Parametric equation of state

It is impossible to find the function h_3 given by the formula (2.2.1) as an explicit function of h_1 and h_2 [72]. Schofield [73, 74] suggested a parametric representation of the thermodynamic functions in the neighborhood of the critical point. The variables r and θ were used, where the parameter r represents a "distance" from the critical point and the angular parameter θ describes a distance around lines of constant r from one side of the coexistence curve to the other. If any thermodynamic property exhibits a singularity in the critical point by a scaling law with a critical exponent, the critical behavior is characterized by variable r. It means, that one can describe the singular behavior using $\psi(r,\theta)$, asymptotically $\Psi(r,\theta) = r^{-x}\psi(\theta)$, where $\psi(\theta)$ is an analytic function and x is a critical exponent [74]. Consequently,

$$h_1 = r^{2-\alpha-\beta}H(\theta), \qquad h_2 = rT(\theta). \tag{3.0.1}$$

Here the functions $H(\theta)$ and $T(\theta)$ are analytic functions of θ. One can use parametric variables in Eq. (2.2.1), and, therefore, the order parameter ϕ_1 can be expressed as

$$\phi_1 = r^{\beta}M(\theta). \tag{3.0.2}$$

$M(\theta)$ in Eq. (3.0.2) is an analytical function of θ.

Schofiled [73] suggested the following forms of the equations

$$h_1 = ar^{2-\alpha-\beta}\theta(1-\theta^2), \qquad h_2 = r(1-b^2\theta^2). \tag{3.0.3}$$

It was found the linear dependence of

$$M(\theta) = k\theta \tag{3.0.4}$$

gives a good experimental data approximation. This choice gives the attractively simple equation and is called the "linear model".

In Eq. (3.0.3), $b^2 = (\gamma - 2\beta)/\gamma(1-2\beta)$ is a universal constant, and a and k are system-dependent constants related to the critical amplitudes [72].

The "cubic model " is given using the approximation [75]

$$M(\theta) = k\theta(1 + c\theta^2), \tag{3.0.5}$$

where c is a universal constant.

3.1 Linear model

The linear model with only an order parameter ϕ_1 is discussed in this chapter,

$$\phi_1 = kr^{\beta}\theta. \tag{3.1.1}$$

The variable θ varies from $\theta = 0$ at $\phi_1 = 0$, $h_2 > 0$, to $\theta = \pm 1/b$ at $h_2 = 0$ and to $\theta = \pm 1$ at $\phi_1 = \pm\phi_{cxc}$ at negative h_2. The linear model does not describe the two phase region for $|\theta| > 1$.

The singular part of the thermodynamic potential is given by [72]

$$h_3 = -akr^{2-\alpha}[f(\theta) - \theta^2(1-\theta^2)] - \frac{ak}{6}r^2(1-b^2\theta^2)^2. \tag{3.1.2}$$

The equation is modified by adding an analytical term. Then the model is fully consistent with the results of the renormalization group theory [71]. In Eq. (3.1.2) $f(\theta)$ is the known function of θ:

$$f(\theta) = f_0 + f_2\theta^2 + f_4\theta^4. \tag{3.1.3}$$

The constants f_0, f_2, f_4 can be expressed in the form

$$f_0 = \frac{\beta(\delta-3) - b^2\alpha\gamma}{2b^4(2-\alpha)(1-\alpha)\alpha}, \tag{3.1.4}$$

$$f_2 = \frac{\beta(\delta-3) - b^2\alpha(1-2\beta)}{2b^2(1-\alpha)\alpha}, \tag{3.1.5}$$

$$f_4 = -\frac{1-2\beta}{2\alpha}. \tag{3.1.6}$$

By differentiation of Eq. (3.1.2) one gets [71]

$$\phi_2 = akr^{1-\alpha}s(\theta) - \frac{akr(1-b^2\theta^2)}{3}, \tag{3.1.7}$$

where

$$s(\theta) = s_0 + s_2\theta^2. \tag{3.1.8}$$

The constants s_0, s_2 can be expressed in the form

$$s_0 = -(2-\alpha)f_0, \tag{3.1.9}$$

$$s_2 = -(2-\alpha)b^2(1-2\beta)f_0 - \gamma f_2. \tag{3.1.10}$$

Using the definition of susceptibilities, one can write Eq. (2.2.3)

$$\chi_1 = \frac{k}{a}r^{-\gamma}c_1(\theta) \tag{3.1.11}$$

$$\chi_2 = akr^{-\alpha}c_2(\theta) - \frac{ak}{3}, \tag{3.1.12}$$

$$\chi_{12} = kr^{\beta-1}c_{12}(\theta). \tag{3.1.13}$$

In the equations

$$c_1(\theta) = \frac{1 - b^2\theta^2(1-2\beta)}{c_0(\theta)} \tag{3.1.14}$$

$$c_2(\theta) = \frac{(1-\alpha)(1-3\theta^2)s(\theta) - 2s_2\beta\delta\theta^2(1-\theta^2)}{c_0(\theta)} \tag{3.1.15}$$

$$c_{12}(\theta) = \frac{\beta\theta(1-\delta-\theta^2(3-\delta)}{c_0(\theta)} \tag{3.1.16}$$

$$c_0(\theta) = (1-3\theta^2)(1-b^2\theta^2) + 2\beta\delta b^2\theta^2(1-\theta^2). \tag{3.1.17}$$

3.2 Critical exponents and Linear model

The linear model is based on the linearity of the function of $M(\theta)$ (see Eq. 3.0.5). The order parameter ϕ_1 is obtained by a differentiation of Eq. (3.1.2) (see the definition of ϕ_1 in Eq. (2.2.2)). The comparison of the result of the differentiation with the form of the linear model in Eq.(3.0.2) yields

$$M(\theta) = -\frac{2b^2(2-\alpha)\theta(f(\theta) - \theta^2 + \theta^4) + (1-b^2\theta^2)(f'(\theta) - 2\theta + 4\theta^3)}{2b^2(\beta+\gamma)\theta^2(1-\theta^2) + (1-3\theta^2)(1-b^2\theta^2)}. \tag{3.2.1}$$

The function $M(\theta)$ must be very close to the linear function θ [74]. The function $M(\theta)$ is a rational function. Constants of the rational function are calculated from the critical-exponent values.

Sengers and Shanks have published a review of experimental critical-exponent values for fluids [67] recently. Pelissetto and Vicari have reviewed the theoretical values of the critical-exponent values [69] - see Table 2.2. We have tested the influence of different sets of exponents on the linearity of the function $M(\theta)$. We have selected

Table 3.1: Coefficients of the linear parametric equation

Set	α	β	γ	δ	b^2	f_0	f_2	f_4
1 [71]	0.110	0.325	1.240	4.815	1.359447	−0.59137	2.019449	−1.59091
2 [69]	0.107	0.324	1.237	4.784	1.352704	−0.60273	2.038911	−1.64486
3 [69]	0.110	0.326	1.239	4.801	1.361406	−0.58549	2.007071	−1.58182
4 [69]	0.113	0.328	1.241	4.818	1.370332	−0.56895	1.976839	−1.52212
5 [67]	0.104	0.314	1.226	4.731	1.311196	−0.61951	2.016681	−1.78846
6 [67]	0.113	0.3245	1.238	4.815	1.355463	−0.57461	1.969705	−1.5531
7 [67]	0.122	0.335	1.250	4.904	1.406061	−0.53233	1.929573	−1.35246

the values presented in [71], and the lower limit, the middle value and the upper limit for experimental [67] and theoretical [69] values of the critical exponents. For each set of exponents we have calculated b^2, f_0, f_2 and f_4. The results are in Table 3.1. One can see the differences from linearity are quite significant for some of the sets of the exponents. If the linear model is used with the set of critical exponent, the test of linearity of function $M(\theta)$ is useful. If the difference of $M(\theta)$ from the linear function is identified, the coefficients f_0, f_2 and f_4 should be re-calculated.

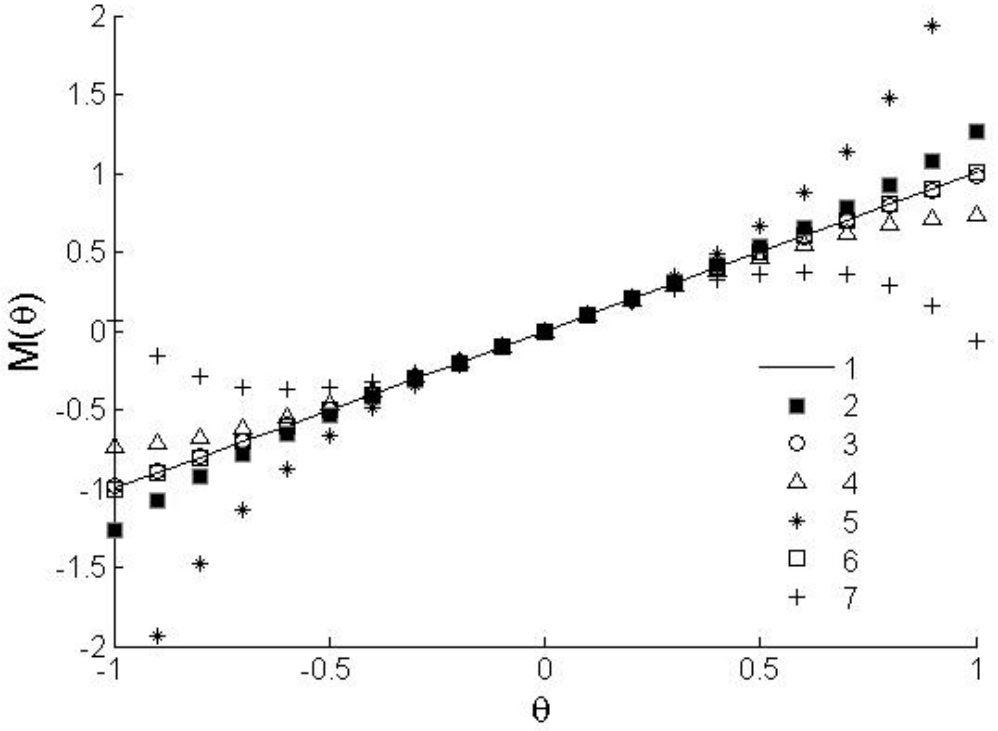

Figure 3.1: Function $M(\theta)$ for the sets of critical exponents. Numbering according to Table 3.1.

Chapter 4

Simple, revised and complete scaling

The simplest model of the phase transition of fluids is the lattice gas. For the lattice gas the scaling fields are [72]:

$$h_1 = \Delta\hat{\mu}, \qquad h_2 = \Delta\hat{T}, \qquad h_3 = \Delta\hat{P}. \tag{4.0.1}$$

The Ising model gives equations describing the behavior of thermodynamic properties asymptotically near the critical point. The concept of background functions was introduced to describe the behavior of the properties in a large distance from the critical point. If X is a property, one can write $X = X_{\rm cr} + X_{\rm b}$, where $X_{\rm cr}$ indicates a critical part of the thermodynamic property, that often shows some singular behavior at the critical point, and $X_{\rm b}$ represents some analytical, regular behavior of the background.

4.1 Simple and revised scaling

If $\Delta\hat{P}$ is a thermodynamic potential, one can write

$$d\Delta\hat{P} = \Delta\hat{\rho}d\hat{\mu} + \Delta(\hat{\rho}\hat{S})d\hat{T}. \tag{4.1.1}$$

Using Eq. (2.2.2) one gets

$$\phi_1 = \Delta\hat{\rho}, \qquad \phi_2 = \Delta(\hat{\rho}\hat{S}). \tag{4.1.2}$$

When the chemical potential is used as a fundamental thermodynamic potential instead of the pressure, we obtain

$$d\Delta\hat{\mu} = \Delta\hat{V}d\hat{P} - \Delta\hat{S}d\hat{T}. \tag{4.1.3}$$

In this case

$$\phi_1 = \Delta\hat{V}, \qquad \phi_2 = -\Delta\hat{S}. \tag{4.1.4}$$

$$\hat{C_P} = \hat{T}\left(\frac{\partial\hat{S}}{\partial\hat{T}}\right)_P = -\hat{T}\chi_2, \tag{4.1.5}$$

$$\hat{\kappa_T} = -\frac{1}{\hat{V}}\left(\frac{\partial\hat{V}}{\partial\hat{P}}\right)_T = -\frac{1}{\hat{V}}\chi_1, \tag{4.1.6}$$

$$\hat{\alpha_V} = \frac{1}{\hat{V}}\left(\frac{\partial\hat{V}}{\partial\hat{T}}\right)_P = \frac{1}{\hat{V}}\chi_{12}. \tag{4.1.7}$$

In the simple-scaling approximation (lattice gas model), the two-phase boundary is symmetric. According to some theoretical models, the coexistence-curve diameter ρ_{d} as function of temperature shows a singular behavior [72]. For this reason a revised-scaling approximation has been proposed [76] with the scaling fields

$$h_1 = \Delta\hat{\mu}, \qquad h_2 = \Delta\hat{T} + b_2\Delta\hat{\mu}, \qquad h_3 = \Delta\hat{P}. \tag{4.1.8}$$

In this case one gets

$$\Delta\hat{\rho} = \phi_1 + b_2\phi_2, \qquad \Delta(\hat{\rho}\hat{S}) = \phi_2. \tag{4.1.9}$$

When the chemical potential is used as a fundamental thermodynamic potential instead of the pressure, one obtains the following relation for various thermodynamic properties:

$$d\Delta\hat{\mu} = \Delta\hat{V}d\hat{P} - \Delta\hat{S}d\hat{T}, \tag{4.1.10}$$

$$h_3 = \Delta\hat{\mu}, \qquad h_1 = \Delta\hat{P}, \qquad h_2 = \Delta\hat{T} + b_2\Delta\hat{P}, \tag{4.1.11}$$

$$\Delta\hat{V} = \phi_1 + b_2\phi_2, \qquad \Delta\hat{S} = -\phi_2, \tag{4.1.12}$$

$$\hat{C_P} = \hat{T}\left(\frac{\partial\hat{S}}{\partial\hat{T}}\right)_P = -\hat{T}\chi_2, \tag{4.1.13}$$

$$\hat{\kappa_T} = -\frac{1}{\hat{V}}\left(\frac{\partial\hat{V}}{\partial\hat{P}}\right)_T = -\frac{1}{\hat{V}}(\chi_1 + 2b_2\chi_{12} + b_2^2\chi_2^2), \tag{4.1.14}$$

$$\hat{\alpha_V} = \frac{1}{\hat{V}}\left(\frac{\partial\hat{V}}{\partial\hat{T}}\right)_P = \frac{1}{\hat{V}}(\chi_{12} + b_2\chi_2). \tag{4.1.15}$$

4.2 Complete scaling

For asymmetric fluids, Fisher and coworkers [77, 78, 79] pointed out the necessity to relate the scaling fields to all physical fields [80, 81]. For one-component fluids, one can write (in linear approximation) [72, 82, 83]:

$$\begin{aligned} h_1 &= a_1\Delta\hat{\mu} + a_2\Delta\hat{T} + a_3\Delta\hat{P}, \\ h_2 &= b_1\Delta\hat{T} + b_2\Delta\hat{\mu} + b_3\Delta\hat{P}, \\ h_3 &= c_1\Delta\hat{P} + c_2\Delta\hat{\mu} + c_3\Delta\hat{T}. \end{aligned} \tag{4.2.1}$$

The dependent field h_3 is a homogeneous function of h_1 and h_2 (Eq. (2.2.1)). If the phase-coexistence locus exhibits a strong curvature, the linear approximation may be insufficient and it is appropriate to include [84, 61] a nonlinear term. The physical properties are given by the thermodynamic relations

$$\hat{\rho} = \left(\frac{\partial\hat{P}}{\partial\hat{\mu}}\right)_{\hat{T}} \tag{4.2.2}$$

$$\hat{\rho}\hat{S} = \left(\frac{\partial\hat{P}}{\partial\hat{T}}\right)_{\hat{\mu}}. \tag{4.2.3}$$

It is possible to use the thermodynamic relations to find a link between physical and scaling densities. First, differentiating the h_3 with respect to $\hat{\mu}$, one gets

$$\left(\frac{\partial h_3}{\partial \hat{\mu}}\right)_{\hat{T}} = c_1 \left(\frac{\partial \hat{P}}{\partial \hat{\mu}}\right)_{\hat{T}} + c_2 = c_1 \hat{\rho} + c_2. \tag{4.2.4}$$

Second, supposing $h_3 = h_3(h_1, h_2)$, one gets

$$\left(\frac{\partial h_3}{\partial \hat{\mu}}\right)_{\hat{T}} = \left(\frac{\partial h_3}{\partial h_1}\right)_{h_2} \left(\frac{\partial h_1}{\partial \hat{\mu}}\right)_{\hat{T}} + \left(\frac{\partial h_3}{\partial h_2}\right)_{h_1} \left(\frac{\partial h_2}{\partial \hat{\mu}}\right)_{\hat{T}},$$

$$\left(\frac{\partial h_3}{\partial \hat{\mu}}\right)_{\hat{T}} = \phi_1 \left(a_1 + a_3 \left(\frac{\partial \hat{P}}{\partial \hat{\mu}}\right)_{\hat{T}}\right) + \phi_2 \left(b_1 + b_3 \left(\frac{\partial \hat{P}}{\partial \hat{\mu}}\right)_{\hat{T}}\right),$$

$$\left(\frac{\partial h_3}{\partial \hat{\mu}}\right)_{\hat{T}} = a_1\phi_1 + a_3\phi_1\hat{\rho} + b_2\phi_2 + b_3\phi_2\hat{\rho}. \tag{4.2.5}$$

Comparing Eqs (4.2.4) and (4.2.5), one gets

$$\hat{\rho} = \frac{a_1\phi_1 + b_2\phi_2 - c_2}{c_1 - a_3\phi_1 - b_3\phi_2}. \tag{4.2.6}$$

When the derivative of h_3 with respect to $\hat{T}$ is calculated, one gets

$$\hat{\rho}\hat{S} = \frac{a_2\phi_1 + b_1\phi_2 - c_3}{c_1 - a_3\phi_1 - b_3\phi_2}.$$

When Eq. (4.2.6) is used, one can write

$$\hat{S} = \frac{a_2\phi_1 + b_1\phi_2 - c_3}{a_1\phi_1 + b_2\phi_2 - c_2}. \tag{4.2.7}$$

Because at the critical point $\hat{\rho} = 1$, $\hat{S} = S_{\mathrm{c}}/R = \hat{S}_{\mathrm{c}}$, $\phi_1 = 0$ and $\phi_2 = 0$, must be

$$\frac{-c_2}{c_1} = 1, \qquad \frac{-c_3}{c_1} = \hat{S}_{\mathrm{c}},$$

and it is possible to select $c_1 = 1$, $c_2 = -1$ and $c_3 = -\hat{S}_{\mathrm{c}}$. Eqs. (4.2.6) and (4.2.7) now change to the form

$$\hat{\rho} = \frac{a_1\phi_1 + b_2\phi_2 + 1}{1 - a_3\phi_1 - b_3\phi_2}, \tag{4.2.8}$$

$$\hat{S} = \frac{a_2\phi_1 + b_1\phi_2 + \hat{S}_{\rm c}}{a_1\phi_1 + b_2\phi_2 + 1}. \tag{4.2.9}$$

While the scaling fields are defined as linear combinations of the physical fields, the physical densities are non-linear combinations of the scaling densities.

At the critical point, using Eqs. (4.2.2, 4.2.3) we obtain

$$\hat{\rho}_{\rm c}\hat{S}_{\rm c} = \left(\frac{\partial\hat{P}}{\partial\hat{T}}\right)_{\hat{\mu},{\rm c}} = \hat{S}_{\rm c}. \tag{4.2.10}$$

Applying the definition of h_1 (Eq. (4.2.1)), along the path for $h_1 = 0$ asymptotically close to the critical point, one gets

$$a_1\left(\frac{\partial\hat{\mu}}{\partial\hat{T}}\right)_{h_1=0,{\rm c}} + a_2 + a_3\left(\frac{\partial\hat{P}}{\partial\hat{T}}\right)_{h_1=0,{\rm c}} = 0. \tag{4.2.11}$$

On the contrary, from the thermodynamic relation $d\mu = -SdT + vdP$ follows, that at the critical point

$$\left(\frac{\partial\hat{\mu}}{\partial\hat{T}}\right)_{h_1=0,{\rm c}} + \hat{S}_{\rm c} - \left(\frac{\partial\hat{P}}{\partial\hat{T}}\right)_{h_1=0,{\rm c}} = 0. \tag{4.2.12}$$

From Eqs. (4.2.11), (4.2.12) one gets,

$$\left(\frac{\partial\hat{\mu}}{\partial\hat{T}}\right)_{h_1=0,{\rm c}} = -\frac{a_2}{a_1} - \frac{a_3}{a_1}\left(\frac{\partial\hat{P}}{\partial\hat{T}}\right)_{h_1=0,{\rm c}} = -\hat{S}_{\rm c} + \left(\frac{\partial\hat{P}}{\partial\hat{T}}\right)_{h_1=0,{\rm c}}. \tag{4.2.13}$$

Although the critical value of entropy can be arbitrarily chosen, a convenient choice will further simplify the scaling equations. Adopting

$$\hat{S}_{\rm c} = \left(\frac{\partial\hat{P}}{\partial\hat{T}}\right)_{h_1=0,{\rm c}}, \tag{4.2.14}$$

one obtains

$$\left(\frac{\partial\hat{\mu}}{\partial\hat{T}}\right)_{h_1=0,{\rm c}} = 0, \qquad a_2 = -a_3\hat{S}_{\rm c}. \tag{4.2.15}$$

It is possible to normalize the scaling fields such a $a_1 = 1$ and $b_1 = 1$ [72]. Hence, in complete scaling there are three system-dependent coefficients, namely a_3, b_2 and b_3. In the approximation, the scaling fields read

$$\begin{aligned} h_1 &= \Delta\hat{\mu} + a_3 \left(\Delta\hat{P} - \left(\frac{d\hat{P}}{d\hat{T}} \right)_{\text{cxc, c}} \Delta\hat{T} \right), \\ h_2 &= \Delta\hat{T} + b_2 \Delta\hat{\mu} + b_3 \Delta\hat{P}, \\ h_3 &= \Delta\hat{P} - \Delta\hat{\mu} + \left(\frac{d\hat{P}}{d\hat{T}} \right)_{\text{cxc, c}} \Delta\hat{T}. \end{aligned} \tag{4.2.16}$$

4.3 Scaled equation of state for supercooled water

Recently, the scaling theory was applied to the liquid-liquid critical point by Fuentevilla and Anisimov and a parametric equation of state was formulated [84, 61]. Here the scaling fields were assumed to be the following combinations of physical fields, the pressure P and the temperature T:

$$h_1 = a_1 \Delta\hat{P} + a_2 \Delta\hat{T} + a_3 \Delta\hat{P}^2, \tag{4.3.1}$$

$$h_2 = b_1 \Delta\hat{T} + b_2 \Delta\hat{P}, \tag{4.3.2}$$

A nonlinear term $a_3 \Delta\hat{P}^2$ was added to account for the strong curvature of the liquid-liquid transition line. Any two coefficients may be absorbed in the scaling function f, the coefficients $a_2 = 1$ and $b_2 = -1$ were adopted. The negative sign of b_2 indicates, that the liquid-liquid phase separation in supercooled water occurs with increasing pressure. Fuentevilla and Anisimov used the data obtained from Mishima *et al.* [1] and the data obtained through personal communication with Mishima. The data for

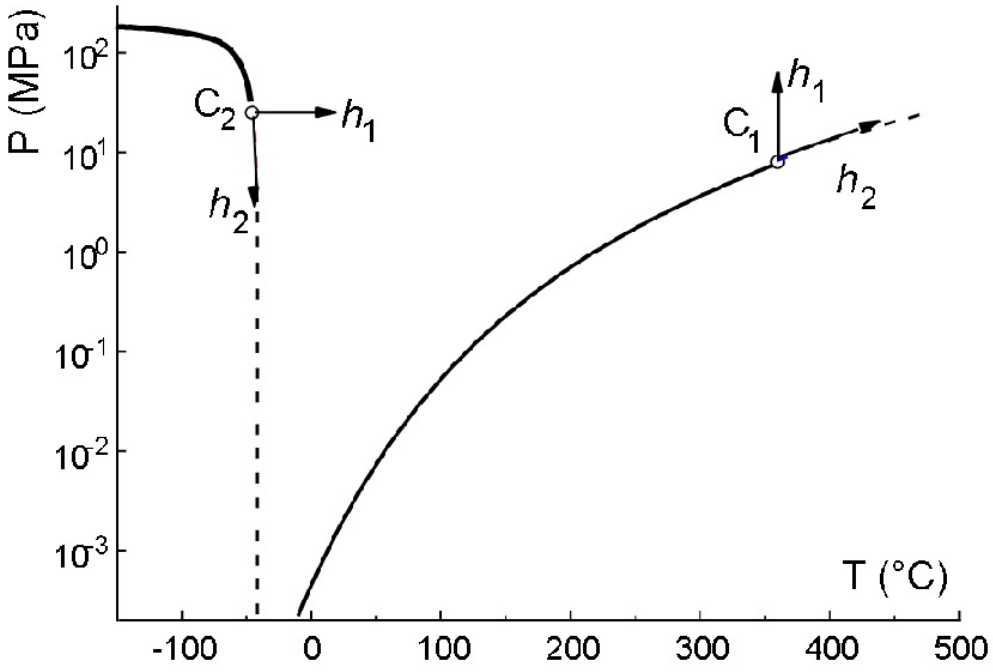

Figure 4.1: Phase diagram for water with vapor-liquid and liquid-liquid critical points.

the Widom line (an analytical continuation of the liquid-liquid transition curve) given by the relation $h_1 = 0$, were fitted by the polynomial expression:

$$T = \mathrm{A} + \mathrm{B}P + \mathrm{C}P^2 = 234.130 - 61.7594 \cdot 10^{-3}P - 952.784 \cdot 10^{-6}P^2. \tag{4.3.3}$$

In the equation the temperature T is in Kelvin and the pressure P in Pascal. The least squares method was used to determine coefficients A, B and C to fit the Mishima data.

In the model (Eqs. (4.3.1 and 4.3.2)) one gets

$$\phi_1 = \frac{b_1\Delta\hat{V} + b_1\Delta\hat{S}}{a_2b_2 - (a_1)_{\mathrm{eff}}b_1}, \tag{4.3.4}$$

$$\phi_2 = \frac{a_2\Delta\hat{V} + (a_1)_{\mathrm{eff}}\Delta\hat{S}}{(a_1)_{\mathrm{eff}}b_1 - a_2b_2}. \tag{4.3.5}$$

Table 4.1: Parameters of the Fuentevilla and Anisimov model

a_1	b_1	a_3	P_c	T_c	a	k
0.0078	0.0078	0.062	27 MPa	232 K	0.47	0.47

In the Fuentevilla - Anisimov model, the critical parts of the dimensionless isobaric heat capacity, isothermal compressibility, and thermal expansivity [84, 61] are:

$$\hat{C}_{P,\mathrm{cr}} = \hat{T}\left(\frac{\partial \hat{S}}{\partial \hat{T}}\right)_{\hat{P}} - \hat{C}_{P,\mathrm{b}} = -\hat{T}(a_2^2\chi_1 + 2a_2b_1\chi_{12} + b_1^2\chi_2), \tag{4.3.6}$$

$$\hat{\kappa}_{T,\mathrm{cr}} = -\frac{1}{\hat{V}}\left(\frac{\partial \hat{V}}{\partial \hat{P}}\right)_{\hat{T}} - \hat{\kappa}_{T,\mathrm{b}} = -\frac{1}{\hat{V}}((a_1)_{\mathrm{eff}}^2\chi_1 + 2(a_1)_{\mathrm{eff}}b_2\chi_{12} + b_2^2\chi_2), \tag{4.3.7}$$

$$\hat{\alpha}_{P,\mathrm{cr}} = \frac{1}{\hat{V}}\left(\frac{\partial \hat{V}}{\partial \hat{T}}\right)_{\hat{P}} - \hat{\alpha}_{P,\mathrm{b}} = -\frac{1}{\hat{V}}((a_1)_{\mathrm{eff}}a_2\chi_1 + [(a_1)_{\mathrm{eff}}b_1 + a_2b_2]\chi_{12} + b_1b_2\chi_2). \tag{4.3.8}$$

The subscript "b" indicates the property background. Fuentevilla and Anisimov used the linear model (Eqs. (4.2.2, 4.2.3)) for the description of the thermodynamic properties of supercooled water. The location of the critical point (T_c and P_c) and the system-dependent amplitudes (a, k) were found from the experimental heat capacity data [7]. The parameters $a_1 = b_1$ and a_3 are based on an estimate of the liquid - liquid phase transition curve (Eq. 4.3.3). The parameters of the model are in Table 4.1.

Mishima [17] measured the volume of water at about $200-275$ K and $40-400$ MPa. He used the model of Fuentevilla and Anisimov. The data for the Widom line given by relation $h_1 = 0$ were fitted by another polynomial expression $P(T)$ (MPa):

$$P = \mathrm{A} + \mathrm{B}T + \mathrm{C}T^2 = -1504 + 19.49T - 0.05613T^2. \tag{4.3.9}$$

Table 4.2: Parameters of the Mishima model

a_1	a_2	a	b	P_c	T_c	V_c	k
12.99	28.44	1	1	40 MPa	225 K	1.04 cm^3/g	3.9

Mishima used the model

$$h_1 = \Delta\hat{P} + a_1\Delta\hat{T} + a_2\Delta\hat{T}^2, \tag{4.3.10}$$

$$h_2 = \Delta\hat{T} - b_1\Delta\hat{P}. \tag{4.3.11}$$

For dimensionless isobaric heat capacity, isothermal compressibility, and thermal expansivity one gets [17]:

$$\hat{V}_{\text{cr}} == -\phi_1 + b_1\phi_2, \tag{4.3.12}$$

$$\hat{C}_{P,\text{cr}} == \hat{T}(w^2\chi_1 + 2w\chi_{12} + \chi_2), \tag{4.3.13}$$

$$\hat{\kappa}_{T,\text{cr}} = -\frac{1}{\hat{V}}((-\chi_1 + 2b_1\chi_{12} - b_1^2\chi_2), \tag{4.3.14}$$

$$\hat{\alpha}_{P,\text{cr}} = \frac{1}{\hat{V}}(-w\chi_1 - (1 - b_1w)\chi_{12} + b_1\chi_2), \tag{4.3.15}$$

where

$$w = a_1 + 2a_2\Delta\hat{T}. \tag{4.3.16}$$

The parameters of the model are in Table 4.2.

Chapter 5

Crossover equation and the vapor pressure of supercooled water

Vapor-pressure equations are often used in atmospheric applications. Also properties of water at temperatures below the triple point are needed for calculating the saturation pressure in clouds, because clouds are often composed of deeply supercooled water. There are many equations used in meteorology that describe the saturation pressure of H_2O also below the triple point. Most of them are based on the Clapeyron equation, because experimental data are not of high quality. Measurements are restricted to temperatures above approximately 233 K, which is the limit of homogenous nucleation. But meteorologists are interested in the vapor pressure of water at temperatures down to 160 K. Minimum temperatures in the Antarctic winter stratosphere could be below 175 K [85]. How does one predict vapor pressures of supercooled water below the limit of homogenous nucleation? Murphy and Koop [85] carried out an evaluation of many vapor-pressure equations. They used the knowledge of the isobaric heat capacity, C_P, above 233 K (where experimental data exist) and the asymptotic behavior of C_P at the temperature limit of amorphous ice (130 K to 150 K) to develop an equation for the vapor pressure of supercooled

liquid water. They made detailed comparisons of the new equation with other vapor-pressure equations and with existing experimental data. The crucial area is the "no man's land" - see Figure 1.1, where experimental data are missing.

The general approach to the "no man's land" area is based on an extrapolation of thermophysical properties. Experimental data are known in the region above 233 K [7, 8, 10] and experimental data on amorphous ice can be used to constrain the thermodynamic functions at 155 K [86, 1]. The problem is that some properties (isobaric heat capacity, thermal expansivity, isothermal compressibility) change dramatically. To describe the properties in the "no man's land" area, it is possible to use the model of Fuentevilla and Anisimov Eqs. (4.3.1, 4.3.2).

There is a very accurate equation for the vapor pressure of water, namely, the Wagner and Pruß equation [16]:

$$\ln P = \ln P_{\rm c} + \frac{T_{\rm c}}{T}(-7.85951783\tau + 1.84408259\tau^{1.5} - 11.7866497\tau^3 + \\ + 22.6807411\tau^{3.5} - 15.9618719\tau^4 + 1.80122502\tau^{7.5}). \qquad (5.0.1)$$

In the equation $P_{\rm c} = 2.2064 \cdot 10^7$ Pa, $\tau = 1 - T/T_{\rm c}, T_{\rm c}$=647.096 K, with P in Pa. This equation is declared to be valid in the range 273.16 K $\leq T \leq$ 647 K. Murphy and Koop [85] have derived

$$\ln P = 54.842763 - \frac{6763.22}{T} - 4.210 \ln T + 0.000367T + \qquad (5.0.2) \\ + \tanh(0.0415(T - 218.8)(53.878 - \frac{1331.22}{T} - 9.44523 \ln T + 0.014025T),$$

with P in MPa. Eq. (5.0.2) is valid in the temperature interval 123 K $< T <$ 332 K.

If the Wagner and Pruß equation is extrapolated down to the temperature 123 K, it is possible to calculate the differences between Eqs. (5.0.2, 5.0.1). The pressure

differences (in percentages) are defined as

$$\text{Deviation} = \frac{\text{P}_{Wagner,Pruß} - \text{P}_{Murphy,Koop}}{\text{P}_{Murphy,Koop}}. \tag{5.0.3}$$

and they are shown in Figure 5.1. We can see the Wagner and Pruß equation can be extrapolated below the triple point (to temperatures near 233 K).

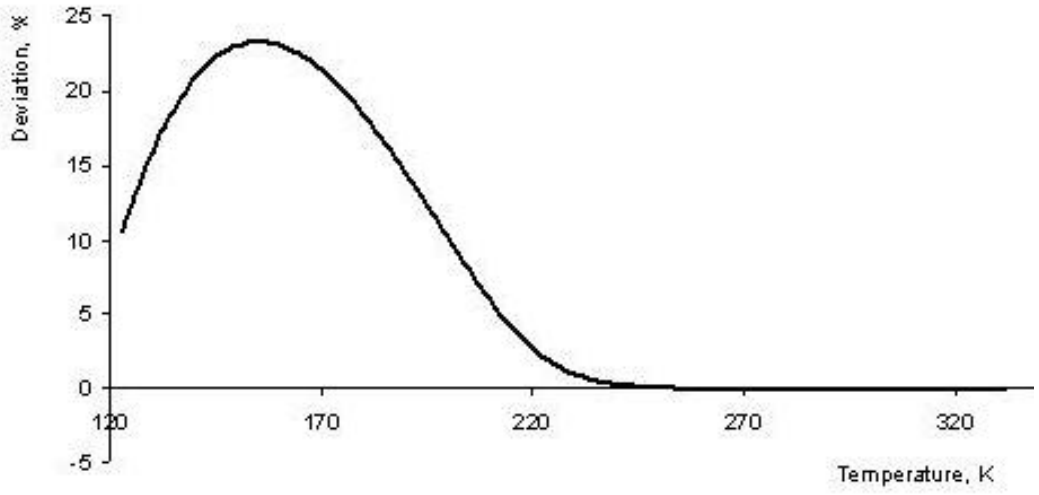

Figure 5.1: Comparison of Eqs. (5.0.2, 5.0.1) for the saturation pressure of water vapor over liquid water.

5.1 Clausius - Clapeyron equation

The Clausius - Clapeyron equation can be used to calculate vapor pressures for temperatures below the triple point, and knowledge of $C_{P,\text{liq}}$ is useful for this purpose. The Clausius - Clapeyron equation extrapolated to the ideal - gas limit can be written as:

$$\frac{d\ln(P)}{dT} = \frac{L_{liq}(T)}{RT^2}, \tag{5.1.1}$$

where $L_{liq}(T)$ is the enthalpy of vaporization as a function of temperature and R=8.314 472 $\mathrm{Jmol^{-1}K^{-1}}$ is the molar gas constant. A starting point is needed for the integration of equation 5.1.1. The integration can start at the triple point (pressure P_{t} =611.657± 0.01 Pa, temperature T_{t} =273.16 K).

It is necessary to know the temperature dependence of $L_{\mathrm{liq}}(T)$ to integrate Eq. (5.1.1). The equation for $L_{\mathrm{liq}}(T)$ was published in [87]:

$$L_{\mathrm{liq}}(T) = L_{\mathrm{liq,t}} + \int_{T_{\mathrm{t}}}^{T} \Delta C_p(T')dT' + \int_{T_{\mathrm{t}}}^{T} \frac{dp}{dT'} \left[(v_{\mathrm{vap}} - v_{\mathrm{liq}}) - T' \left(\frac{\partial (v_{\mathrm{vap}} - v_{\mathrm{liq}})}{\partial T'} \right)_p \right] dT', \tag{5.1.2}$$

where $L_{\mathrm{liq,t}}$ is the enthalpy of vaporization at the triple-point temperature T_{t}, ΔC_P is the difference in isobaric molar heat capacities ($\Delta C_P = C_{P,\mathrm{liq}} - C_{P,\mathrm{vap}}$), v_{vap} and v_{liq} are the molar volumes of vapor and liquid, respectively. The second integral is very small compared to the first one. For example, if $v_{\mathrm{vap}} >> v_{\mathrm{liq}}$ and the behavior of the vapor is approximated by an ideal-gas equation, the second integral is zero. The enthalpy of vaporization at the triple point is $L_{\mathrm{liq,t}}$ =45054.7 $\mathrm{J{\cdot}mol^{-1}}$ [16] (IAPWS-95). Equation (5.1.2) can be written

$$L_{\mathrm{liq}}(T) = 45054.7 + \int_{T_{\mathrm{t}}}^{T} \Delta C_P(T')dT'. \tag{5.1.3}$$

From [85], one can obtain the relation for $C_{P,\mathrm{vap}}$ (in $\mathrm{J{\cdot}mol^{-1}K^{-1}}$):

$$C_{P,\mathrm{vap}} = 33.2618 + 0.00187T - 0.06165T \exp\left(-\left(\frac{T}{129.85} \right)^2 \right) + 0.06163T \exp\left(-\left(\frac{T}{125.1} \right)^2 \right). \tag{5.1.4}$$

Therefore it is sufficient to know only $C_{P,\mathrm{liq}}$ at atmospheric pressure to be able to calculate $L_{\mathrm{liq}}(T)$. It is assumed that at temperatures near 155 K, the heat capacity

of the liquid water is close to the heat capacity of ice [85, 86], namely, $C_{P,\mathrm{liq}}$ is equal to $C_{P,\mathrm{ice}}$ of hexagonal ice plus 2 J·mol^{-1}K^{-1}. Murphy and Koop [85] obtained the equation for $C_{P,\mathrm{ice}}$ (in Jmol^{-1}K^{-1}):

$$C_{P,\mathrm{ice}} = -2.0572 + 0.14644T + 0.06163T \exp\left(-\left(\frac{T}{125.1}\right)^2\right). \tag{5.1.5}$$

It is therefore possible to write in the temperature range between 123 K and 167 K (in Jmol^{-1}K^{-1}):

$$C_{P,\mathrm{liq}} = -0.0572 + 0.14644T + 0.06163T \exp\left(-\left(\frac{T}{125.1}\right)^2\right). \tag{5.1.6}$$

From Eqs.(5.1.4, 5.1.6) one can obtain :

$$\Delta C_P(T) = -33.319 + 0.14457T + 0.06165T \exp\left(-\left(\frac{T}{129.85}\right)^2\right). \tag{5.1.7}$$

There are several ways to get $C_{P,\mathrm{liq}}$ for temperatures between 236 K and 273 K. The data for $C_{P,\mathrm{liq}}$ from [10, 88] are used in the temperature interval.

5.2 Isobaric heat capacity

From Eq. (4.3.6)

$$C_P = C_{P,\mathrm{cr}} + C_{P,\mathrm{b}} = -R \cdot \frac{T}{T_\mathrm{c}}(a_2^2\chi_1 + 2a_2b_1\chi_{12} + b_1^2\chi_2) + C_{P,\mathrm{b}}. \tag{5.2.1}$$

We have used the following steps to obtain the background function $C_{P,\mathrm{b}}$:

A) It is assumed in the region of temperatures between 123 K and 167 K, that C_P is equal to $C_{P,\mathrm{ice}}$ of hexagonal ice plus 2 J·mol^{-1}K^{-1}. We use Eq. (5.1.6).

B) Pátek et al. [88] developed equations for the properties of water at ambient pressure for temperatures between 253 K and 383 K. The properties are based on

IAPWS-95 (within tolerances). We use C_P from this work in this temperature interval.

C) The data of Archer and Carter [10] are used for temperatures between 236 and 250 K.

D) The critical part of C_P is calculated from Eq.(5.2.1) for all temperature intervals.

E) The critical part is subtracted from values obtained in steps A), B) and C). As a result, the $C_{P,\mathrm{b}}$ values are obtained in the temperature intervals. It is possible to fit the values with some analytical function - the least-squares method was used.

F) The background $C_{P,\mathrm{b}}$ is fitted with some analytical functions, and we suppose that the background function is valid in the entire temperature interval between 130 K and 383 K. One can calculate the critical part of Eq.(5.2.1) and obtain
$C_P = C_{P,\mathrm{cr}} + C_{P,\mathrm{b}}$.

Changing the value of coefficient a_2 in Eq.(4.3.1) from 1 to 1.25 [89] was suggested to eliminate the undesirable behavior of the background function. For the background function $C_{P,\mathrm{b}}$, the behavior is displayed in Figure 5.2.

$$C_{P,\mathrm{b}} = 6725.474 + 6462.0717 \cdot \tau - 552.53268 \cdot e^{-\tau^3} + 88.473461 \cdot e^{-(4-\tau)^4} - 12454.046 \cdot \tau^{1/2} - 500.781 \cdot \tau^2, \quad (5.2.2)$$

where $\tau = T/100$. The values of C_P together with the background function are shown in Figure 5.3. We can use the Murphy and Koop equation to get values of C_P. From Eqs.(5.1.1,5.1.3), it is possible to express

$$C_{P,\mathrm{liq}} = C_{P,\mathrm{vap}} - \frac{d}{dT}\left(RT^2 \frac{d\ln p}{dT}\right). \quad (5.2.3)$$

From Eqs.(5.0.2,5.2.3) one can calculate the values of C_P and compare them. The

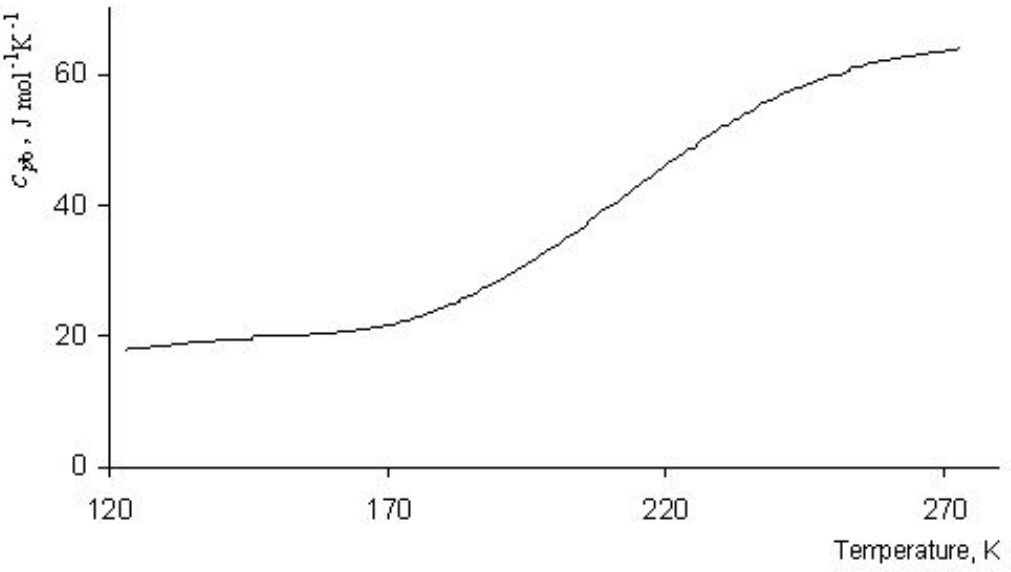

Figure 5.2: Background function $C_{P,\mathrm{b}}$ Eq.(5.2.2) with $a_2 = 1.25$.

comparison is displayed in Figure 5.4. We can see differences in extrapolation into the "no man's land" region between C_P from Eq.(5.2.3) and values gained by using the scaled equation. We believe that our extrapolation gives more accurate results, because only the background function is extrapolated while the critical part of C_P is given by a scaled equation.

5.3 Calculation of vapor pressure

The values of $C_{P,\mathrm{liq}}$ and $C_{P,\mathrm{vap}}$ can be substituted in Eq.(5.1.3) for the calculation of L_{liq}. A numerical integration has been performed. The obtained values are displayed in Figure 5.6. If the Clausius-Clapeyron equation is integrated (numerically), then the values for the vapor pressure are obtained.

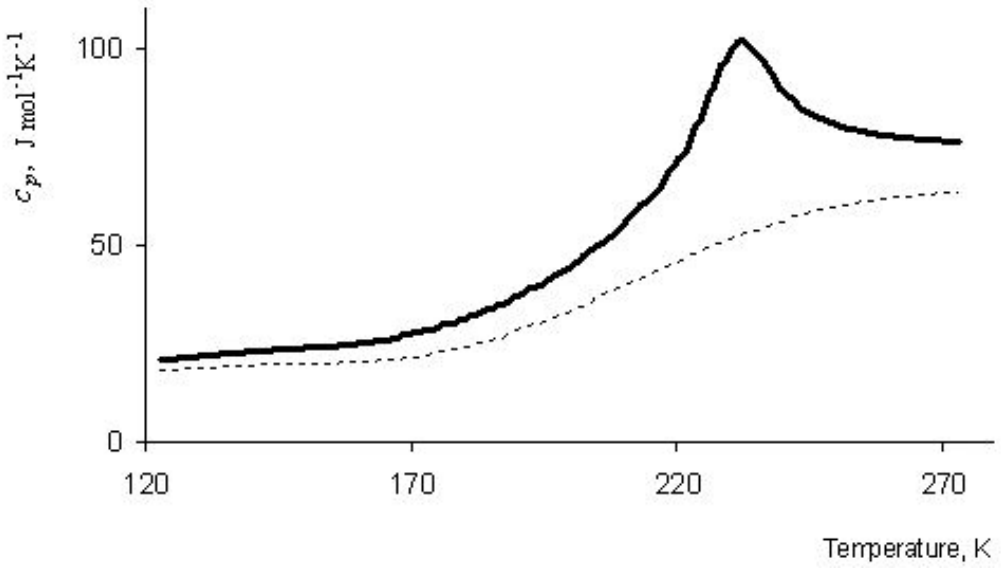

Figure 5.3: Isobaric heat capacity calculated with Eq.(5.2.1) in the interval 123 K - 273 K (solid line) and the background function from Eq.(5.2.2) (dashed line).

We used the fact that the Wagner-Pruß equation describes the calculated vapor-pressure data very well in the region below the triple point to temperatures near -30°C (Figure 5.1). We added correction terms to the Wagner-Pruß equation. The terms are significant only in the region 130 K - 250 K. The resulting equation is

$$\ln P = \ln(2.2064 \cdot 10^7) + \left(\frac{T_c}{T}\right)(-7.85951783 \cdot \tau + 1.84408259 \cdot \tau^{1.5}$$
$$-11.7866497 \cdot \tau^3 + 22.6807411 \cdot \tau^{3.5} - 15.9618719 \cdot \tau^4 + 1.80122502 \cdot \tau^{7.5})$$
$$-0.05611 \cdot e^{-\tau_2^4} - 14.2133 \cdot \tau_1^{-8} + 46.174 \cdot \tau_1^{-9} - 32.52 \cdot \tau_1^{-10}, \quad (5.3.1)$$

where $\tau = 1 - T/T_c, T_c$ =647.096 K, $\tau_1 = T/100$ K, $\tau_2 = (T - 182\text{ K})/35$ K, with P in Pa.

The deviations $100(P - P_{Eq.(5.3.1)})/P_{Eq.(5.3.1)}$ are displayed in Figure 5.6.

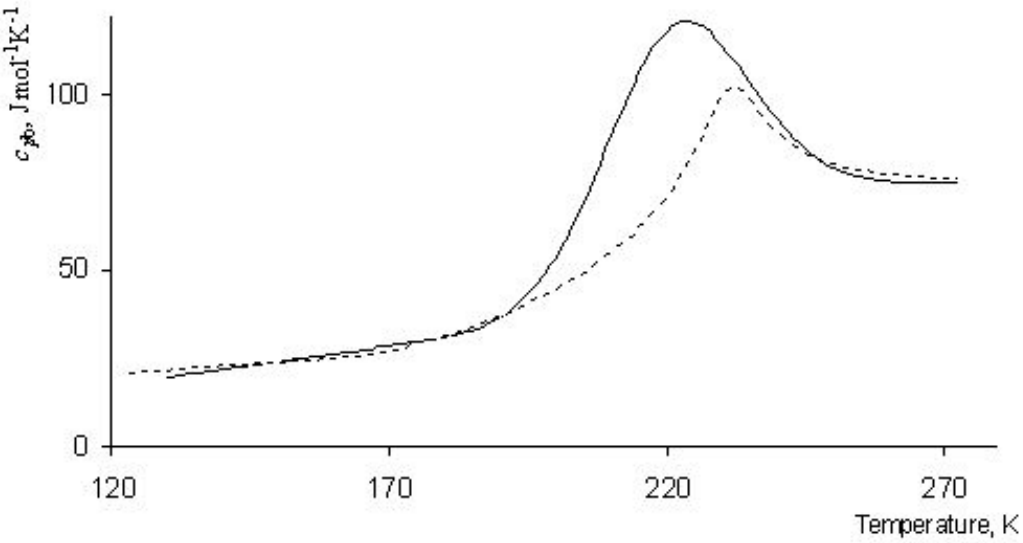

Figure 5.4: Isobaric heat capacity in the interval from 123 K to 273 K (the dashed line for C_P calculated from the scaled equation (5.2.1) and the solid line for values calculated from Eq.(5.2.3))

5.4 Vapor pressure - Conclusion

In the chapter we have constructed noncritical background functions for isobaric heat capacity and we have used this knowledge to calculate vapor pressure data in the wide interval of temperatures from 123 K to 273.16 K. We have used the Murphy and Koop vapor pressure equation to calculate the values of isobaric heat capacity, and compared them with isobaric heat capacity calculated from the scaled equation. We believe that the extrapolation gives more accurate results, because only the background function is extrapolated. We have proved that the Wagner-Pruß equation can be used down to -30°C, and we have developed some additional terms to the equation to describe the behavior of the vapor pressure down to 123 K. Eq.(5.3.1) describes the vapor pressure of water in the interval of temperatures from 123 K to 647 K.

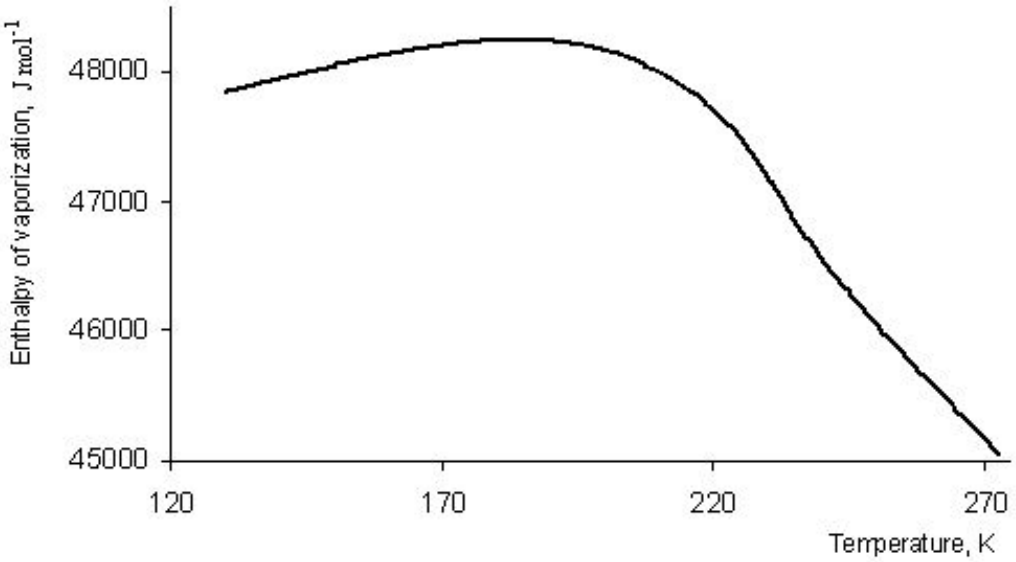

Figure 5.5: Enthalpy of vaporization as a function of temperature-values obtained from numerical integration of Eq.(5.1.3).

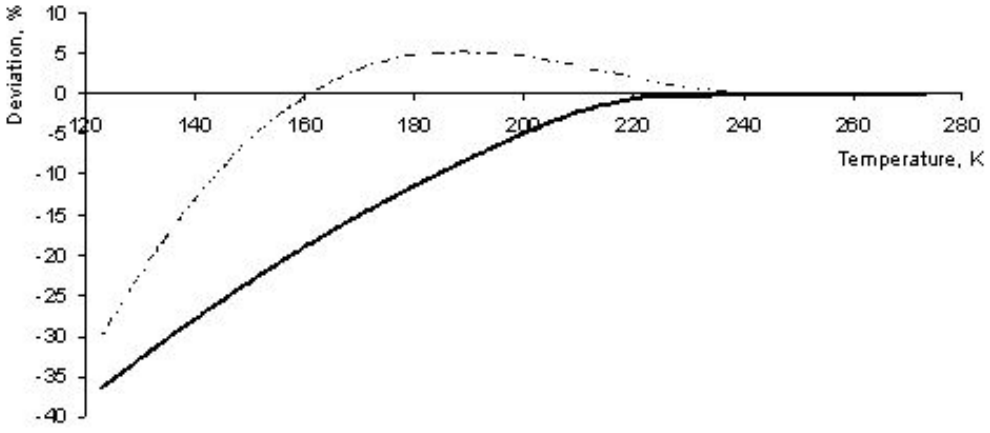

Figure 5.6: Deviations of Eq.(5.0.2) (dashed line) and Eq.(5.0.1) (solid line) from Eq.(5.3.1).

Chapter 6

Surface tension of water

Liquid-vapor interface attracts a wide research interest in recent several years because of its importance in atmospheric phenomena, biological and technical applications. It is this force of the surface tension that allows insects to walk on water. The surface tension allows water to rise in a capillary tube. Water has especially the large surface tension compared to some simple liquids owing hydrogen-bonding structure at the surface. Surface tension properties of supercooled liquid water have importance in the atmosphere. Cloud droplets have shown to stay liquid water down to 235 K. Homogeneous and heterogeneous nucleation processes transforming supercooled droplets into ice crystals have significant importance to radiative forcing and climate.

6.1 Introduction

Much has been written about a second inflection point of the temperature dependence of the water surface tension, but this theme still remains subject of controversy [90, 91, 92]. The same data can be used to support different hypotheses. When the surface tension above 0°C is explored, the inflection point is either very weak, or it does not exist at all [90]. We have decided to include the data of the surface

tension from the supercooled water region [5, 3, 4]. Because of lower accuracy of the experimental data in this region, it was reasonable to include results of the molecular dynamics study [92, 6] into our research.

The International Association for the Properties of Water and Steam (IAPWS) issued the Release on the Surface Tension of Ordinary Water Substance in 1994 [2] . For temperatures between 0.01°C and 374 °C, this release contains critically evaluated data of the surface tension σ, with estimated values of an uncertainty $\Delta\sigma$. A very elegant interpolating equation was recommended in the aforesaid IAPWS release in 1994:

$$\sigma = B\tau^{\mu}(1 + b\tau), \tag{6.1.1}$$

where B=235.8 mN·m^{-1}, $\tau = 1 - \frac{T}{T_c}$, T_c = 647.096 K, μ = 1.256, $b = -0.625$, T is temperature in K. The range of validity of Eq.(6.1.1) is between the temperature of the triple point 273.16 K and the critical temperature T_c=647.096 K.

6.2 Inflection point

An excellent review of recent equations describing the surface tension of supercooled water at ambient pressure is possible to find in [93, 94]. Using the evaluated data gained in [2], we have recalculated coefficients of IAPWS equation (6.1.1) and obtained new coefficients that give a better fit. The original and new values of coefficients, inflection point and sum of squares are shown in the Table 6.1.

To create as simple equation as possible, we rounded coefficients of the new fit in the next step. Deviations from evaluated data [2] are displayed in Figure 6.1.

Table 6.1: IAPWS and new fits

Equation	Description	B	b	μ	Inflection point T[K]	Sum of squares
IAPWS	IAPWS	235.8	-0.625	1.256	529.6	0.0534
N	Best fit	237.2	-0.6297	1.2595	529.1	0.0296
R	Rounded	237.4	-0.63	1.26	528.9	0.038

Resulting from Eq. (6.1.1), the inflection points (Tab. 6.1) are given by conditions

$$\frac{d^2\sigma}{d\tau^2} = \mu B \tau^{\mu-2}((\mu-1) + b(\mu+1)\tau) = 0. \tag{6.2.1}$$

Such a formula yields only just one value of the inflection point T_i for each equation (Tab. 6.1):

$$T_\mathrm{i} = T_\mathrm{c}(1 + \frac{\mu-1}{b\cdot(\mu+1)}). \tag{6.2.2}$$

These values T_i correspond well with the value of 525 K presented in [92]. Many authors have searched the weak inflection point [90, 92, 6] in the vicinity of 0°C. Using data above 0°C, it is difficult to get a proof of an existence of the second inflection point, because of the experimental uncertainties.

Gittens [90] set that new experimental method is needed to get accuracy of measurements at least 0.001 mN·m^{-1}. Provided the IAPWS evaluated data are the best existing data for the surface tension above 0°C, a function of temperature dependence is concave in this region (see Figure 6.2).

That is why the data below 0°C are necessary for test of the second inflection point existence. Experimental data for supercooled water [5, 3, 4] are presented in Figure 6.3.

As we can see in Figure 6.3, uncertainties of experimental values in the supercooled region are larger than for temperatures above 0°C. Data gained by Hacker [3] are used

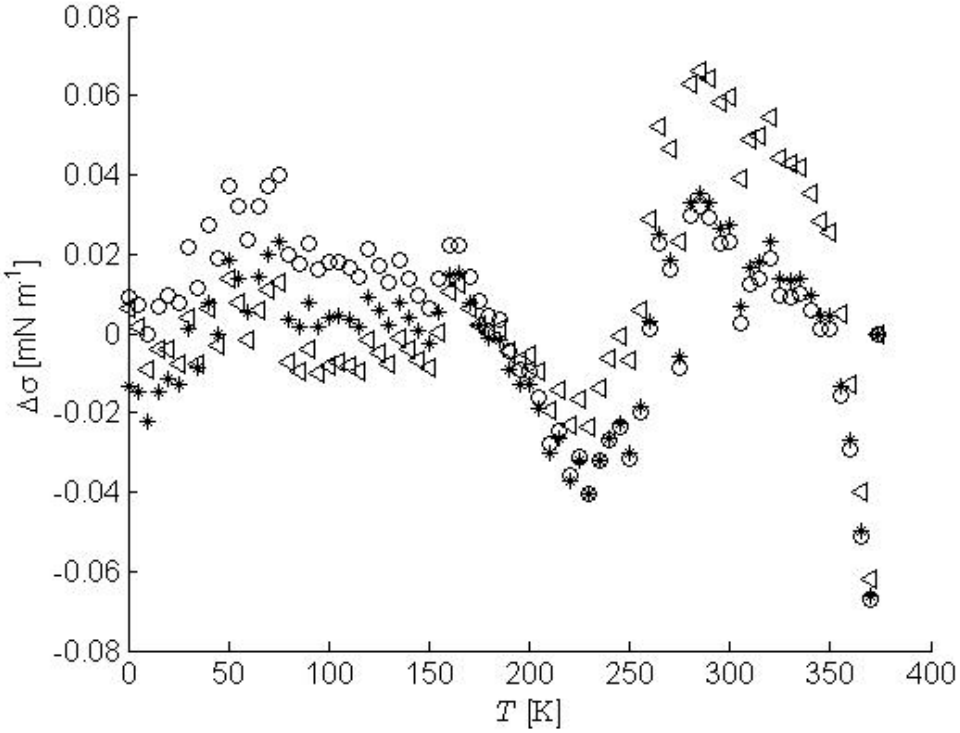

Figure 6.1: Deviations of data yielded from equations with various coefficients (Table 6.1) and evaluated data (IAPWS - [2]). Triangles - deviations of original IAPWS approximation 6.1.1, asterisks - deviations of the new equations (N), circles - rounded coefficients of the new equation (R).

in the book by Pruppacher and Klett [87]. The authors have also taken into account an assumption of singularity behavior of liquid water near -45°C. They presented [87] the equation for the surface tension σ [mN·m^{-1}]:

$$\sigma = \sum_{n=0}^{6} a_n t^n, \tag{6.2.3}$$

where t is temperature in °C, $a_0 = 75.93$, a_1 =0.115·10^{-6}, a_2 =6.818·10^{-2}, a_3 =6.511·10^{-3}, a_4 =2.933·10^{-4}, a_5 =6.283·10^{-6}, a_6 =5.285·10^{-8}.

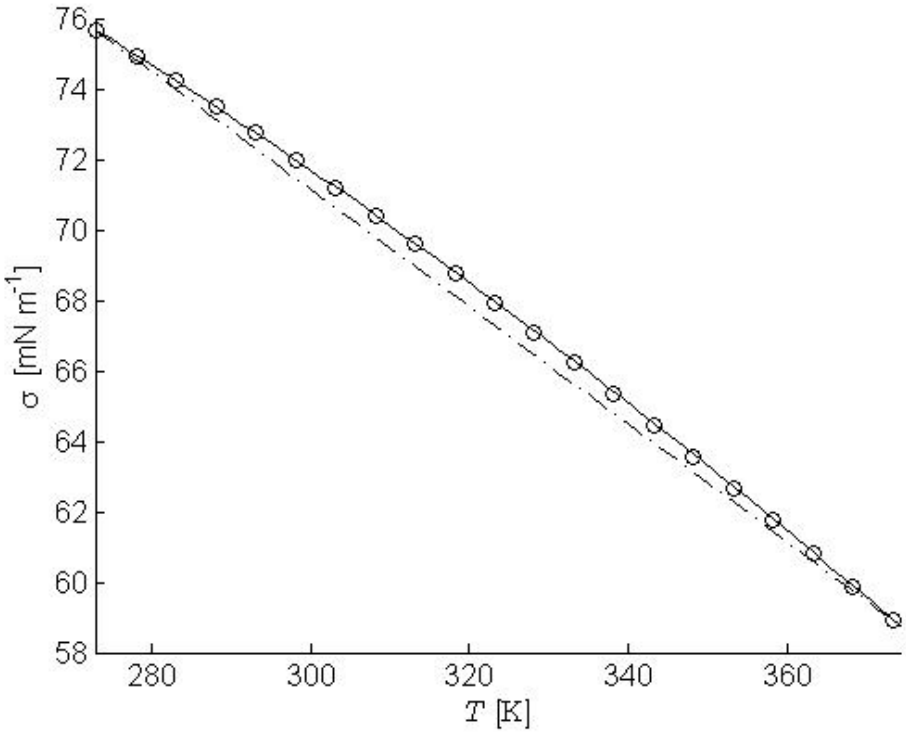

Figure 6.2: The IAPWS formulation for the temperature dependence of the surface tension is a concave function in the temperature interval from 0°C to 100°C. Solid line - IAPWS approximation Eq.(6.1.1), dashed line - the line connected values of the surface tension at 0°C and 100°C, circles - IAPWS evaluated data [2].

Unfortunately, Eq. (6.2.3) does not meet the values of IAPWS at 0°C. The polynomial fitted only to negative temperatures and it is not possible to use it for any temperatures above 0°C. The singularity assumption of the surface tension near −45°C as it was used in [87] is not valid [95]. There exist two basic sets of experimental data of the surface tension at negative temperatures. The data ICT [95] exist only down to -8°C and cannot directly influence a searching of the inflection point. Hacker data [3] show higher values in the supercooled water region than Floriano and Angell data [4]. Floriano and Angell data show higher dispersion mainly in the region of

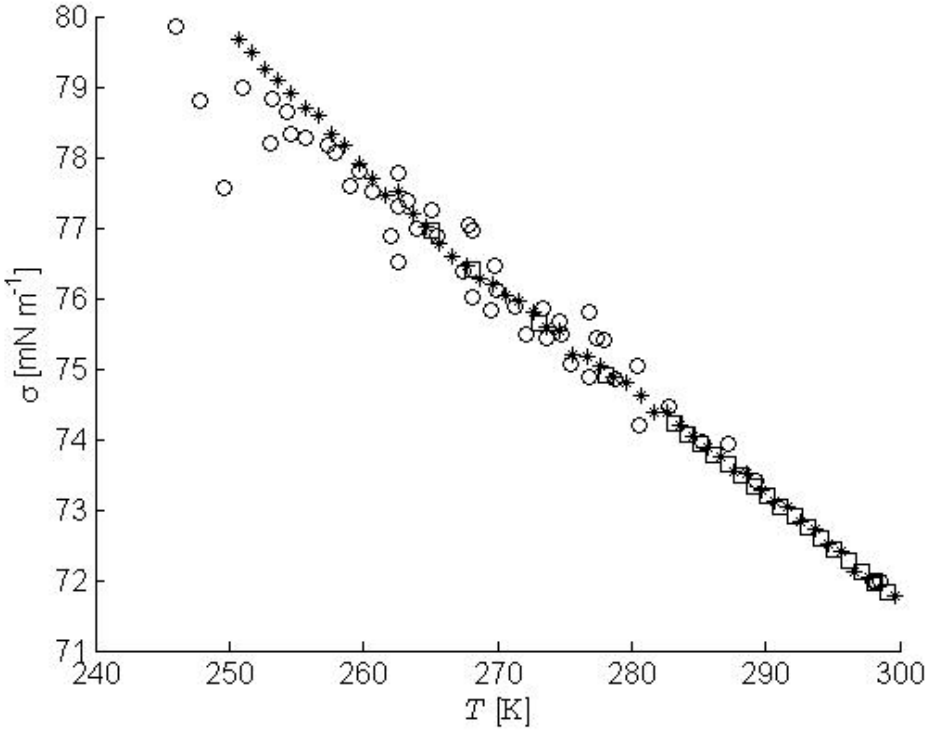

Figure 6.3: Experimental data for the surface tension in the region of supercooled water. Asterisks - [3], circles - [4], squares - [5].

lower temperatures. It is difficult to predict the form of an extrapolation without further information.

We have used the molecular dynamics (MD) study [6] on surface properties of supercooled water. The extended simple point charge (SPC/E) potential was used, to calculate the surface tension in a temperature range from 228 K to 293 K. Because the results of simulations in supercooled region are in a good agreement with experimental data, we have assumed we can use the data down to 228 K from this study. These data, IAPWS [2] and Prupacher and Klett [87] extrapolations are displayed in Figure 6.4.

One can see that Prupacher and Klett approximation (6.2.3) gives a good fit of

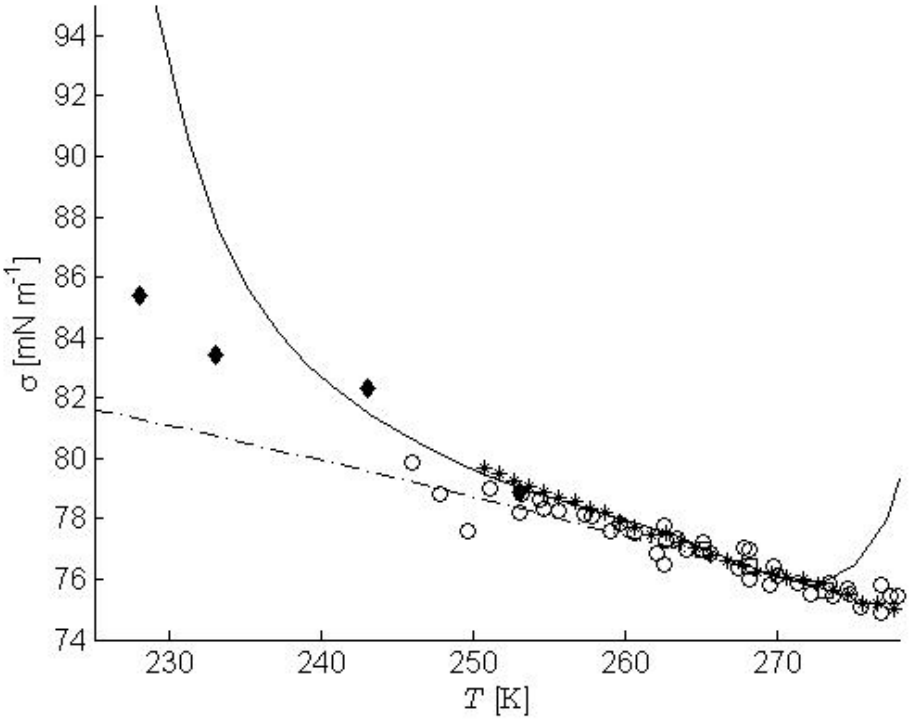

Figure 6.4: Experimental data for supercooled water and extrapolations: Asterisks - [3], circles - [4], squares - [5], diamonds - [6], dashed line - Eq.(6.1.1), solid line - Eq.(6.2.3)

the Hacker data [3] and it is not possible to use them for temperatures below $-38°$C and above 0°C. On the contrary, the extrapolation (6.1.1) satisfactorily describes the Floriano and Angell data [4]. As it was mentioned above, Eq.(6.1.1) does not yield any inflection point in this temperatures region. Even an absolute value of the second derivative of a temperature dependence of the surface tension is growing, if the temperatures go down. It means the IAPWS function (6.1.1) is concave also in the negative temperatures region. The IAPWS form of the temperature dependence of the surface tension Eq.(6.1.1) is very accurate for the description of values above 0°C. In the negative temperatures region, IAPWS equation (6.1.1) describes only

experimental data [4]. A correction of this equation is needed. We tried to find such a correction in the form:

$$\sigma = B\tau^{\mu}(1 + b\tau + c\tau^{n}). \tag{6.2.4}$$

Here c is a new parameter (probably positive) and n is an unknown power. We wanted to keep the IAPWS equation (6.1.1) for temperatures above 0°C, and fix the parameters B, b in the first step. One can read

$$\sigma = \tau^{\mu}(B + C\tau + D\tau^{n}), \tag{6.2.5}$$

where $C = B \cdot b$ and $D = B \cdot c$. Whence follows:

$$D \cdot \tau^{n} = \frac{\sigma}{\tau^{\mu}} - B - C \cdot \tau. \tag{6.2.6}$$

To find the correction, we calculated the right side of Eq.(6.2.6) for all experimental and calculated data [5, 3, 4, 6] and used a regression method to find coefficients D,n values. Using this, we have got the optimal values $D = 1.1868 \cdot 10^{7}$ and n=3 (only a natural exponent n was the target).

As shown in Figure 6.5, there exists the second inflection point in this temperature dependence of the surface tension. This inflection point value was calculated at the temperature of about 1.5°C. Deviations of the surface tension values calculated using (Eq. 6.2.5) from IAPWS evaluated data [2] are graphed in a Fig. 6.6. All deviations are in a range of uncertainties tabulated in [2].

We can optimize the parameters of (Eq. 6.2.5) subsequently (to the IAPWS evaluated data [2]) and we obtain values B=235.8, C=-147.424, D=1.2038·10^{7}, n=33, μ=1.256. Such an optimization yields slightly better approximation of evaluated data [2], as shown in Fig. 6.7.

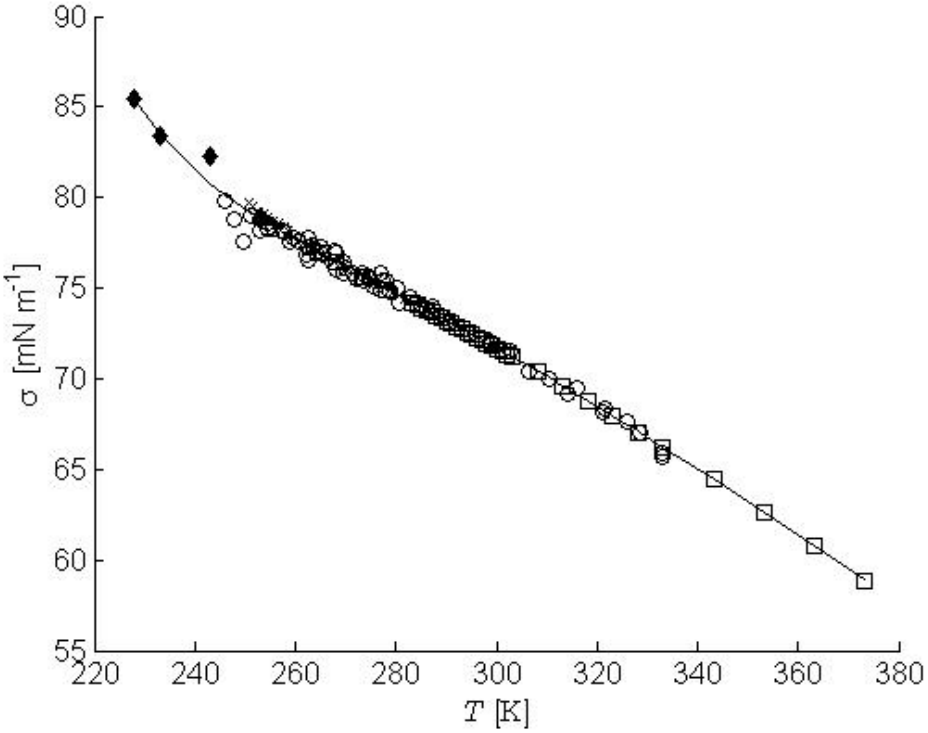

Figure 6.5: The temperature dependence of the surface tension from 6.2.5. Experimental data [3] - asterisks, [4] - circles, [5] - squares. Calculated data [6] - diamonds.

6.3 Inflection point - conclusions

We have modified parameters of Eq.(6.1.1) to get smaller deviations from evaluated data [2]. Even our approximation of Eq.(6.1.1) parameters to the lower number of decimal places leads to better results than IAPWS Eq.(6.1.1). The possibility of an existence of the second inflection point in the temperature dependence of the surface tension is discussed. The analysis of experimental data for the surface tension of supercooled water was made. These data were completed with values calculated using molecular dynamic [6]. Next term has been added to Eq.(6.1.1) to fit all of data. Eq. 6.2.5 follows from this. As it is shown in presented work, this equation

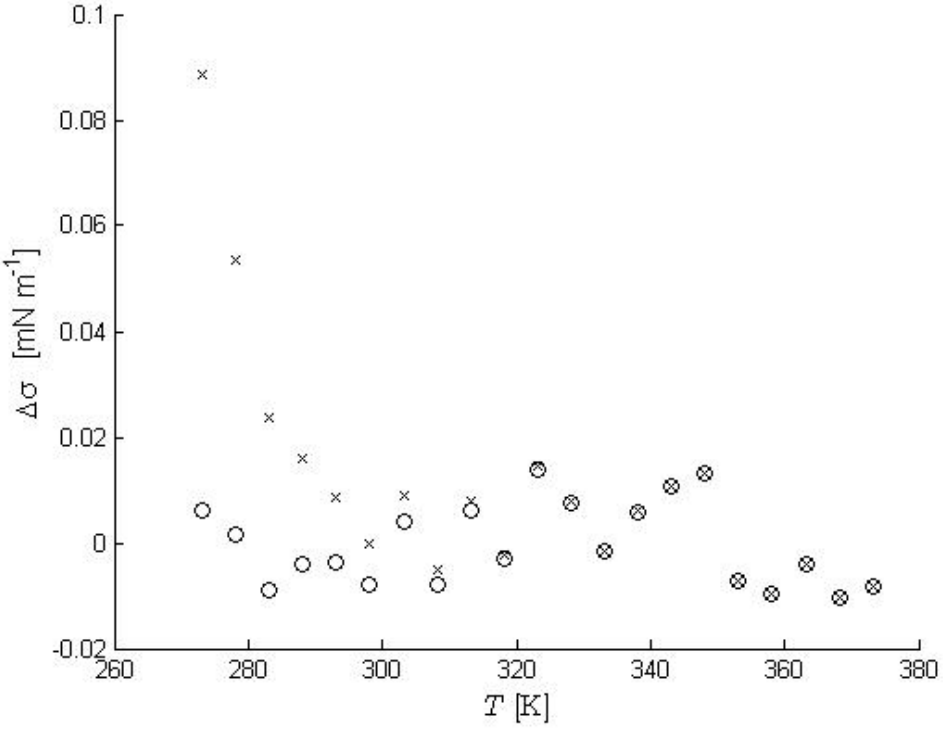

Figure 6.6: Deviations of Eq. (6.2.5) (crosses) and the deviations of IAPWS Eq. (6.1.1) (open circles) from IAPWS evaluated data [2].

leads to the inflection point value at the temperature of about 1.5°C. Parameters of Eq.(6.2.5) were done more precise in the next step. This leads to the relation describing the surface tension values of ordinary water between 228 K and 647 K.

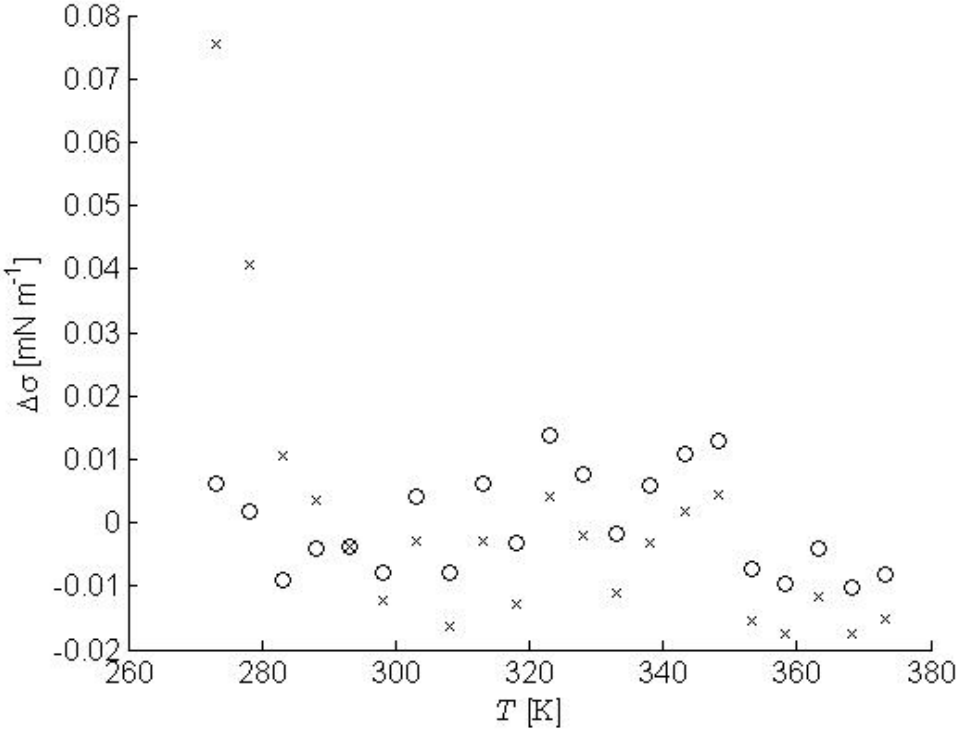

Figure 6.7: Deviations of Eq. (6.2.5) with optimized parameters (crosses) and deviations of IAPWS Eq. (6.1.1) (open circles) from data evaluated by IAPWS [2].

Chapter 7

Supercooled water - recent development

Basic principles of supercooled water behavior were further described in various papers [11, 96, 55]. A brief summary of new findings is given in this chapter.

Recently, Stokely et al. [97] have shown, how all four scenarios can be described by varying two quantities, the strength of the hydrogen bonds and the cooperation of the hydrogen bonds. Three of the scenarios are discussed in Chapter 1, the fourth scenario is the critical-point free (CPF) scenario hypothesis. This scenario supossed a first-order phase transition line separating two liquid phases and extending to $P < 0$ down to the (superheated) limit of liquid water stability [98]. No critical point is presented in this scenario.

7.1 Bertrand - Anisimov model

Bertrand and Anisimov [11] used a particular choice of the critical entropy, $\hat{S}_c = 0$. In the paper, the scaling fields were assumed to be the following combination of physical

fields, the pressure P and the temperature T:

$$h_1 = \Delta\hat{T} + a'\Delta\hat{\mu}, \tag{7.1.1}$$

$$h_2 = -\Delta\hat{\mu}, \tag{7.1.2}$$

$$h_3 = \Delta\hat{P} - \Delta\hat{\mu}. \tag{7.1.3}$$

In the equations a' coefficients of the model represent the slope $-d\hat{T}/d\hat{P}$ along the liquid - liquid transition line ($h_1 = 0$). In this case, molar entropy and molar density are given by

$$\Delta\hat{S} = \phi_1, \tag{7.1.4}$$

$$\Delta\hat{\rho} = -\phi_2 + a'\phi_1. \tag{7.1.5}$$

The following relation for the Widom line was used

$$T = \mathrm{A} + \mathrm{B}P + \mathrm{C}P^2 = 231.4 - 147.8 \cdot 10^{-3} \cdot P - 339.9 \cdot 10^{-6} \cdot P^2. \tag{7.1.6}$$

In the equation the temperature T is in K and the pressure P is in Pa.

For critical parts of physical response functions, namely the isothermal compressibility, the isobaric thermal expansivity and the isobaric heat capacity, one gets:

$$\left(\hat{\rho}^2\hat{\kappa}_T\right)_{\mathrm{cr}} = \left(\frac{\partial\hat{\rho}}{\partial\hat{\mu}}\right)_{\hat{T},\mathrm{cr}} = \chi_2 - 2a'\chi_{12} + (a')^2\chi_1, \tag{7.1.7}$$

$$\left(\hat{\rho}\hat{\alpha}_{\hat{P}}\right)_{\mathrm{cr}} = -\left(\frac{\partial\hat{\rho}}{\partial\hat{T}}\right)_{\hat{P},\mathrm{cr}} = \chi_{12} - a'\chi_1 + \hat{S}\left(\hat{\rho}^2\hat{\kappa}_T\right)_{\mathrm{cr}}, \tag{7.1.8}$$

$$\left(\hat{\rho}\frac{\hat{C}_P}{\hat{T}}\right)_{\mathrm{cr}} = \left(\hat{\rho}\frac{\partial\hat{S}}{\partial\hat{T}}\right)_{\hat{P},\mathrm{cr}} = \chi_1 + 2\hat{S}\left(\hat{\rho}\hat{\alpha}_{\hat{P}}\right)_{\mathrm{cr}} - \hat{S}^2\left(\hat{\rho}^2\hat{\kappa}_T\right)_{\mathrm{cr}}. \tag{7.1.9}$$

Reduced entropy per mol in the equations is

$$\hat{S} = \frac{\hat{S}_{\mathrm{c}} + \phi_1}{1 - \phi_2 + a'\phi_1}. \tag{7.1.10}$$

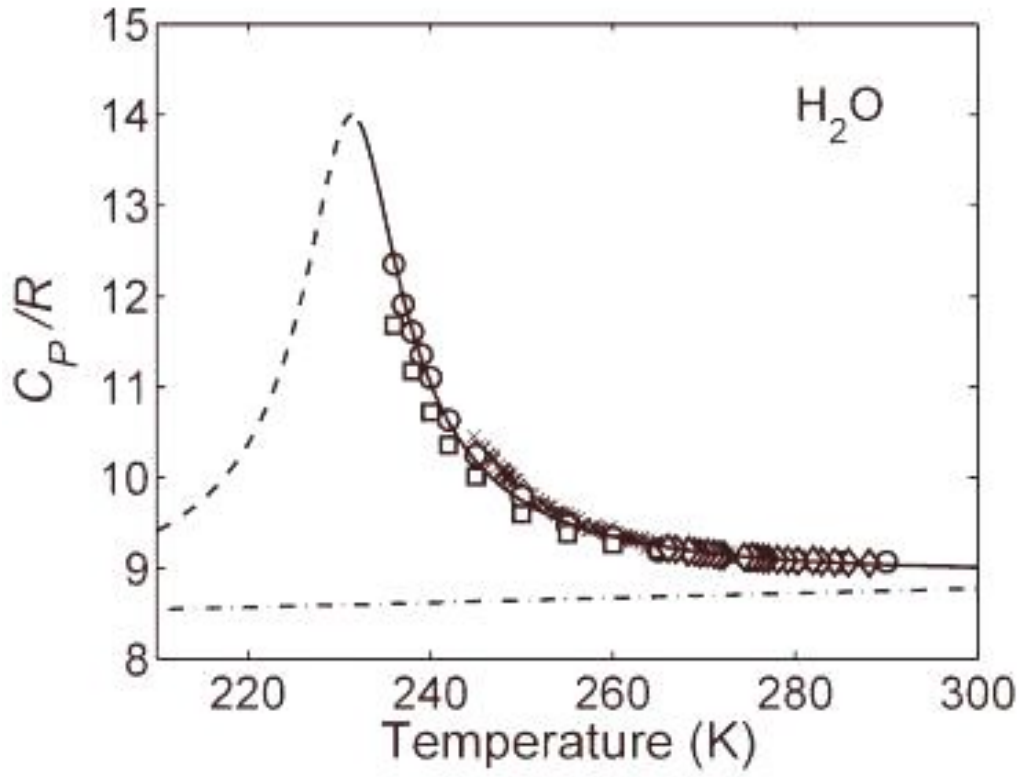

Figure 7.1: Isobaric heat-capacity experiments for H_2O (open circles [7], crosses [8], diamonds [9] and squares [10]) and the prediction of the scaling parametric equation of state (solid curve in the metastable region and dashed curve in the unstable region). The estimated noncritical background is plotted as a dotted-dashed line. Figure copied from [11].

The comparison with experimental data is shown in Figures (7.1, 7.2, 7.3). The background functions for the Bertrand and Anisimov model are described in Table 7.1. The parameters of the model are in Table 7.2.

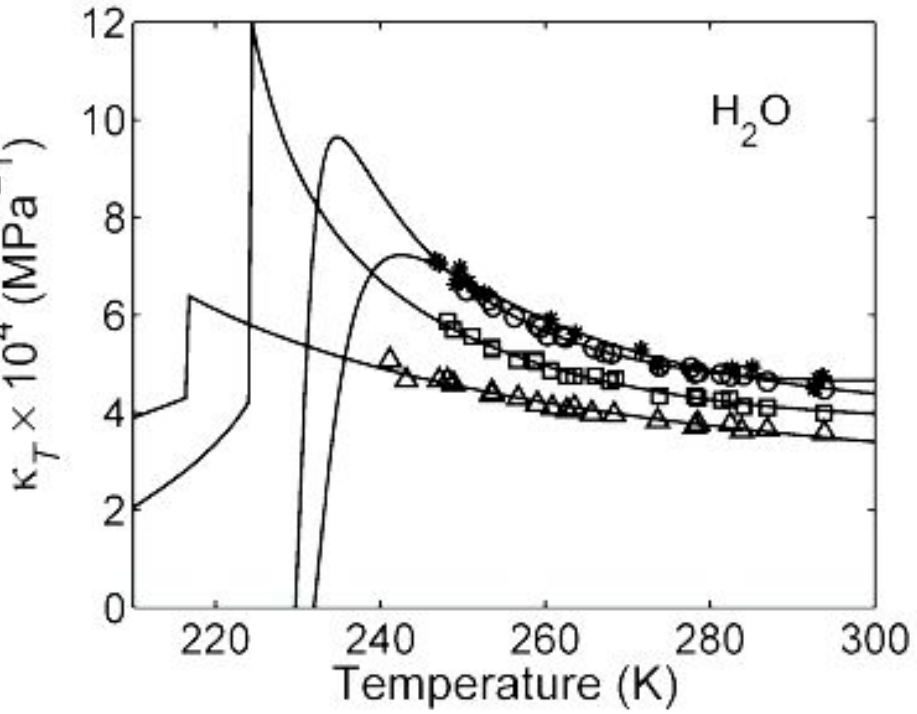

Figure 7.2: Isothermal compressibility experimental data for H_2O along isobars [12, 13](0.1 MPa (stars), 10 MPa (open circles), 50 MPa (squares) and 100 MPa (triangles)) compared with the scaling prediction at the same pressures (solid curves). Figure copied from [11].

7.2 HBAS model

A new paper describing thermodynamic properties of supercooled water was published recently [96]. We will call this model the HBAS model (Holten-Bertrand-Anisimov-Sengers). The following model was adopted:

$$h_1 = \Delta\hat{T} + a'\Delta\hat{P}, \tag{7.2.1}$$

$$h_2 = -\Delta\hat{P} + b'\Delta\hat{T}, \tag{7.2.2}$$

$$h_3 = \Delta\hat{P} - \Delta\hat{\mu} + \Delta\hat{\mu}^r. \tag{7.2.3}$$

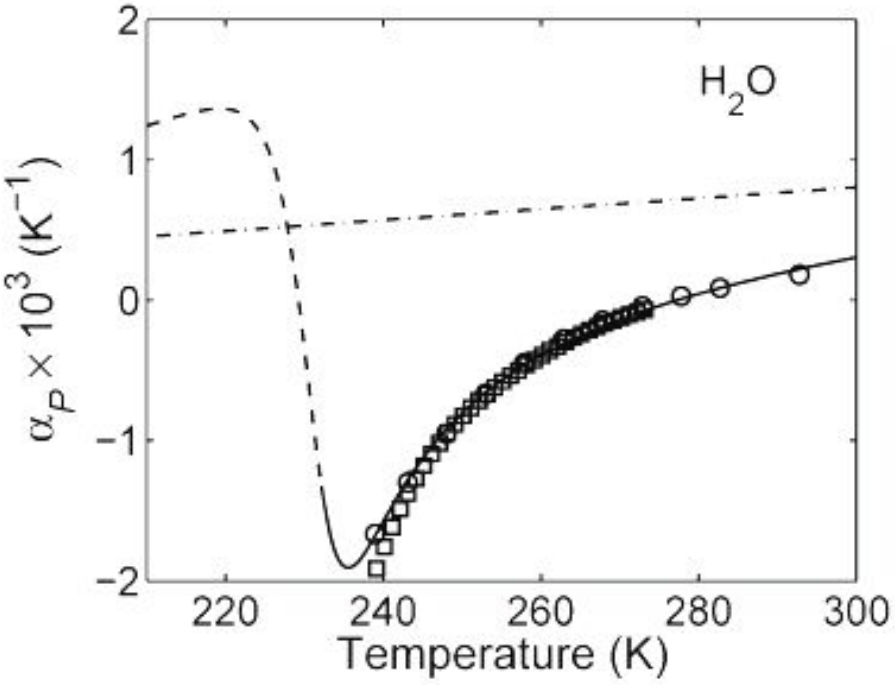

Figure 7.3: Thermal expansivity experimental data for H_2O at 0.1 MPa (open circles [14] and squares [15] and the prediction of the scaling parametric equation of state (solid curve in the metastable region and dashed curve in the unstable region). The estimated noncritical background is plotted as the dotted-dashed line. Figure copied from [11].

In the equations, a' is a coefficient of the model representing the slope $-d\hat{T}/d\hat{P}$ of the phase coexistence or the Widom line at the critical point, b' is a coefficient describing the asymmetry of the phase transition of supercooled water in terms of the entropy order parameter. To obtain the complete behavior of the thermodynamic properties, the previous works [84, 89, 11] included temperature - dependent background functions of each property separately, it means the description of the properties could be mutually thermodynamically inconsistent. In the paper, the background is added to

Table 7.1: Background functions of the Bertrand-Anisimov model

Property	*Pressure*(MPa)
$(\hat{C_P})_{\mathrm{b}} = 0.588\Delta\hat{T} + 8.585$	0.1
$(\kappa_T)_{\mathrm{b}} = 9.808\Delta\hat{T} - 17.60[10^{-4}\mathrm{MPa}^{-1}]$	0.1
$(\kappa_T)_{\mathrm{b}} = 12.15\Delta\hat{T} - 17.73[10^{-4}\mathrm{MPa}^{-1}]$	10
$(\kappa_T)_{\mathrm{b}} = 7.305\Delta\hat{T} - 14.33[10^{-4}\mathrm{MPa}^{-1}]$	50
$(\kappa_T)_{\mathrm{b}} = 2.431\Delta\hat{T} - 10.53[10^{-4}\mathrm{MPa}^{-1}]$	100
$(\alpha_P)_{\mathrm{b}} = 0.892\Delta\hat{T} + 0.527[10^{-3}\mathrm{K}^{-1}]$	0.1

Table 7.2: Parameters of the Bertrand and Anisimov model

a'	P_{c}	T_{c}	a	k
0.066	27.5 MPa	227.1 K	0.34	0.34

the chemical potential and all other background functions can be calculated according to thermodynamic rules. The regular contribution to the chemical potential is represented by the truncated Taylor-series expansion around the critical point:

$$\Delta\hat{\mu}^r = \sum_{m,n} c_{mn}(\Delta\hat{T})^m(\Delta\hat{P})^n. \tag{7.2.4}$$

The coefficient $c_{00} = 0$ because it is supposed that $\Delta\hat{\mu}^r_{cr} = 0$. The coefficient $c_{01} = \Delta\hat{V} = 0$ and because the zero entropy $\Delta\hat{S}$ was chosen, $c_{10} = 0$. In this case, the molar volume and the entropy molar density are given by

$$\Delta\hat{V} = \left(\frac{\partial\hat{\mu}}{\partial\hat{P}}\right)_T = -a'\phi_1 + \phi_2 + \Delta\hat{\mu}^r_{\hat{P}}, \tag{7.2.5}$$

$$\Delta\hat{S} = -\left(\frac{\partial\hat{\mu}}{\partial\hat{T}}\right)_P = \phi_1 + b'\phi_2 - \Delta\hat{\mu}^r_{\hat{T}}. \tag{7.2.6}$$

For $\Delta\hat{\mu}^r$ the subscript $\hat{P}$ indicates the derivative with respect to $\hat{P}$ at constant $\hat{T}$, and the subscript $\hat{T}$ indicates the derivative with respect to $\hat{T}$ at constant $\hat{P}$.

For the critical parts of the physical response function, namely the isothermal compressibility, the isobaric thermal expansivity and the isobaric heat capacity, one

Table 7.3: Parameters of the HBAS model

P_c	27.5 MPa	c_{11}	1.5363×10^{-1}
T_c	224.23 K	c_{12}	-6.4879×10^{-3}
ρ_c	948.77 kg m^{-3}	c_{13}	7.7090×10^{-3}
a	0.22924	c_{20}	-3.8888×10^{0}
k	0.37704	c_{21}	1.7347×10^{-1}
a'	0.090	c_{22}	-6.4157×10^{-2}
c_{02}	7.1779×10^{-2}	c_{23}	-6.9850×10^{-3}
c_{03}	-4.0936×10^{-4}	c_{30}	6.9813×10^{-1}
c_{04}	-1.0996×10^{-3}	c_{31}	-1.1459×10^{-1}
c_{05}	2.9497×10^{-4}	c_{32}	7.5006×10^{-2}

gets:

$$\hat{\kappa}_{T,\mathrm{cr}} = -\frac{1}{\hat{V}}\left(\frac{\partial \hat{V}}{\partial \hat{P}}\right)_T = \frac{1}{\hat{V}}\left[\chi_2 - 2a'\chi_{12} + (a')^2\chi_1 - \Delta\hat{\mu}^r_{\hat{P}\hat{P}}\right], \tag{7.2.7}$$

$$\hat{\alpha}_{V,\mathrm{cr}} = -\frac{1}{\hat{V}}\left(\frac{\partial \hat{V}}{\partial \hat{T}}\right)_P = \frac{1}{\hat{V}}\left[b'\chi_2 + (1 - a'b')\chi_{12} - a'\chi_1 + \Delta\hat{\mu}^r_{\hat{T}\hat{P}}\right], \tag{7.2.8}$$

$$\hat{C}_{P,\mathrm{cr}} = \hat{T}\left(\frac{\partial \hat{S}}{\partial \hat{T}}\right)_{\hat{P}} = \hat{T}\left[\chi_1 + b'^2\chi_2 + 2b'\chi_{12} - \Delta\hat{\mu}^r_{\hat{T}\hat{T}}\right]. \tag{7.2.9}$$

The parameters of the HBAS model are in Table 7.3.

The HBAS model implies a linear liquid-liquid transition (LLT) line. The model with parameters of Table 7.3 is called the asymptotic model and the validity of the model is restricted to the pressures not exceeding 150 MPa [96]. The value of the parameter a' is restricted to the range of 0.065 to 0.090. Because the position of the LLT line is not exactly known, the deviation of the critical point was from the Mishima's curve was tolerated up to 3 K. The model was not very sensitive to the critical pressure, P_c was constrained to the value $P_c = 27.5$ MPa, the value obtained from the Bertrand and Anisimov model. The mixing coefficient b' was set to zero. The value of β was set to the value 0.3265 (Pelissetto and Vicari [69]). The fitted model is valid up to 300 K and from 0 to 150 MPa.

Table 7.4: Parameters of the extended HBAS model

P_c	56.989 MPa	c_{12}	-4.6569×10^{-3}
T_c	213.89 K	c_{13}	2.3627×10^{-3}
ρ_c	949.87 kg m^{-3}	c_{14}	-2.8697×10^{-4}
a	0.11624	c_{20}	-3.6144×10^{0}
k	0.43280	c_{21}	-1.5009×10^{-2}
a'	0.10898	c_{22}	-2.4609×10^{-2}
c_{02}	4.0793×10^{-2}	c_{23}	9.8679×10^{-4}
c_{03}	-6.7912×10^{-4}	c_{30}	5.4267×10^{-1}
c_{04}	-7.5669×10^{-6}	c_{31}	1.0620×10^{-1}
c_{05}	1.0922×10^{-5}	c_{32}	1.2759×10^{-2}
c_{11}	1.9547×10^{-1}	c_{41}	-7.9970×10^{-2}

The paper [96] introduced so called extended scaling model in which any constraints on the slope of the LLT line and on the critical parameters were removed. The semi-empirical extended model is based on the addition of two background terms, and the model is then able to describe experimental data up to 400 MPa.

Chapter 8

Supercooled water - mean field approximation

8.1 Testing of the properties of the mean field approximation

During a research fellowship at the University of Maryland, the mean field approximation of the scaled equation of state was tested. For relationships between the scaling fields and the physical fields near the liquid-liquid critical point in supercooled water, we adopteded [99]

$$h_1 = \Delta\hat{T} + a_1\Delta\hat{P} + a_2(\Delta\hat{P})^2, \tag{8.1.1}$$

$$h_2 = -\Delta\hat{P} + b_1\Delta\hat{T}, \tag{8.1.2}$$

$$h_3 = -\Delta\hat{\mu} + \Delta\hat{P} - \hat{S}_c\Delta\hat{T}. \tag{8.1.3}$$

In the equations we have neglected a contribution from the additional physical field $\Delta\hat{\mu}$ to h_1 and h_2, since such contributions only become significant in highly asymmetric systems [100, 82]. In the relations above, a_1, a_2 and b_1 are system-dependent coefficients. The coefficients a_1 and a_2 represent the limiting slope and curvature of the

phase-coexistence or Widom line $h_1 = 0$. The coefficient b_1 is a so-called mixing coefficient in the revised scaling approximation [82]. While near the vapor-liquid critical point the leading term in the expansion of the ordering field h_1 is $\Delta\hat{\mu}$, the leading term in the expansion of h_1 near the liquid-liquid critical point in supercooled water is $\Delta\hat{T}$, since the entropy yields now the major contribution to the order parameter and not the density. The selected model differs from the model of Bertrand and Anisimov [11] for supercooled water in two aspects. First, following Fuentevilla and Anisimov [84], we have added a quadratic pressure contribution in the expansion of h_1 to accommodate a curvature of the phase-coexistence line and the Widom line as a function of pressure. Secondly, we have preferred to formulate the scaling laws in terms of the physical potential $\mu(T, P)$ rather than in terms of $P(T, \mu)$ as was done by Bertrand and Anisimov, because it leads to simpler expressions for some thermodynamic properties. The equation (8.1.3) can be further simplified by taking $\hat{S}_{\rm c} = 0$. One can express the volume $\hat{V}$ and the entropy $\hat{S}$:

$$\hat{V} = 1 - a_{1,\rm eff}\phi_1 + \phi_2, \tag{8.1.4}$$

$$\hat{S} = \hat{S}_{\rm c} + \phi_1 + b_1\phi_2, \tag{8.1.5}$$

with

$$a_{1,\rm eff} = a_1 + 2a_2\Delta\hat{P}. \tag{8.1.6}$$

The theoretical model only applies to critical parts of various thermodynamic properties. Hence, to investigate whether the theory can account for the anomalous temperature dependence of the response functions, we separated the isobaric heat capacity $\hat{C}_P$, the isothermal compressibility $\hat{\kappa}_T$, and the thermal expansivity $\hat{\alpha}_V$ into a critical

part and a noncritical background part [11]:

$$\hat{C}_P = \hat{C}_{P,\mathrm{cr}} + \hat{C}_{P,\mathrm{b}}, \tag{8.1.7}$$

$$\hat{\kappa}_T = \hat{\kappa}_{T,\mathrm{cr}} + \hat{\kappa}_{T,\mathrm{b}}, \tag{8.1.8}$$

$$\hat{\alpha}_V = \hat{\alpha}_{V,\mathrm{cr}} + \hat{\alpha}_{V,\mathrm{b}}. \tag{8.1.9}$$

The theoretical model only yields expressions for the critical parts of these response functions:

$$\hat{C}_{P,\mathrm{cr}} = \hat{T}[\chi_1 + 2b_1\chi_{12} + b_1^2\chi_2], \tag{8.1.10}$$

$$\hat{\kappa}_{T,\mathrm{cr}} = \frac{1}{\hat{V}}[a_{1,\mathrm{eff}}^2\chi_1 - 2a_{1,\mathrm{eff}}\chi_{12} + \chi_2 + 2a_2\phi_1], \tag{8.1.11}$$

$$\hat{\alpha}_{V,\mathrm{cr}} = \frac{1}{\hat{V}} - [a_{1,\mathrm{eff}}\chi_1 + (1 - 2a_{1,\mathrm{eff}}b_1)\chi_{12} + b_1\chi_2]. \tag{8.1.12}$$

In the mean-field approximation ($\alpha = 0, \beta = 1/2$), the field h_3 can be represented by the asymptotic Landau expansion [34, 101, 102]:

$$-h_3 = \frac{1}{2}a_0h_2\phi_1^2 + \frac{1}{4}u_0\phi_1^4 - h_1\phi_1, \tag{8.1.13}$$

where a_0 and u_0 are two system-dependent coefficients. Minimization of the potential as a function of ϕ_1 at constant h_1 yields the condition

$$u_0\phi_1^3 + a_0h_2\phi_1 - h_1 = 0, \tag{8.1.14}$$

from which one can derive expressions for the scaling density ϕ_2 and for the scaling susceptibilities in term of the order parameter ϕ_1:

$$\phi_2 = -\frac{1}{2}a_0\phi_1^2, \tag{8.1.15}$$

$$\chi_1 = \frac{1}{3u_0\phi_1^2 + a_0h_2}, \tag{8.1.16}$$

$$\chi_2 = a_0^2 \phi_1^2 \chi_1, \tag{8.1.17}$$

$$\chi_{12} = -a_0 \phi_1 \chi_1. \tag{8.1.18}$$

We have compared the theoretical model for liquid-liquid critical behavior in the

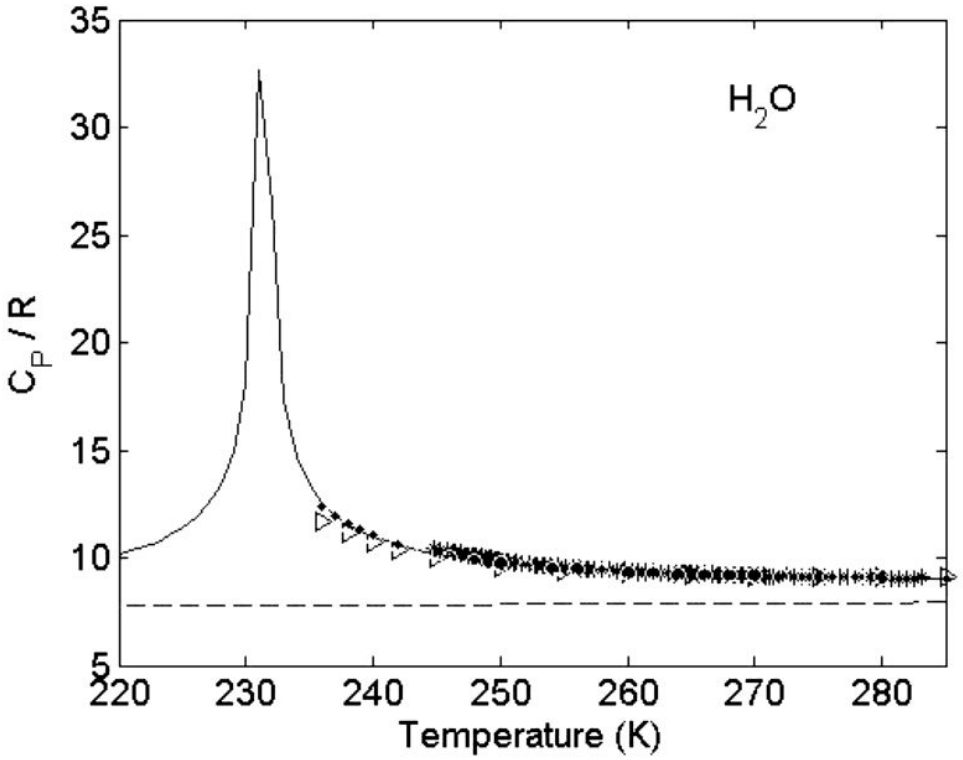

Figure 8.1: Comparison of mean-field equation of state with experimental data for the isobaric heat capacity at ambient pressure as a function of temperature. The curves represent values calculated from the scaled equation. The symbols indicate experimental data (diamonds [7], triangles [10], stars [8]. The estimated noncritical background contribution is plotted as a dashed line.

mean-field approximation with experimental data for the isobaric heat capacity, the isothermal compressibility and the thermal expansivity of supercooled water. The background contributions in Eqs. (8.1.7-8.1.9) should be smooth analytic functions of temperature and pressure and should not display any singular behavior as a function

of temperature or pressure [89]. We have tried the simplest background representation possible, namely a linear function of temperature for each experimental isobar:

$$\hat{C}_{P,\mathrm{b}} = A + B\hat{T}, \tag{8.1.19}$$

$$\hat{\kappa}_{T,\mathrm{b}} = C + D\hat{T}, \tag{8.1.20}$$

$$\hat{\alpha}_{V,\mathrm{b}} = E + F\hat{T}, \tag{8.1.21}$$

where A, B, C, D, E, F are adjustable constants that parametrically depend on the pressure. The coefficients a_1 and a_2 in Eq. (8.1.1) have been calculated from a fit to the data for the Widom line as specified by Mishima [17]:

$$h_1 = \Delta\hat{T} + a_1\Delta\hat{P} + a_2(\Delta\hat{P})^2 = 0. \tag{8.1.22}$$

We found the coefficient b_1 in Eq. (8.1.2) to be very small, indicating little asymmetry in the liquid-liquid critical behavior of supercooled water. Hence, in the final fit the coefficient b_1 was set equal to zero. The experimental data for the response functions have been obtained as a function of temperature and pressure. At each T and P, the scaling fields h_1 and h_2 are calculated from Eqs.(8.1.1,8.1.2) and then the order parameter ϕ_1 from Eq.(8.1.14). The molar volumes in Eqs.(8.1.11),(8.1.12) were estimated from an extrapolation of the IAPWS-95 Formulation for the Thermodynamic Properties of Ordinary Water Substance for General and Scientific Use [103]. Following Fuentevilla and Anisimov [84], we have neglected the small contribution from the term $2a_2\phi_1$ in Eq.(8.1.11).

The coefficients a_0 and u_0 in the classical Landau expansion (Eq.(8.1.11)) and the coefficients of the linear temperature dependence of the non-critical background contributions given by Eqs.(8.1.19-8.1.21) were determined from fits to the experimental

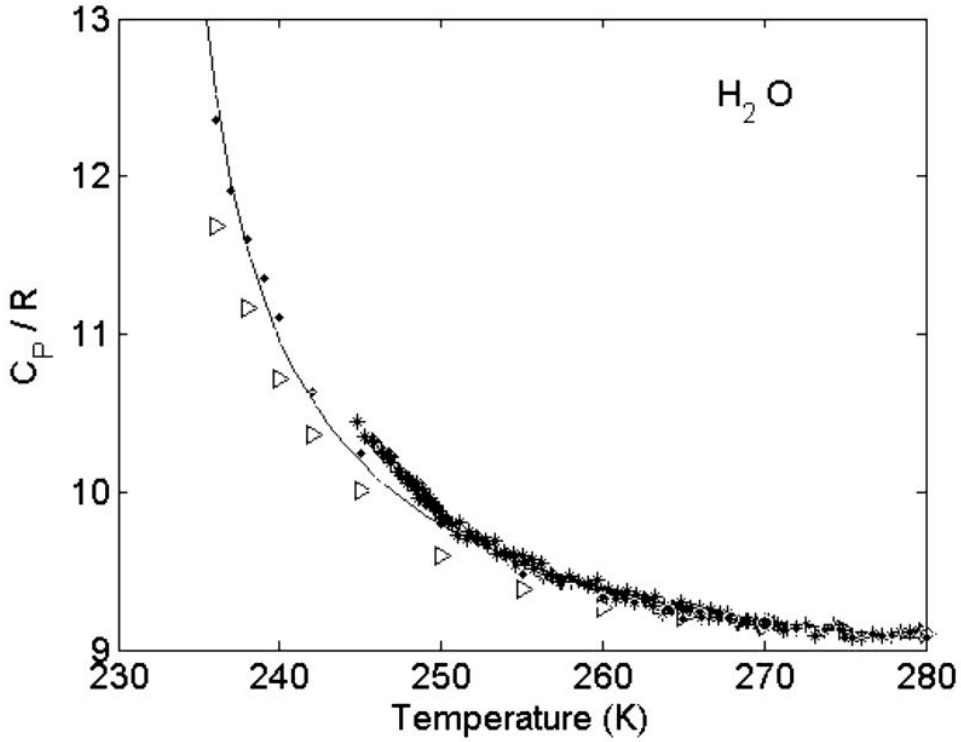

Figure 8.2: Comparison of mean-field equation of state with experimental data for the isobaric heat capacity at ambient pressure as a function of temperature in more detail

data. The critical parameters were also treated as adjustable constants but subject to the condition that they must be located on the Widom line as given by Eq.(8.1.22). The resulting values for the coefficients of the scaled equation of state are presented in Table 8.1.

For the critical parameters we found $P_c = 17$ MPa and $T_c = 229$ K. However, the chi-square of the fit depends relatively weakly on the values chosen for the critical parameters P_c and T_c, so that they could not be determined accurately from the fits.

The comparison of our mean-field thermodynamic model with experimental data for the heat capacity is shown in Figure 8.1, in detail in Figure 8.2, with experimental data for the isothermal compressibility in Figure 8.3 , and with experimental data for

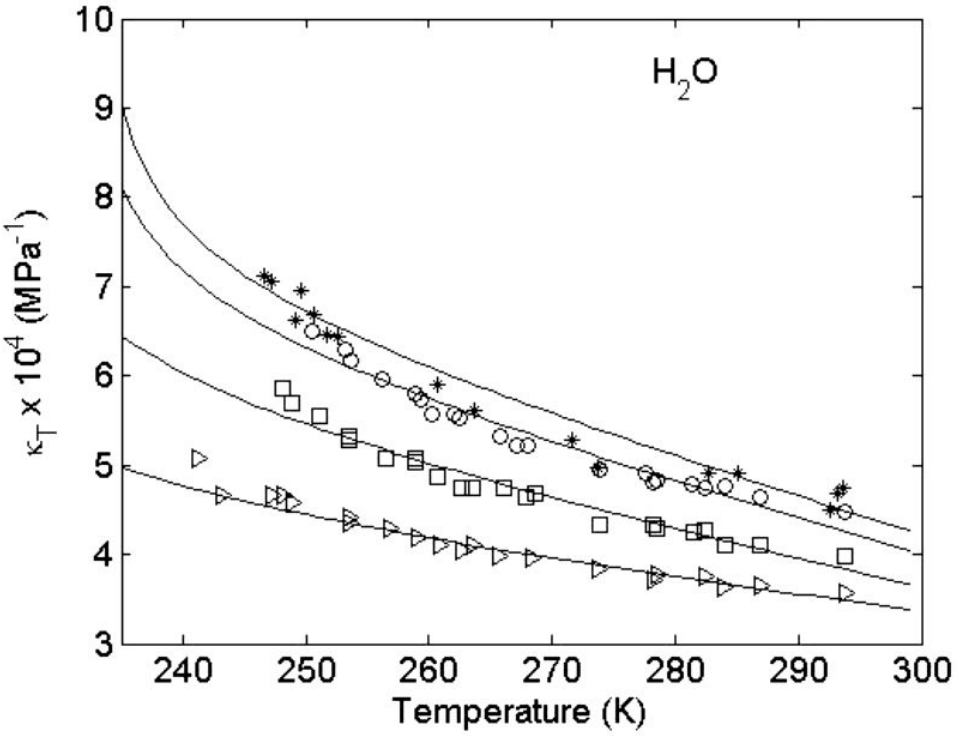

Figure 8.3: Comparison of mean-field equation of state with experimental data for the isochoric compressibility along isobars as a function of temperature. The curves represent calculated values, symbols indicate experimental data (stars 0.1 MPa [12], open circles 10 MPa [13], squares 50 MPa [13], triangles 100 MPa [13]).

the thermal expansivity data in Figure 8.4. These figures confirm that the assumption of liquid-liquid critical behavior of supercooled water already in a mean-field approximation yields a physically realistic explanation of the anomalous temperature dependence of the isobaric heat capacity, the isothermal compressibility, and the thermal expansivity observed experimentally in supercooled water.

Table 8.1: Parameters of the mean-field model

P_c		17 MPa
T_c		229 K
a_0		0.017
u_0		0.98
a_1		0.0734
a_2		0.0165
b_1		0.
$\hat{C}_{P,b} = A + B\hat{T}$	$P = 0.1$ MPa	$\hat{C}_{P,b} = 7.161 + 0.615\hat{T}$
$\hat{\alpha}_{V,b} = C + D\hat{T}$	$P = 0.1$ MPa	$\hat{\alpha}_{V,b} = -1.273 + 1.102\hat{T}$
	$P = 40$ MPa	$\hat{\alpha}_{V,b} = -0.549 + 0.550\hat{T}$
	$P = 70$ MPa	$\hat{\alpha}_{V,b} = -0.0755 + 0.162\hat{T}$
	$P = 100$ MPa	$\hat{\alpha}_{V,b} = 0.362 - 0.199\hat{T}$
$\hat{\kappa}_{T,b} = E + F\hat{T}$	$P = 0.1$ MPa	$\hat{\kappa}_{T,b} = 0.163 - 0.0942\hat{T}$
	$P = 10$ MPa	$\hat{\kappa}_{T,b} = 0.151 - 0.0866\hat{T}$
	$P = 50$ MPa	$\hat{\alpha}_{V,b} = 0.120 - 0.0655\hat{T}$
	$P = 100$ MPa	$\hat{\alpha}_{V,b} = 0.0738 - 0.0339\hat{T}$

8.2 Most recent results in the research of the mean-field approximation

Holten et al.[55] have applied the mean field approximation to the HBAS model. Recently, it has been shown that by assuming the existence of a liquid–liquid critical point, the theory of critical phenomena can give an accurate account of the experimental thermodynamic-property data up to the pressure of 150 MPa [11, 96]. In addition, a phenomenological extension of the theoretical model can account for all available experimental data of ordinary and heavy supercooled water up to 400 MPa [96] within experimental accuracy, thus establishing a benchmark for any further developments in this area. In the works [11, 96] an asymptotic scaled equation was used to describe the critical parts of the thermodynamic properties. However, the

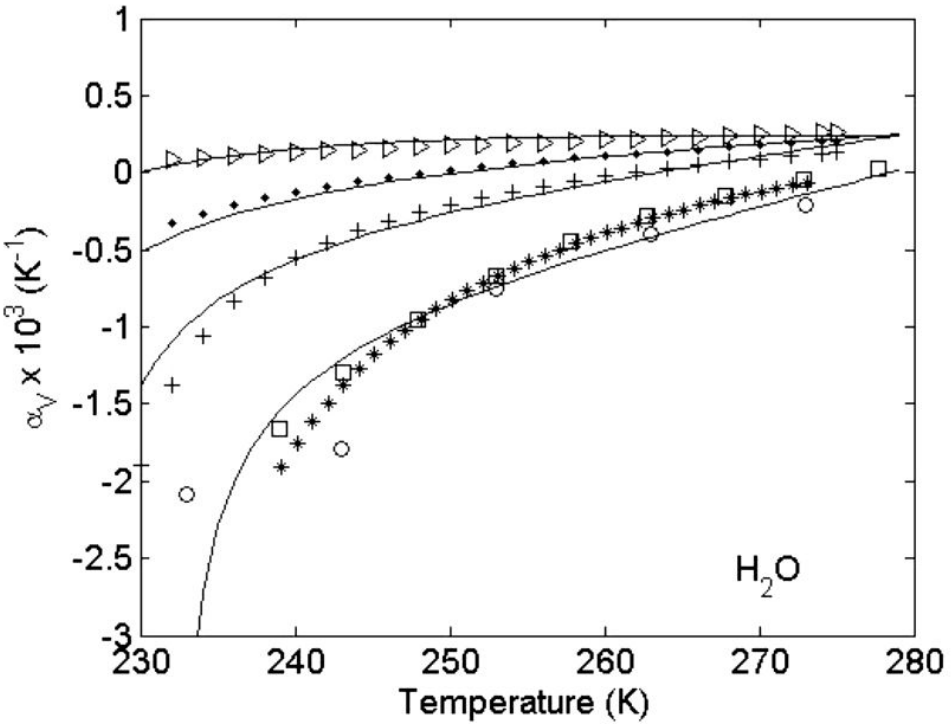

Figure 8.4: Comparison of mean-field equation of state with experimental data for the thermal expansivity along isobars as a function of temperature. The curves represent values calculated from the equations presented in this thesis. The symbols indicate experimental data (squares 0.1 MPa [14], stars 0.1 MPa [15], open circles 0.1 MPa [16], plus 40 MPa [17], diamonds 70 MPa [17], triangles 100 Mpa [17]).

actual experimental data are located in a non-asymptotic temperature range and pressure range, not closer than 5 % (in relative temperature and pressure) from the assumed location of the critical point. Any non-asymptotic features of the thermodynamic properties were effectively absorbed by the adjustable analytic backgrounds. The available numerical data in the critical region of the Ising model are known to exhibit a crossover from scaled critical behavior asymptotically close to the critical point to mean-field critical behavior further away from the critical point [104]. The crossover from asymptotic scaled critical behavior to mean-field critical behavior has also been observed in ionic solutions [105] and in polymer solutions [106]. Hence,

the question arises whether the available experimental data in supercooled water can also be effectively described in terms of a mean-field approximation. An advantage is that mean-field equations for critical thermodynamic behavior are very simple and suitable for practical applications if they do give a representation of the available property data within experimental accuracy. Following Holten et al. [96], for the relationships between the scaling fields and the physical fields near the liquid–liquid critical point in supercooled water we adopt:

$$h_1 = \Delta\hat{T} + a'\Delta\hat{P}, \tag{8.2.1}$$

$$h_2 = -\Delta\hat{P}, \tag{8.2.2}$$

$$h_3 = \Delta\hat{P} - \Delta\hat{\mu} + \Delta\hat{\mu}^r. \tag{8.2.3}$$

In (8.2.1), the system-dependent coefficient a' represents the limiting slope of the phase-coexistence or the Widom line $h_1 = 0$. In Ref. [96], Eq. (8.2.2) contains an additional mixing term $b'\Delta\hat{T}$ on the right-hand side. Since this mixing term was not found to improve the description [96], we have not included it. The equation (2.2.1) only represents the asymptotic behavior of the so-called singular critical contributions to the thermodynamic properties. To obtain a complete representation of the thermodynamic properties, we need to add a regular (i.e., analytic) background contribution. As common practice in developing scaled equations of state in fluids near the vapor-liquid critical point suggests [72, 107], the regular background contribution is represented by the truncated Taylor-series expansion around the critical point:

$$\Delta\hat{\mu}^r = \sum_{m,n} c_{mn}(\Delta\hat{T})^m(\Delta\hat{P})^n, \tag{8.2.4}$$

with $c_{00} = c_{10} = c_{01} = 0$. The first two terms in the temperature expansion of $\Delta\hat{\mu}^r$ depend on the choice of zero entropy and energy and do not appear in the expressions of

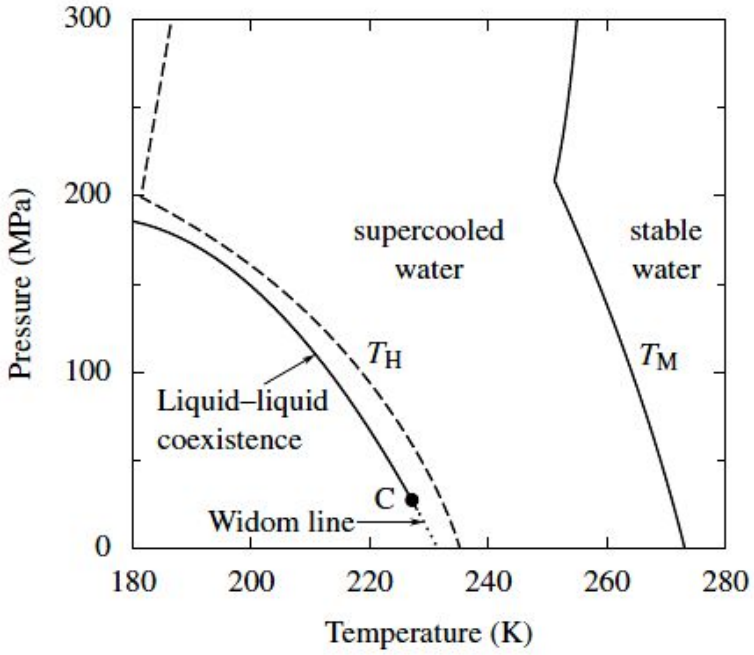

Figure 8.5: Hypothetical phase diagram of cold water. T_M is the melting line [18, 19]. T_H is the line of homogeneous ice nucleation [20, 21]. The location of the liquid–liquid coexistence curve is shown as suggested by Mishima [17], and the location of the LLCP (C), about 27 MPa, as suggested in Ref. [11]. The continuation of the liquid coexistence curve into the one-phase region is the line of maximum fluctuations, the Widom line [22].

any of the physically observable thermodynamic properties. Hence, these coefficients may be set to zero. Furthermore, the coefficient $c_{01} = V_c - 1 = 0$. Strictly speaking, critical fluctuations also yield an analytic contribution to h_3 [102, 71]. In this thesis we incorporate this contribution into the linear background contribution as has also been done in Ref. [96]. From Eqs. (8.2.1–8.2.3) and the fundamental thermodynamic differential relation can be written

$$d\hat{\mu} = \hat{V}d\hat{P} - \hat{S}d\hat{T}. \tag{8.2.5}$$

One finds for the volume $\hat{V}$ and entropy $\hat{S}$ that

$$\hat{V} = \left(\frac{\partial \hat{\mu}}{\partial \hat{P}}\right)_T = 1 - a'\Phi_1 + \Phi_2 + \Delta\hat{\mu}^r_{\hat{P}}, \tag{8.2.6}$$

$$\hat{S} = -\left(\frac{\partial \hat{\mu}}{\partial \hat{T}}\right)_P = \phi_1 - \Delta\hat{\mu}^r_{\hat{T}}. \tag{8.2.7}$$

We adopt the convention that the subscript $\hat{P}$ indicates a derivative with respect to $\hat{P}$ at constant $\hat{T}$ and the subscript $\hat{T}$ indicates a derivative with respect to $\hat{T}$ at constant $\hat{P}$. Finally, the dimensionless experimental susceptibilities, isothermal compressibility $\hat{\kappa}_T$, expansivity coefficient $\hat{\alpha}_V$, and isobaric heat capacity $\hat{C}_P$, can be expressed in terms of the theoretical scaling susceptibilities

$$\hat{\kappa}_T = -\frac{1}{\hat{V}}\left(\frac{\partial \hat{V}}{\partial \hat{P}}\right)_T = \frac{1}{\hat{V}}\left[\chi_2 - 2a'\chi_{12} + (a')^2\chi_1 - \Delta\hat{\mu}^r_{\hat{P}\hat{P}}\right], \tag{8.2.8}$$

$$\hat{\alpha}_V = \frac{1}{\hat{V}}\left(\frac{\partial \hat{V}}{\partial \hat{T}}\right)_P = \frac{1}{\hat{V}}\left[\chi_{12} - a'\chi_1 + \Delta\hat{\mu}^r_{\hat{T}\hat{P}}\right], \tag{8.2.9}$$

$$\hat{C}_P = \hat{T}\left(\frac{\partial \hat{S}}{\partial \hat{T}}\right)_{\hat{P}} = \hat{T}\left[\chi_1 - \Delta\hat{\mu}^r_{\hat{T}\hat{T}}\right]. \tag{8.2.10}$$

These equations contain fewer terms than the ones in Ref. [96] because we have not included the mixing term $b'\Delta\hat{T}$ in Eq. (8.2.2) as explained above. In the linear model the explicit relationships between the variables (h_1, h_2, ϕ_1) and (r, θ) are

$$h_1 = ar^{\beta+\gamma}\theta(1-\theta^2), \tag{8.2.11}$$

$$h_2 = r(1 - b^2\theta^2), \tag{8.2.12}$$

$$\phi_1 = kr^\beta\theta, \tag{8.2.13}$$

where a and k are system-dependent amplitudes, $\gamma = 2 - \alpha - 2\beta$, and where b is a universal constant, $b^2 = (\gamma - 2\beta)/[\gamma(1-2\beta)] \simeq 1.36$. The scaling properties are

analytic functions of θ. The weakly fluctuating scaling density derived from this equation of state is

$$\phi_2 = akr^{1-\alpha}s(\theta), \tag{8.2.14}$$

and the scaling susceptibilities are given by

$$\chi_1 = \frac{k}{a}r^{-\gamma}c_1(\theta), \tag{8.2.15}$$

$$\chi_{12} = kr^{\beta-1}c_{12}(\theta), \tag{8.2.16}$$

$$\chi_2 = akr^{-\alpha}c_2(\theta), \tag{8.2.17}$$

where the analytic functions s, c_1, c_{12}, and c_2 are given in Chapter 3, "Parametric equation of state". In the mean-field approximation ($\alpha = 0$, $\beta = 1/2$) the field h_3, given by Eq. (2.2.1), can be represented by the truncated Landau expansion Eq. (8.1.13). One can find that for $h_2 < 0$, Eq. (8.1.14) also has a metastable solution for a certain range of h_1 values around zero. This range is limited by the spinodals located at

$$\phi_1 = \pm\left(\frac{2a_0|h_2|}{u_0}\right)^{1/2}, \qquad h_1 = \pm\frac{(2a_0|h_2|)^{3/2}}{3u_0^{1/2}}. \tag{8.2.18}$$

On the binodal ($h_1 = 0$ and $h_2 < 0$), the values of ϕ_1 are

$$\phi_1 = \pm\left(\frac{6a_0|h_2|}{u_0}\right)^{1/2}. \tag{8.2.19}$$

The linear model can also be used in the mean-field approximation. In this approximation, the values of the critical exponents are $\alpha = 0$, $\beta = 1/2$, and $\gamma = 1$, and the value of b^2 is $3/2$ [71]. The scaling densities and susceptibilities are

$$\phi_1 = kr^{1/2}\theta, \qquad \phi_2 = -\tfrac{1}{2}akr\theta^2, \tag{8.2.20}$$

$$\chi_1 = \frac{k}{a}r^{-1}, \qquad \chi_{12} = -kr^{-1/2}\theta, \qquad \chi_2 = ak\theta^2. \tag{8.2.21}$$

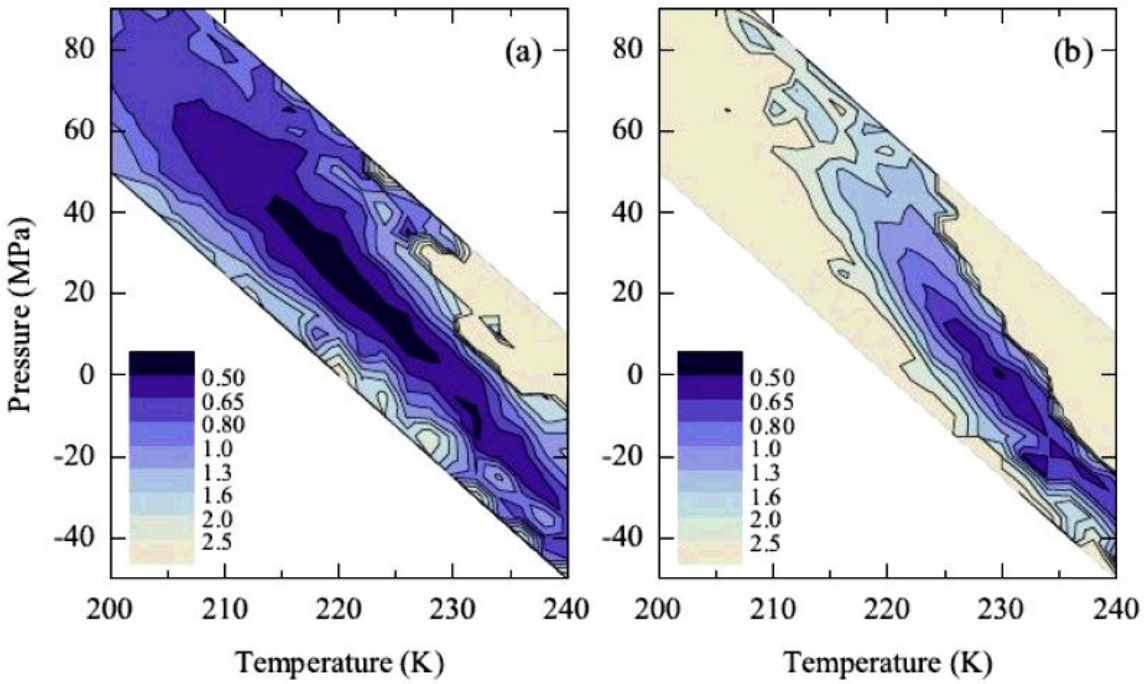

Figure 8.6: Reduced sum of squared residuals as a function of the location of the liquid–liquid critical point. (a) Unconstrained fit; (b) Constrained fit: slope of the liquid–liquid transition line a' restricted to the range 0.065–0.090.

The coefficients a_0 and u_0 in Eq. (8.1.13) are related to a and k according to

$$a_0 = a/k, \qquad u_0 = 3a/k^3. \tag{8.2.22}$$

For the computation of properties from the mean-field model, we did not use the linear-model variables given above. Instead, the scaling fields h_1 and h_2 were computed from Eqs. (8.2.1), (8.2.2), and the scaling densities ϕ_1 and ϕ_2 followed from Eqs. (8.1.13) and (8.1.15). The scaling susceptibilities were calculated with Eqs. (8.1.16–8.1.18), and the thermodynamic properties followed from Eqs. (8.2.6–8.2.10). Nevertheless, the linear-model equations allow comparing the values of the Landau-expansion coefficients a_0 and u_0 with the linear-model amplitudes a and k obtained by the scaling model. In particular, the mean-field values $a \simeq 0.17$ and $k \simeq 0.58$,

Table 8.2: Parameters for EOS with P_c fixed at 0 MPa

Parameter	Value[a]	Parameter	Value
T_c (K)	229.25	c_{11}	3.9564×10^{-1}
P_c (MPa)	0.00	c_{12}	-1.5833×10^{-2}
ρ_c (kg m^{-3})	923.71	c_{13}	2.9268×10^{-3}
a_0	0.29828	c_{20}	-3.4876×10^{0}
u_0	2.6209	c_{21}	1.9529×10^{-2}
a'	0.087272	c_{22}	-3.8655×10^{-2}
c_{02}	4.6287×10^{-2}	c_{23}	-3.1951×10^{-3}
c_{03}	3.3954×10^{-3}	c_{30}	5.4631×10^{-1}
c_{04}	-9.5250×10^{-4}	c_{31}	-3.3151×10^{-2}
c_{05}	1.1948×10^{-4}	c_{32}	5.6790×10^{-2}

[a] Final digits of parameter values are given to allow reproducing the values of properties calculated with the model but do not have physical significance.

calculated from Eq. (8.2.22) with a_0 and u_0 taken from Table 8.2, can be compared with the scaling-model values $a \simeq 0.29$ and $k \simeq 0.38$ [96]. Not surprisingly, these values are of the same order.

While the liquid-liquid transition (LLT) is likely curved in the pressure-temperature plane, as it is shown in Figure (8.5), we have used a linearized LLT, like in previous studies [11, 96]. The mean-field critical model was fitted to the experimental property data of supercooled and stable water up to 150 MPa in the same manner as described by Holten et al. [96] for a scaled non-analytic parametric equation. With a completely unrestricted slope and position of the LLT, the fit was found to be insensitive to the critical pressure. As shown in Figure 8.6a, good fits could be obtained for critical pressures from about -30 MPa to 60 MPa. To reduce the uncertainty in the location of the critical point, the constraints used in Ref. [96] were adopted: a', the slope of the LLT, was restricted to the range 0.065–0.090, and the critical point was allowed

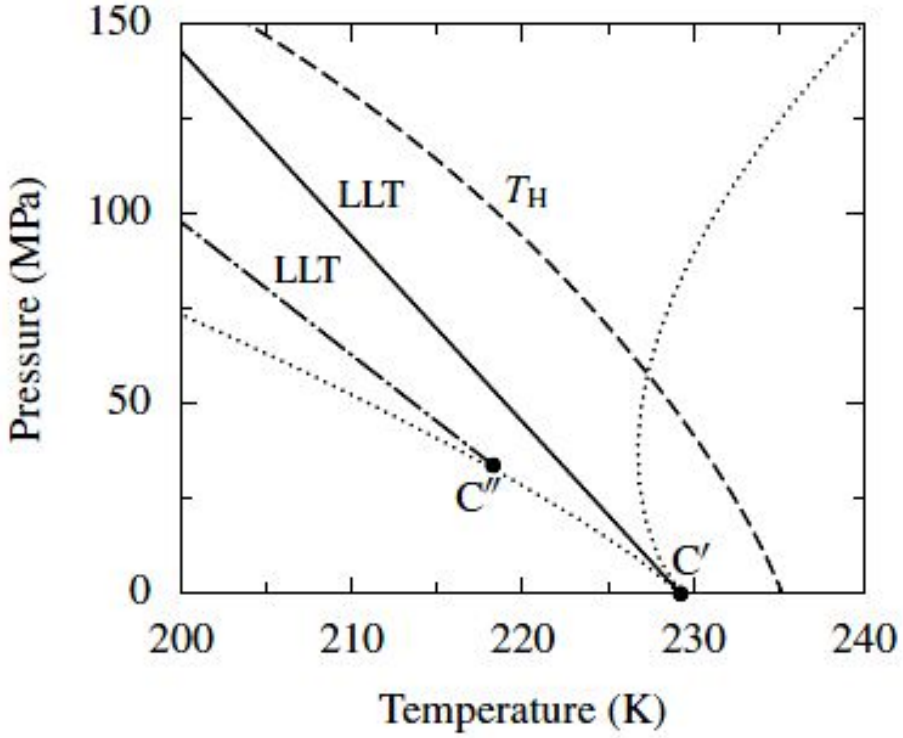

Figure 8.7: Location of the liquid-liquid transition (LLT) lines of the limited-pressure-range model (solid) and the extended-pressure-range model (dash-dotted). The dashed curve is the experimental homogeneous ice nucleation temperature T_{H} [20, 21]. The liquid–liquid critical points are denoted by C′ (limited model) and C″ (extended model). The spinodals (Eq.(8.2.18)) of the limited model are shown as dotted curves.

to deviate at most 3 K from the LLT curve suggested by Mishima [17]. With these constraints, good fits were found for critical pressures in the range of about -10 MPa to 10 MPa, as one can see in Figure 8.6b. The quality of the fit was insensitive to the critical pressure for values in this range, so the critical pressure for this particular model was set to zero. The resulting optimized parameters are given in Table 8.2, and the location of the LLT is shown in Figure 8.6. The densities calculated from the model are compared with experimental data in Figure 8.8. Good agreement with the data is found, and the temperature of maximum density, shown in Figure 8.9, is

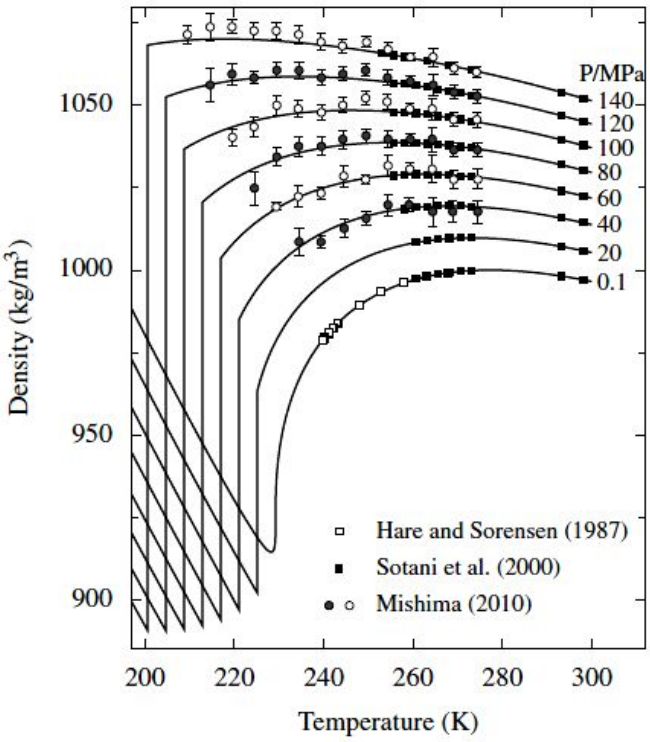

Figure 8.8: Densities of H_2O according to the model (curves). The symbols represent experimental data of Mishima [17], Sotani et al. [23] and Hare and Sorensen [15]. The symbols for Mishima's densities on different isobars are alternatingly open and filled to guide the eye.

also well represented. The expansivity coefficient and isothermal compressibility calculated with the model are graphed in Figures 8.10 and 8.11. The predicted isobaric heat capacity agrees with the data of Archer and Carter [10], to which the model was fitted. The predicted isochoric heat capacity becomes negative and diverges at about 229 K (at 0.1 MPa), which means that the liquid becomes thermally unstable below that temperature. At lower temperatures, the liquid state also becomes mechanically unstable, as is illustrated in Figure 8.13. The reversal of thermal and mechanical stability in supercooled water was also found on the basis of a scaled non-analytic equation of state [96]. In the previous study of Bertrand and Anisimov [96], it was

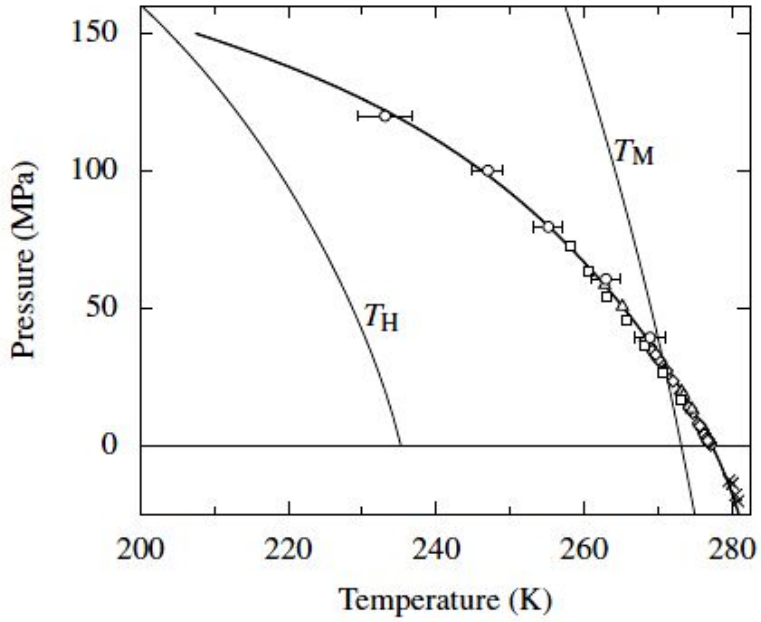

Figure 8.9: Temperature of maximum density of H_2O as a function of pressure according to the model (thick solid curve). T_M marks the melting curve [18, 19] and its extension to negative pressures [24]; T_H denotes the homogeneous nucleation limit [20]. Symbols represent experimental data [25, 26, 27, 23, 17]. The temperatures of maximum density for Mishima's data [17] were determined by locating the maxima of fits to his density data.

concluded that the mean-field equation of state could fairly describe the heat capacity and thermal expansivity with linear background terms, while the compressibility was not accurately represented. However, as shown in this work, with a certain freedom of the location of the LLT line, we can describe all properties with the same quality as the scaling model.

It is possible to extend the model in such a way that all experimental data of supercooled water, up to the pressure of 400 MPa, can be represented. Such an extension must be regarded as semi-empirical, since far away from the critical point critical fluctuations are of no importance, and the non-critical regular part dominates

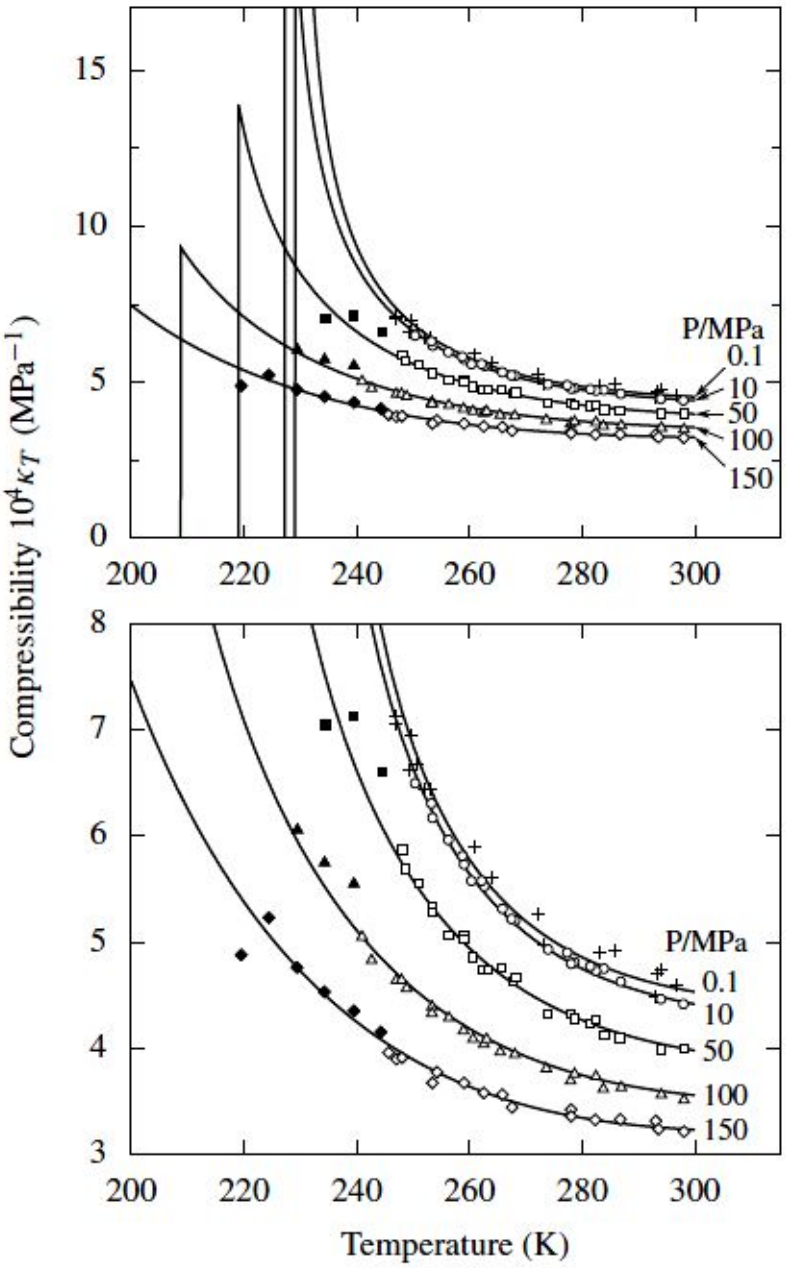

Figure 8.10: Isothermal compressibility of H_2O according to the model (curves). For clarity, the curves are not shown for temperatures below the LLT line in the bottom graph. Symbols represent experimental data of Speedy and Angell [12], Kanno and Angell [13], and Mishima [17]. Solid and open symbols of the same shape correspond to the same pressure.

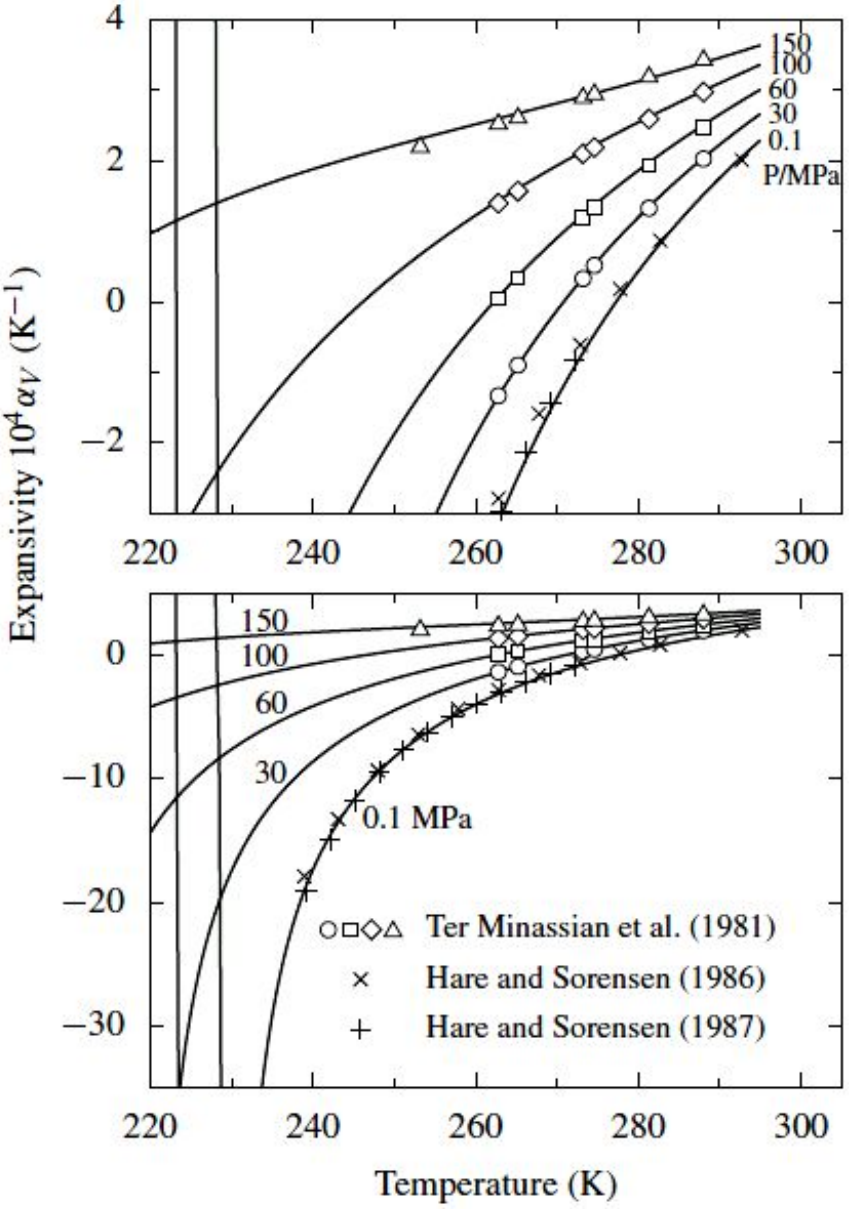

Figure 8.11: Expansivity coefficient of H_2O according to the model (curves). Symbols represent experimental data of Ter Minassian et al. [26] and Hare and Sorensen [14, 15].

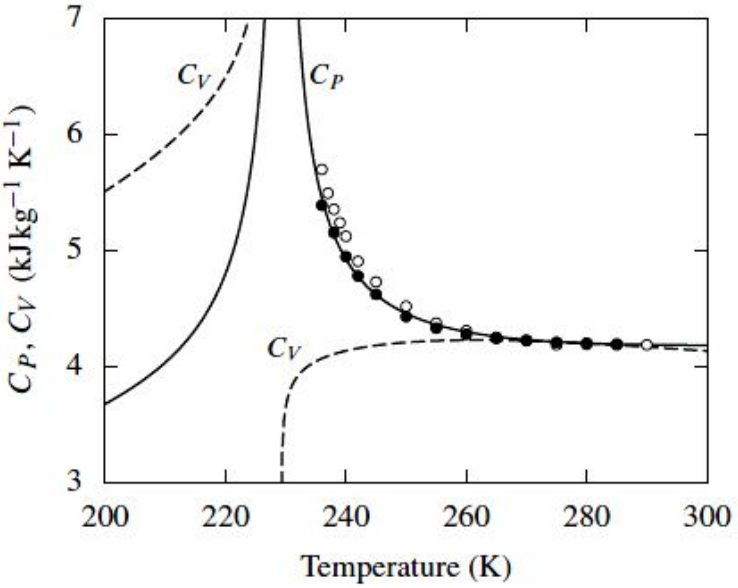

Figure 8.12: Isobaric and isochoric heat capacity of H_2O versus temperature at 0.1 MPa according to the model. Symbols represent experimental data of Angell et al. [7] and Archer and Carter [10].

the thermodynamic properties. Moreover, a linearization of the LLT for pressures up to 400 MPa is unlikely to be a good approximation of a curved LLT. Nevertheless, by allowing the location and slope of the linearized LLT to be unconstrained, and by adding two background parameters, all data could be represented. The optimized parameters are given in Table 8.3, and the location of the LLT is shown in Figure 8.7. For the fit given here, the critical point is located at about 218 K and 34 MPa. However, similarly to the limited-pressure model, a good fit can be obtained for critical point locations in a certain range, in this case from about -10 MPa to 60 MPa. The resulting description of the thermodynamic properties is similar to the limited-pressure model, so only the result for the density is given here (Figure 8.14).

We have shown that a mean-field approximation of the theory of critical phenomena can describe the anomalous thermodynamic properties of supercooled water

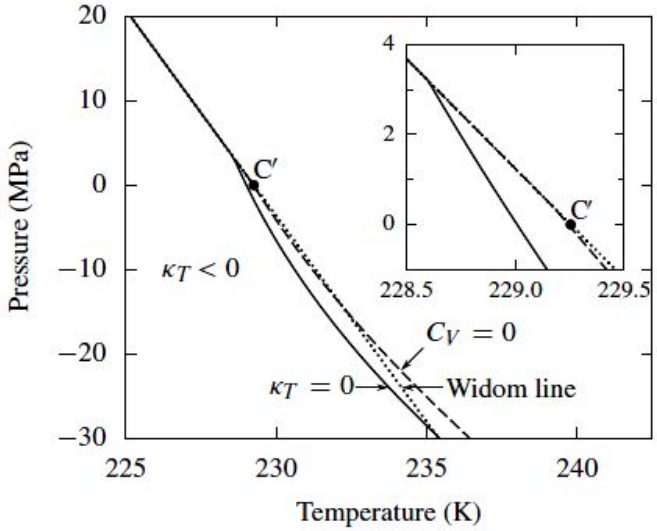

Figure 8.13: Absolute stability limit of the liquid state, predicted by the limited-pressure-range model. Solid line: limit of mechanical stability, where the isothermal compressibility κ_T is zero. Dashed line: limit of thermal stability, where the isochoric heat capacity C_V is zero. C′ indicates the liquid–liquid critical point of the model. The dotted line, at which $h_1 = 0$ (8.2.1), indicates the liquid–liquid transition line and its extension below the critical pressure, the Widom line. The inset shows the stability limits in the vicinity of the critical point, which is located in the mechanically and thermally stable region.

Table 8.3: Parameters for the semi-empirical equation of state

Parameter	Value	Parameter	Value
T_c(K)	218.27	c_{12}	-2.0115 $\times 10^{-2}$
P_c (MPa)	33.822	c_{13}	2.7532 $\times 10^{-3}$
ρ_c(kg m^{-3})	932.67	c_{14}	-2.0219 $\times 10^{-4}$
a_0	0.28726	c_{20}	-3.3946 $\times 10^{0}$
u_0	3.6547	c_{21}	-1.0517 $\times 10^{-1}$
a'	0.12275	c_{22}	-7.8267 $\times 10^{-3}$
c_{02}	4.1231 $\times 10^{-2}$	c_{23}	2.0144 $\times 10^{-4}$
c_{03}	5.5959 $\times 10^{-4}$	c_{30}	4.8304 $\times 10^{-1}$
c_{04}	-2.3590 $\times 10^{-4}$	c_{31}	1.5453 $\times 10^{-1}$
c_{05}	2.5739 $\times 10^{-5}$	c_{32}	5.1032 $\times 10^{-3}$
c_{11}	3.7040 $\times 10^{-1}$	c_{41}	-7.9993 $\times 10^{-2}$

with the same accuracy and with the same number of adjustable parameters as the scaling theory. The reason of the insensitivity to a particular form of the equation of state is the lack of experimental data in the region asymptotically close to the critical point. In particular, without assumptions or independent information regarding the position of the liquid-liquid transition line, the exact location of the critical point becomes uncertain and cannot be accurately determined from the available thermodynamic property data alone. However, we have verified that it is impossible to represent the experimental data in terms of a polynomial representation that does not include any divergent critical behavior of the thermodynamic response functions.

The mean-field approximation has advantages and disadvantages compared to the scaling-theory equation of state. Computationally, the mean-field equation of state is simpler than the one based on the scaling theory and is therefore easier for engineering use. On the other hand, the mean-field approximation neglects critical fluctuations, thus lacking an important physical feature of critical phenomena. In particular, it is known that the critical fluctuations shift the location of the critical point, characterized by $P_c/\rho_c RT_c$, by 10–15 % with respect to the mean-field prediction [108]. For the liquid–liquid point in supercooled water, it would mean a fluctuation-induced increase in the critical-pressure value by 10–15 MPa. When more experimental information becomes available in the supercooled region, it may be possible to develop a crossover equation of state, for example, based on a two-state model of water as suggested by Bertrand and Anisimov [96], which would both incorporate critical fluctuations and provide a correct mean-field description far away from the critical point [108].

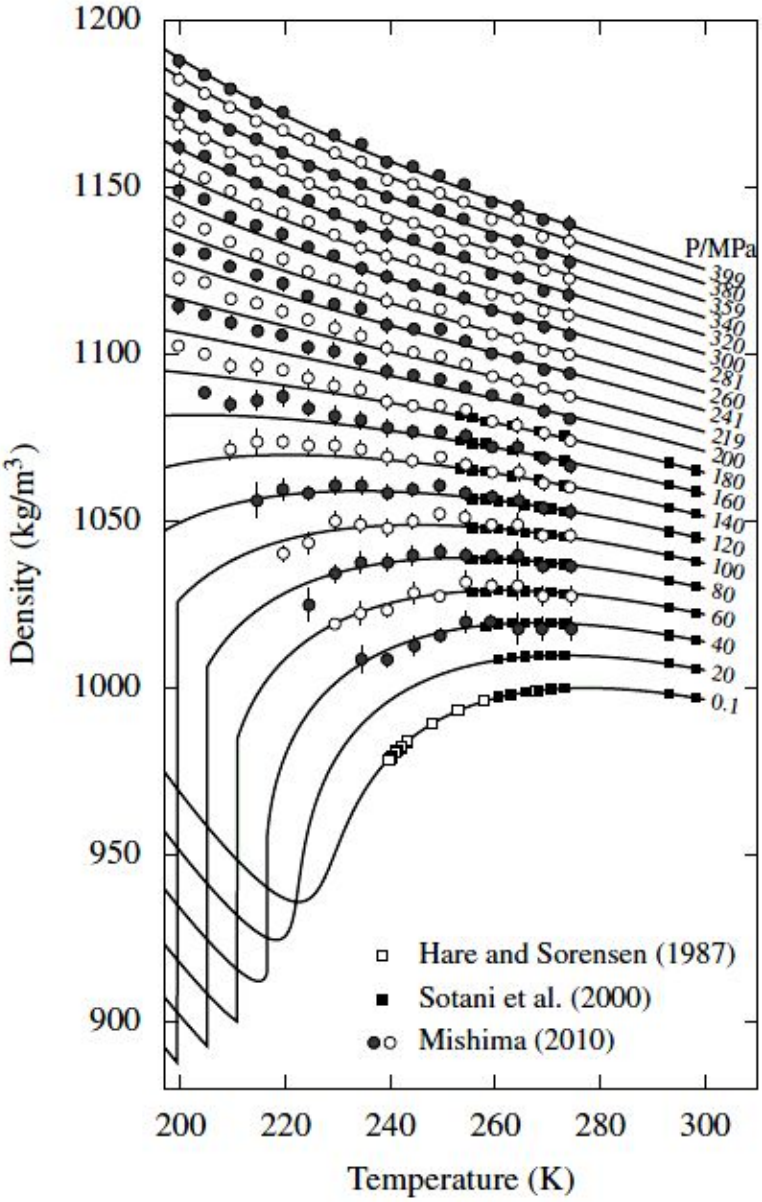

Figure 8.14: Densities of H_2O according to the extended, semi-empirical model (curves). The symbols represent experimental data of Mishima [17], Sotani et al. [23] and Hare and Sorensen [15]. The symbols for Mishima's densities on different isobars are alternatingly open and filled to guide the eye.

Chapter 9

Summary

9.1 Conclusions

- The equation for vapor pressure was developed on the basis of the mean-field approximation of the scaled equation for supercooled water. The range of validity of the vapor pressure equation is from 130 K to 647 K. The Wagner and Pruß equation is possible to be used already for temperatures above 243 K, not only in the range of validity from 273 K to 647 K. The results were presented at the XV. IAPWS conference in Berlin (2008) and at the 17th Symposium on Thermophysical properties in Boulder (2009).

- The analytic background functions for the Fuentevilla and Anisimov model in the mean-field approximation were calculated and comparisons with experimental data were made. The results were presented at the XV. IAPWS conference in Berlin (2008).

- The evaluation of the influence of the new calculated and measured values of critical exponents on the linear model of the parametric equation of state was shown. The results were published in the Journal Littera Scripta, 2011 (in Czech).

- The mean-field approximation of the equation of state of supercooled water was tested and the comparison with experimental data was carried out. This research was executed at the University of Maryland and was supported by a grant from the International Association for the Properties of Water and Steam. The paper with the results has been submitted to the International Journal of Thermophysics and is under review.

- Properties of the surface tension of supercooled water were studied and a new relation describing the surface tension from 228 K to 647 K was developed. The second inflection point of the temperature dependence of the surface tension was calculated at the temperature about 1.5 C. This work is prepared to be published.

9.2 Future work

- The papers [11, 96] show, that the description of D_2O is very similar to ordinary water, only parameters are shifted. Mean-field approximation of properties of D_2O will be needed.

- Further testing of the developed models to all existing experimental data is needed.

- A new practical state equation for supercooled water, suitable for meteorology, studies of the aircraft icing, for atmospheric boundary layer physics or in biology, etc. should be developed.

- We would like to continue in the cooperation with the world known research group of Professors Mikhail A. Anisimov and Jan V. Sengers from the University of Maryland, U.S.A. and with working groups of the International Association for the properties of water and steam.

Bibliography

[1] O. Mishima and H. E. Stanley. The relationship between liquid, supercooled and glassy water. *Nature*, 396:329–335, 1998.

[2] IAPWS release on surface tension of ordinary water substance. Available at http://www.iapws.org, 1994.

[3] P. T. Hacker. *Experimental values of the surface tension of supercooled water, Technical Note 2510.* National Advisory Committee for Aeronautics, Washington, 1951.

[4] M. A. Floriano and M. A. Angell. Surface tension and molar surface free energy and entropy of water to -27.2 °C. *J. Phys. Chem.*, 94:4199–4202, 1990.

[5] E. W. Washburn. *International Critical Tables.* McGraw-Hill, New York, 1928.

[6] Y. Lü and B. Wei. A molecular dynamics study on surface properties of supercooled water. *Science in China Series G: Physics, Mechanics and Astronomy*, 49:616–625, 2006.

[7] C. A. Angell; M. Oguni and W. J. Sichina. Heat capacity of water at extremes of supercooling and superheating. *J. Phys. Chem.*, 86:998 – 1002, 1982.

[8] E. Tombari; C. Ferrari and G. Salvetti. Heat capacity anomaly in a large sample of supercooled water. *Chem. Phys. Lett.*, 300:749 – 751, 1999.

[9] M. A. Anisimov; A. V. Voronel; N. S. Zaugolnikova and G. I. Ovodov. Specific heat of water near the melting point and Ornstein-Zernike fluctuation corrections. *JETP Letters*, 15:449 – 452, 1972.

[10] D. G. Archer and R. W. Carter. Thermodynamic properties of the NaCl + H_2O system. 4. Heat capacities of H_2O and NaCl(aq) in cold-stable and supercooled states. *J. Phys. Chem. B*, 104:8563 – 8584, 2000.

[11] C. E. Bertrand and M. A. Anisimov. Peculiar thermodynamics of the second critical point in supercooled water. *J. Phys. Chem. B*, 115:14099 – 14111, 2011.

[12] R. J. Speedy and C. A. Angell. Isothermal compressibility of supercooled water and evidence for a thermodynamic singularity at -45 °c. *J. Chem. Phys.*, 65:851 – 858, 1976.

[13] H. Kanno and C. A. Angell. Water: Anomalous compressibilities to 1.9 kbar and correlation with supercooling limits. *J. Chem. Phys.*, 70:851 – 858, 1979.

[14] D. E. Hare and C. M. Sorensen. Densities of supercooled H_2O and D_2O in 25 μ glass capillaries. *J. Chem. Phys.*, 84:5085 – 5089, 1986.

[15] D. E. Hare and C. M. Sorensen. The density of supercooled water. ii. bulk samples cooled to the homogeneous nucleation limit. *J. Chem. Phys.*, 87:4840 – 4845, 1987.

[16] W. Wagner and A. Pruß. International equations for the saturation properties of ordinary water substance. Revised according to the international temperature scale qof 1990. *Physica A*, 323:51 – 66, 2003.

[17] O. Mishima. Volume of supercooled water under pressure and the liquid - liquid critical point. *J. Chem. Phys.*, 133:144503, 2010.

[18] IAPWS revised release on the pressure along the melting and sublimation curves of ordinary water substance. Available at http://http://www.iapws.org/relguide/MeltSub2011.pdf, 2011.

[19] W. Wagner; T. Riethmann; R. Feistel and A. H. Harvey. New equations for the sublimation pressure and melting pressure of H_2O ice Ih . *J. Phys. Chem. Ref. Data*, 40:043103 – 043113, 2011.

[20] H. Kanno; R. J. Speedy and C. A. Angell. Supercooling of water to -92c under pressure. *Science*, 12:880 – 881, 1975.

[21] H. Kanno and K. Mizata. The location of the second critical point of water. *Chem. Phys. Lett.*, 242:507 – 512, 2006.

[22] L. Xu; P. Kumar; S. V. Budyrev; S. H. Chen; P. H. Poole; F. Sciortino and H. E. Stanley. Relation between the widom line and dynamic crossover in systems with a liquid-liquid phase transitions. *PNAS*, 102:16558 – 16562, 2005.

[23] T. Sotani; J. Arabas; H. Kubota; M. Kijima and S. Asada. Volumetric behaviour of water under high pressure at subzero temperature. *High Temp. High Pressures*, 32:433 – 440, 2000.

[24] S. J. Henderson and R. J. Speedy. Melting temperature of ice at positive and negative pressures. *J. Phys. Chem.*, 91:3069 – 3072, 1987.

[25] D. R. Caldwell. The maximum-density points of pure and saline water. *Deep-Sea Res.*, 25:175–181, 1978.

[26] L. Ter Minassian; P. Pruzan and A. Soulard. Thermodynamic properties of water inder pressure up to 5 Kbar and between 28 and 120 c. estimations in the supercooled region down to -40 *c. J. Chem. Phys.*, 75:3064 – 3072, 1981.

[27] S. J. Henderson and R. J. Speedy. Temperature of maximum density in water at negative pressure. *J. Phys. Chem.*, 91:3062 – 3068, 1987.

[28] P. G. Debenedetti and H. E. Stanley. Supercooled and glassy water. *Physics Today*, 56:40–46, 2003.

[29] R. E. Apfel. Water superheated to 279,5 °C at atmospheric pressure. *Nature Phys. Sci.*, 238:63–64, 1972.

[30] Q. Zheng; D. J. Durben; G. H. Wolf and C. A. Angell. Liquids at large negative pressures: Water at the homogeneous nucleation limit. *Science*, 254:829–832, 1991.

[31] P. G. Debenedetti. *Metastable Liquids. Concepts and Principles.* Princeton University Press, Princeton, 1996.

[32] S. B. Kiselev. Kinetic boundary of metastable states in superheated and stretched liquids. *Physica A*, 269:252 – 268, 1999.

[33] S. B. Kiselev and J. F. Ely. Curvature effect on the physical boundary of metastable states in liquids. *Physica A*, 299:357 – 370, 2001.

[34] A. Z. Patashinskii and V. L. Pokrovskii. *Fluctuation Theory of Phase Transitions.* Pergamon Press, New York, 1979.

[35] J. W. Gibbs. *The Scientific Papers of J. Willard Gibbs, Ph.D.,LL.D.I. Thermodynamics.* Dover, New York, 1961.

[36] V. P. Skripov and V. P. Koverda. *Spontaneous Crystallization of Supercooled Liquids.* Nauka, Moskva, 1984.

[37] V. P. Skripov. *Metastable Liquids.* John Wiley, New York, 1974.

[38] V. P. Skripov and P. A. Pavlov. Explosive boiling of liquids and fluctuation nucleus formation. *High Temp.*, 8:782–787, 1970.

[39] O. Mishima. Polyamorphism in water. *Proc. Jpn. Acad, Ser. B*, 86:165–175, 2010.

[40] O. Mishima; L. D. Calvert and E. Whalley. Melting ice I at 77 k and 10 kbar: a new method of making amorphous solids. *Nature*, 310:393 – 395, 1984.

[41] O. Mishima; L. D. Calvert and E. Whalley. An apparently first-order transition between two amorphous phases of ice induced by pressure. *Nature*, 314:76 – 78, 1985.

[42] A. V. Voronel. Thermodynamic quantities near the crystallization points of liquids. *JETP Letters*, 14:174 – 177, 1971.

[43] J. A. Schufle. The specific gravity of supercooled water in a capillary. *Chemistry and Industry*, 16:690, 1965.

[44] J. A. Schufle and M. Venugopalan. Specific volume of liquid water to -40 °C. *J. Geophys. Res.*, 72:3271 – 3275, 1967.

[45] B. V. Zheleznyi. The density of supercooled water. *Russ. J. Phys. Chem.*, 43:1311, 1969.

[46] D. H. Rasmussen and A. P. MacKenzie. Clustering in supercooled water. *J. Chem. Phys.*, 59:5003 – 5013, 1973.

[47] C. M. Sorensen. Densities and partial molar volumes of supercooled aqueous solutions. *J. Chem. Phys.*, 79:1455 – 1461, 1983.

[48] F. Mallamace; C. Branca; M. Broccio; C. Corsaro; Ch. Mou and S. Chen. The anomalous behavior of the density of water in the range 30 K $< T <$ 373 K. *PNAS*, 104:18387 – 18391, 2007.

[49] D. H. Rasmussen; A. P. MacKenzie; C. A. Angell and J. C. Tucker. Anomalous heat capacities of supercooled water and heavy water. *Science*, 181:342 – 344, 1973.

[50] C. A. Angell; J. Shuppert and J. C. Tucker. Anomalous properties of supercooled water. heat capacity, expansivity and proton magnetic resonance chemical shift from 0 to -38. *J. Phys. Chem.*, 77:3092 – 3099, 1973.

[51] R. J. Speedy. Stability-limit conjecture. an interpretation of the properties of water. *J. Phys. Chem.*, 86:982 – 991, 1982.

[52] R. J. Speedy. Limiting forms of the thermodynamic divergences at the conjectured stability limits in superheated and supercooled water. *J. Phys. Chem.*, 86:3002 – 3005, 1982.

[53] P. G. Debenedetti. Supercooled and glassy water. *J. Phys.: Condens. Matter*, 15:R1669, 2003.

[54] P. G. Debenedetti. Reply to comment on 'supercooled and glassy water'. *J. Phys.: Condens. Matter*, 16:6815, 2004.

[55] V. Holten; J. Kalová; M. A. Anisimov and J. V. Sengers. Thermodynamics of liquid - liquid criticality in supercooled water in mean-field approximation. *Int. J. Thermophys., submitted.*

[56] S. Sastry; P. G. Debenedetti; F. Sciortino and H. E. Stanley. Singularity free interpretation of the thermodynamic of supercooled water. *Phys. Rev. E*, 53:6144 – 6154, 1996.

[57] H. E. Stanley and J. Teixeira. Interpretation of the unusual behavior of H_2O and D_2O.

[58] P. H. Poole; F. Sciortino; U. Essmann and H. E. Stanley. Phase behavior of metastable water. *Nature*, 360:324 – 328, 1992.

[59] P. H. Poole; U. Essmann; F. Sciortino and H. E. Stanley. Phase diagram for amorphous solid water. *Phys. Rev. E*, 48:4605 – 4610, 1993.

[60] S. Sastry; F. Sciortino and H. E. Stanley. Limits of stability of the liquid phase in a lattice model with water-like properties. *J. Chem. Phys.*, 98:9863 – 9872, 1993.

[61] D. A. Fuentevilla. A scaled parametric equation of state for the liquid-liquid critical point in supercooled water. Master's thesis, University of Maryland, 2007.

[62] M. A. Leontovich. *Introduction to thermodynamics. Statistical physics.* Nauka, Moscow, 1983.

[63] L. D. Landau and E. M. Lifshitz. *Statistical physics. 3rd edition Part 1.* Butterworth-Heinemann, Oxford, 1980.

[64] L. Onsager. Crystal statistics. I. A two-dimensional model with an order-disorder transition. *Phys.Rev.*, 65:117 – 149, 1944.

[65] J. M. H. Levelt Sengers; R. J. Hocken and J. V. Sengers. Critical-point universality and fluids. *Physics Today*, 30:42 – 51, 1977.

[66] M. E. Fisher. The renormalization group in the theory of critical behavior. *Rev. Mod. Phys.*, 46:597 – 616, 1974.

[67] J. V. Sengers and J. G. Shanks. Experimental critical-exponent values for fluids. *J. Stat. Phys.*, 137:857 – 877, 2009.

[68] M. E. Fisher and S.-Y. Zinn. The shape of the Van der Waals loop and universal critical amplitude ratios. *J. Phys. A*, 31:L629 – L635, 1998.

[69] A. Pelissetto and E. Vicari. Critical phenomena and renormalization-group theory. *Phys. Rep.*, 368:549 – 727, 2002.

[70] J. G. Shanks. A light-scattering study of static critical phenomena in binary liquid mixtures. Master's thesis, University of Maryland, 1986.

[71] M. A. Anisimov; V. A. Agayan and P. J. Collings. Nature of the Blue-phase-III isotropic critical point: An analogy with the liquid-gas transition. *Phys. Rev. E*, 57:582 – 595, 1998.

[72] H. Behnejad; J. V. Sengers and M. A. Anisimov. *Thermodynamic Behavior of Fluids near Critical Points*. Applied Thermodynamics of Fluids, edited by A. Goodwin; C. Peters and J. V. Sengers, Chapter 10. Royal Society of Chemistry, Cambridge, 2010.

[73] P. Schofield. Parametric representation of the equation of state near a critical point. *Phys. Rev. Letters*, 22:606 – 608, 1969.

[74] P. Schofield; J. D. Litster and J. T. Ho. Correlation between critical coefficients and critical exponents. *Phys. Rev. Letters*, 23:1098 – 1102, 1969.

[75] J. T. Ho and J. D. Litster. Faraday rotation near ferromagnetic critical temperature of $CrBr_3$. *Phys. Rev. B*, 2:4523 – 4532, 1970.

[76] J. J. Rehr and N. D. Mermin. Revised scaling equation of state at the liquid-vapor critical point. *Phys. Rev. A*, 8:472 – 480, 1973.

[77] G. Orkoulas; M. E. Fisher and C. stn. The yangyang relation and the specific heats of propane and carbon dioxide. *J. Chem. Phys.*, 113:7530 – 7545, 2000.

[78] M. E. Fisher and G. Orkoulas. The yang-yang anomaly in fluid criticality: Experiment and scaling theory. *Phys. Rev. Lett.*, 85:696 – 699, 2000.

[79] Y. C. Kim; M. E. Fisher and G. Orkoulas. Asymmetric fluid criticality. I. scaling with pressure mixing. *Phys. Rev. E*, 67:061506, 2003.

[80] M. A. Anisimov; E. E. Gorodetskii; V. D. Kulikov and J. V. Sengers. Crossover between vapor-liquid and consolute critical phenomena. *Phys. Rev. E*, 51:1199 – 1215, 1995.

[81] M. A. Anisimov; E. E. Gorodetskii; V. D. Kulikov; A. A. Povodyrev and J. V. Sengers. A general isomorphism approach to thermodynamic and transport properties of binary fluid mixtures near critical points. *Physica A*, 220:277 – 324, 1995.

[82] J. T. Wang and M. A. Anisimov. Nature of vapor-liquid asymmetry in fluid criticality. *Phys. Rev. E*, 75:051107, 2007.

[83] J. T. Wang; C. A. Cerdeirina; M. A. Anisimov and J. V. Sengers. Principle of isomorphism and complete scaling for binary - fluid criticality. *Phys. Rev. E*, 77:031127, 2008.

[84] D. A. Fuentevilla and M. A. Anisimov. Scaled equation of state for supercooled water near the liquid-liquid critical point. *Phys. Rev. Letters*, 97:195702, 2006.

[85] D. M. Murphy and T. Koop. Review of the vapour pressures of ice and supercooled water for atmospheric applications. *Q. J. R. Meteorol. Soc.*, 131:1539 – 1565, 2005.

[86] F. W. Starr; C. A. Angell and H. E. Stanley. Prediction of entropy and dynamic properties of water below the homogeneous nucleation temperature. *Physica A*, 323:51 – 66, 2003.

[87] H. R. Prupacher and J. D. Klett. *Microphysics of Clouds and Precipitation.* Springer, Dordrecht, 2010.

[88] J. Pátek; J. Hrubý; J. Klomfar; M. Součková and A. H. Harvey. Reference correlations for thermophysical properties of liquid water at 0.1 Mpa. *J. Phys. Chem. Ref. Data*, 38:21 – 29, 2009.

[89] J. Kalová and R. Mareš. *Equations for the thermodynamic properties at the saturation line in the supercooled water region.* Proceedings of the 15th International Conference on the Properties Water and Steam, Berlin/Germany, 2008.

[90] G. J. Gittens. Variation of surface tension of water with temperature. *Journal of Colloid and Interface Science*, 30:406–412, 1969.

[91] W. Drost-Hansen. Aqueous interfaces - methods of study and structural properties. Part two. *Ind. Eng. Chem.*, 57:18–37, 1965.

[92] Y. Lü and B. Wei. Second inflection point of water surface tension. *Applied Physics Letters*, 89:18–37, 2006.

[93] V. Holten. *Water nucleation. Wave tube experiments and theoretical considerations.* PhD thesis, Eindhoven University of Technology, 2009.

[94] J. Hrubý. *Nucleation and a new thermodynamic model of supercooled water.* Nucleation and Atmospheric Aerosols 2004: 16th International Conference, Kyoto University Press, 2004.

[95] M. R. Feeney and P. G. Debenedetti. A theoretical study of the interfacial properties of supercooled water. *Ind. Eng. Chem. Res.*, 42:6396–6405, 2003.

[96] V. Holten; C. E. Bertrand; M. A. Anisimov and J. V. Sengers. Thermodynamics of supercooled water. *J. Chem. Phys.*, 136:094507, 2012.

[97] K. Stokely; M. G. Mazza; H. E. Stanley and G. Franzese. Effect of hydrogen bond cooperativity on the behavior of water. *Proc. Natl. Acad. Sci. U. S. A.*, 107:1301 – 1306, 2010.

[98] C. A. Angell. Insights into phases of liquid water from study of its unusual glass-forming properties. *Science*, 319:582 – 587, 2008.

[99] J. Kalová; R. Mareš; M. A. Anisimov and J. V. Sengers. *Scaled equation of state for supercooled water in the mean-field approximation.* Technical Report prepared for the International Association for the Properties of Water and Steam, Pilsen, September 2011.

[100] M. A. Anisimov and J. T. Wang. Nature of asymmetry in fluid criticality. *Phys. Rev. Lett.*, 97:025703, 2006.

[101] M. A. Anisimov. *Critical Phenomena in Liquids and Liquid Crystals.* Gordon and Breach, Philadelphia, 1991.

[102] M. A. Anisimov; S. B. Kiselev; J. V. Sengers and S. Tang. Crossover approach to global critical phenomena in fluids. *Physica A*, 188:487 – 525, 1992.

[103] W. Wagner and A. Pruß. The IAPWS formulation 1995 for the thermodynamic properties of ordinary water substance for general and scientific use. *J. Phys. Chem. Ref. Data*, 31:387 – 535, 2002.

[104] Y. C. Kim; M. A. Anisimov; J. V. Sengers and E. Luijten. Crossover critical behavior in the three dimensional ising model. *J. Stat. Phys.*, 110:591 – 609, 2003.

[105] J. V. Sengers K. Gutkowski, M. A. Anisimov. Crossover criticality in ionic solutions. *J. Chem. Phys.*, 114:3133 – 3148, 2001.

[106] M. A. Anisimov; A. F. Kostko; J. V. Sengers and I. K. Yudin. Competition of mesoscales and crossover to theta-point tricriticality in near-critical polymer solutions. *J. Chem. Phys.*, 123:164901 – 164917, 2005.

[107] F. W. Balfour J. M. H. Levelt Sengers; B. Kamgar-Parsi and J. V. Sengers. Thermodynamic properties of steam in the critical region. *J. Phys. Chem. Ref. Data*, 12:1 – 28, 1983.

[108] A. Kostrowicka Wyczalkowska; J. V. Sengers and M. A. Anisimov. Critical fluctuations and the equation of Van der Waals. *Physica A*, 334:482 – 512, 2004.

Publications and Conferences

HOLTEN V., KALOVÁ J., ANISIMOV M.A. and SENGERS J.V.: Thermodynamics of liquid-liquid criticality in supercooled water in a mean-field approximation, *Int. J. Thermophys.* (submitted)

KALOVÁ J., MAREŠ R.: Second inflection point of surface tension of water, *Int. J. Thermophys.* (submitted)

KALOVÁ J., MAREŠ R., ANISIMOV M.A. and SENGERS J.V.: Scaled equation of state for supercooled water in the mean-field approximation, *Technical report prepared for the International Association for the Properties of Water and Steam*, Pilsen, (2011)

KALOVÁ J., MAREŠ R.: Few remarks to the van der Waals equation, *Littera Scripta*, 4, 1, ISSN 1802-503X (2011), cze

MAREŠ R., KALOVÁ J.: Critical exponents values for fluids and linear scaled equation of state, *Littera Scripta*, 4, 1, ISSN 1802-503X (2011), cze

KALOVÁ J., MAREŠ R.: The surface tension temperature dependence of water, *10th Conference with international participation on Power System Engineering, Thermodynamic and Fluid Flow, ES 2011*, Pilsen. ISBN 978-80-261-0004-1, cze

KALOVÁ J., MAREŠ R.: Dependence of surface tension on geometric shape of phase interface, *Proceedings of 30th meeting of departments of fluids mechanics and hydromechanics*, Liberec, 2011. ISBN 978-80-7372-747- 5, cze

KALOVÁ J., MAREŠ R.: Crossover Equation and the Vapor Pressure of Supercooled Water, *Int. J. Thermophys.*, 31, 756, Netherlands : Springer Netherlands, (2010). ISSN 1572-9567.

KALOVÁ J., MAREŠ R.: Calculation of the vapor pressure of supercooled water using Excel, *Littera Scripta*, ISSN 1802-503X (2009), cze

KALOVÁ J., MAREŠ R.: Density of water at ambient pressure. *The Annual IAPWS Meeting*, Doorwerth, The Netherlands (2009)

KALOVÁ J.: Strange water, *Rozhledy matematicko-fyziklní*, 84, 2, ISSN 0035-9343 (2009), cze

KALOVÁ J., MAREŠ R.: Density of water at atmospheric pressure in the range from -40°C to 40°C. *Mechanical Engineering Journal*, ISSN 1335-2938 (2009), cze

MAREŠ R., KALOVÁ J.: A new international formulation for the viscosity of water and vapor pressure in industrial calculations, *8th Conference with international participation on Power System Engineering, Thermodynamic and Fluid Flow, ES 2009.* ISBN 978-80-7043-665-3, cze

KALOVÁ J., MAREŠ R.: Density of water at atmospheric pressure. *Littera Scripta*, 2, 1, ISSN 1802-503X (2009), cze

KALOVÁ J., MAREŠ R.: The linear expansion of an ideal gas. *Littera Scripta*, 2, 2, ISSN 1802-503X (2009), cze

MAREŠ R., KALOVÁ J.: Thermophysical Properties Converted from Data and Equations Based on Old Temperature Scales, *Proceedings of the 15th International Conference on the Properties Water and Steam*, Berlin, Germany, (2008). ISBN 978-3-931384-64-7.

KALOVÁ J., MAREŠ R.: Equations for the Thermodynamic Properties at the Saturation Line in the Supercooled Water Region. *Water, Steam, And Aqueous Solutions, Advances in Science and Technology for Power Generation.* Berlin, Germany : VDI-Gesellschaft Energie Technik (2008). ISBN 978-3-931384-64-7.

KALOVÁ J., MAREŠ R.: Scaled Equation of State for Supercooled Water - Comparison with Experimental Data and IAPWS 95. *Proceedings of the 15th International Conference on the Properties Water and Steam*, Berlin, Germany (2008). ISBN 978-3-931384-64-7.

MAREŠ R., KALOVÁ J.: New basis for thermophysical properties of water and steam, *7th conference with international participation on Power System Engineering, Thermodynamic and Fluid Flow, ES 2008*. ISBN 978-80-7043-665-3, cze

KALOVÁ J., MAREŠ R.: Supercooled water, *Proceedings of 28th meeting of departments of fluids mechanics and hydromechanics*, Pilsen, 2008.ISBN 978-80-7043-666-0.

Talks at Conferences

- 10th Conference with international participation on Power System Engineering, Thermodynamic and Fluid Flow, ES 2011, Pilsen, The Czech Republic (2011)
- 30th Meeting of Departments of Fluids Mechanics and Hydromechanics, Liberec, The Czech Republic (2011)
- 17th Symposium on Thermophysical Properties, National Institute of Standards and Technology, Boulder, Colorado, U.S.A. (2009)
- The Annual IAPWS Meeting, Doorwerth, The Netherlands (2009)
- The 15th International Conference on the Properties of Water and Steam, Berlin, Germany (2008)
- 28th Meeting of Departments of Fluids Mechanics and Hydromechanics, Pilsen, The Czech Republic (2008)

Academic Stay

Institute for Physical Science and Technology University of Maryland, U.S.A, Young Scientist IAPWS Fellowship Project (2010, 01/07)

Proffessional Membership

Member of IAPWS Working Group on Thermophysical Properties of Water and Steam